ELECTRONIC SIMULATION OF AUTOMOTIVE ENGINE OPERATION

by

Santai Hwang

Submitted in Partial Fulfillment of the Requirements
for the Degree of
Master of Science in Engineering
in the
Electrical Engineering
Program

Signature Panuccio 12/4/86
Adviser Date

Sally M. Hotchkiss December 15, 1986
Dean of the Graduate School

YOUNGSTOWN STATE UNIVERSITY
DEC, 1986

ABSTRACT

ELECTRONIC SIMULATION OF AUTOMOTIVE ENGINE OPERATION

Santai Hwang

Master of Science in Engineering

Youngstown State University, 1986

Three automotive systems are discussed and simulated to provide the understanding and insight necessary to design a more efficient combustion system. The systems simulated are the: (1) digital engine speed display (2) ignition's spark advance, and (3) fuel injection.

In addition the requirements of the sensors needed to provide the inputs for the microcomputers which control the combustion process are discussed and described.

A DC motor, whose speed is adjusted by a voltage transformer and monitored by a digital readout, is used to simulate the engine. The control and operation of the automotive syetems are simulated by using a timing light, a stepper motor, and 4 seven segment LED displays. The timing light is used to check the advance angles of spark plug ignition. The stepper motor is used to control the quantity of fuel being injected. The displays are used to indicate the engine speed.

ACKNOWLEDGEMENTS

I dedicate this thesis to my parents and wife, Shiow Ming, who encouraged and supported my decision to come to America and study electrical engineering at Youngstown State University. I acknowledge my deep gratitude to my adviser, Dr. Salvatore Pansino for his guidance during my transition into electrical engineering at Youngstown State University. I thank Dr. Pansino and the other members of my graduate thesis committee, Dr. Jalal Jalali and Professor Raymond Kramer, for their assistance in developing and reviewing this thesis. Their assistance is deeply appreciated. I also acknowledge my gratitude for the valuable assistance and advice provided by the staff of the Electronics Laboratory, Rich Laughlin and friends Min-Eig Lee, Crown-Sen Shieh, and Margarito Susa. Finally I thank the Demichael & Son Auto Service Company and the Schulte Auto Wrecking Company for donating the auto parts which I used to build the simulated automotive systems.

TABLE OF CONTENTS

LIST OF SYMBOLS

SYMBOL	DEFINITION	UNITS OR REFERENCE
A	Area	$in.^2$
a	A half length of bar	in.
B	Base of transistor	none
c	Collector of transistor	none
D	Diameter of circular	in.
D	Displacement of cylinder	in^3
E	Energy	eV
E	Young's module	psi
E	Emitter of transistor	none
e	the Charge of electronic	coul
F	Force	lb.
f	Frequency	HZ (cps)
g	Acceleration of gravit	ft/sec
h	Thickness	in.
$h\nu$	Photon Energy	eV
h_{FE}	DC current gain of transistor	none
I	current	Amp
I_{CEO}	Dark current gain of transistor	Amp
i	Current density	Amp/cm^2
L	Length	in.
Mr, Mt, Ma,	Radial, tangential, axial bending moment	ft-lb
$\dot{m}$	Mass flow rate	lb/sec
m	10^{-3} Number of charge carrier	

n	Revolution speed	rpm
Q	Shear force	lb
P.tr	Phototransistor	none
q	Load intensity	lb/in^2
Q1	Transistor	none
R	Resistor	ohm
r	Radius	in.
rg	Specific weight	lb/ft^3
γ	Shear strain	none
s	Stress	psi
Sa	STrain sensitivity	none
Ssc	Piezoresistivity of semiconductor	none
Sc	Circuit sensitivity	V
T	Temperature	^oF
T	Period	sec/cycle
Ta	Temperature of environment	^oF
u	10^{-6}	
Vf	Forward voltage	V
V	Base-Emitter voltage	V
v	Velocity	ft/sec
w	Deflection of bending bar	in.
ρ_c	Curvature	in.
ρ_a	Density of air	lb/ft^3
ρ_r	resistivity	ohm-in.
θ	Angle	rad
ϕ	Angle	rad
ϵ_r, ϵ_t	Axial, transverse strain	none

ν	1 Poisson's ratio	none
	2 Frequency of light	cps
η_v	Volumetric efficiency	none

LIST OF FIGURES

LIST OF TABLES

CHAPTER I

INTRODUCTION

1.1 Introduction

The 1986 automobiles differ from those of 1960 in three ways. Looking under the hood, it is obvious that the 1986 models have a considerably more complex array of electronic components and electrical wiring surrounding the engine. The dashboard has also changed drastically, reflecting the advances in digital electronics and system concepts. Finally, comparing performances, we find that the 1986 models are much more economical and safe to drive. The driving forces for those changes were:

(1) stringent Federal Emission Standards requiring auto manufacturers to produce more fuel efficient and less pollutive automobiles.

(2) competition from foreign auto manufacturers and greater expectations from customers for fuel economy, safety, comfort, ease of operation, performance, and maintenance.

(3) advances in electronics and related technologies.

My interest is in the electronic and related technological advances. These include:

(1) The development of low cost per function digital electronics capable of operating in the hostile automotive environment.

(2) Availability of electronic and solid state devices which make it possible to replace mechanical automotive parts such as distributors and carburetors.

(3) Sensors and control systems that make it possible to monitor and control more automotive functions.

(4) Programmable nature of microprocessors allows one to easily make adjustments for the different requirements of a variety of vehicles operating in various climates and conditions.

(5) The ability to perform automotive system functions electrically with a very high degree of accuracy and reliability.

These were the significant factors in determining the objectives and extent of this thesis. One of these objectives is to investigate the feasibility of performing ignition and carburetor functions electrically. Another is to explore some of the shortcomings of present sensor performance and to determine the needs for future sensor development.

1.2 Trends in Automotive Electronics

The incorporation of electronics into automobiles has been slow due to the trade-offs between costs and benefit. The first electronics was introduced during the 1930's in the form of AM radio receivers. During the late 1950's and early 1960's there were attempts to introduce electronic ignition and electronically controlled fuel

injection. Customers, however, did not want such options and they were discontinued.

Electronics is now being used to control engine operation in order to minimize exhaust emissions and maximize fuel economy, to monitor the vehicle perfomance, and to diagnosis on-board system malfunctions. In the future electronics will be incorporated at an increasingly accelerated rate to provide increased safety and convenience. Two ongoing developments are control of vehicle motion and drive line control. There are basically three categories of future applications:

(1) Driver information center: includes displays for monitoring the speed, distance, time, temperature, fuel level, generator, battery, and communications.

(2) Safety control center: includes theft, seat belt, and oil alarms, brake controls, road condition correction, and head light adjustments.

(3) Engine and transmission center: includes (see page 1 bottom).

1.3 Overview of the Project

In this project (Fig. 1) three automotive systems are simulated by electronic devices with microcomputer control. A DC motor is used in place of the engine. The three simulated systems are (1) the display of engine speed (2) the ignition system (3) the fuel injection system. In the traditional car, gears are used to transmit

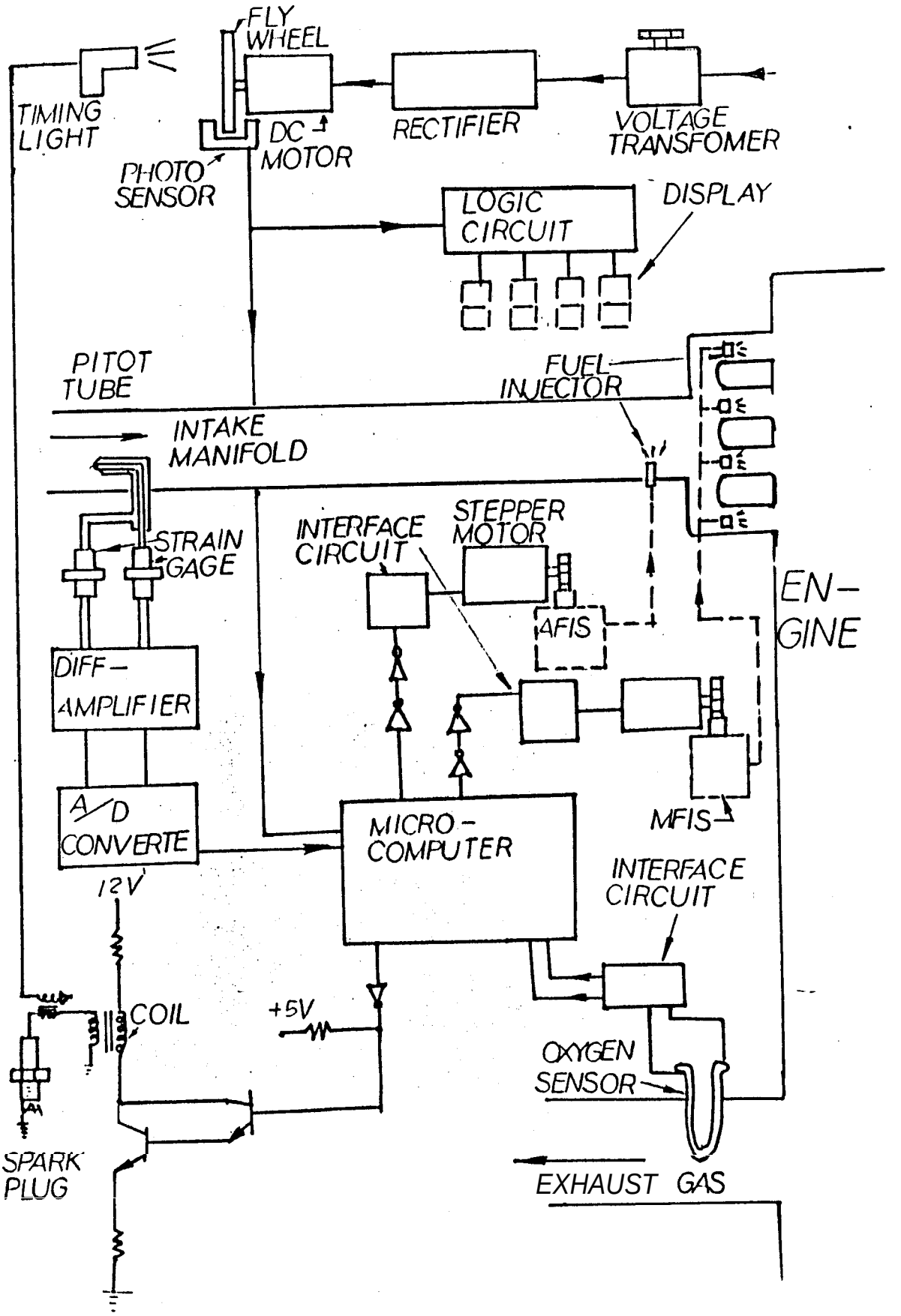

Fig. 1. ELECTRONIC SYMULATION OF ENGINE OPERATION

te the engine motion from the crankchaft (or camshaft) to the distributor shaft, which opens the breaker points to control the timing of spark advance ignition. In this research, a DC motor is used in place of the automobile engine, and a photo sensor is used to detect the revolution of the motor. The signal is used to control the timing of the spark ignition. Consequently, by using these simulations, the mechanical constructions of vacuum advance, centrifugal advance, the distributor, and the breaker points were studied. This provided the basis for modeling the automotive systems with the electronic devices as explained in chapter VII. In addition, the carburetor can be replaced by an air flow meter and a fuel injection system which consists of a stepper motor and fuel injectors to meter the air/fuel ratio. The functions of sensors which are used in this project are introduced as follows:

Chapter II - Photo sensor: To detect the engine speed.

Chapter III - Strain gage: To detect the pressure of air flow.

Chapter IV - Oxygen sensor: To detect whether the combustion is complete or not.

Chapter V - Air flow meter: To measure the air flow mass rate.

The three simulated systems are introduced as follows:

Chapter VI - The digitized speed engine display

Chapter VII - The ignition system

Chapter VIII - The fuel injection system.

The results are discussed and evaluated in chapter IX.

CHAPTER II

PHOTO SENSOR

2.1 Introduction

The behavior of light is explained by two different theories - the particle theory and the wave theory. Since the photoelectric effect is based on Einstein's photon concept the particle theory is the applicable one to analyze how a photo sensor works. Photo devices are divided into three categories:

(1) Light Emitters: such as an LED which converts electrical energy into optical radiation.

(2) Photodetectors: such as photo diodes and phototransistor which converts optical radiation into an electrical signal.

(3) Energy Cells: such as a solar cell which converts optical energy into electrical energy.

2.2 Photo Detective System

There are two basic types of photo detective systems. Both types of systems consist of a light emitter and a light detector which converts the light into an electrical signal. The two types, the photo interrupt and reflective systems, are depicted in Fig. 2.. This study is limited to the photo interrupt system. A GsAs infrared

LED and a phototransistor are generally used as the light emitter and detector. This system has the advantages of fast response, long life, and small size.

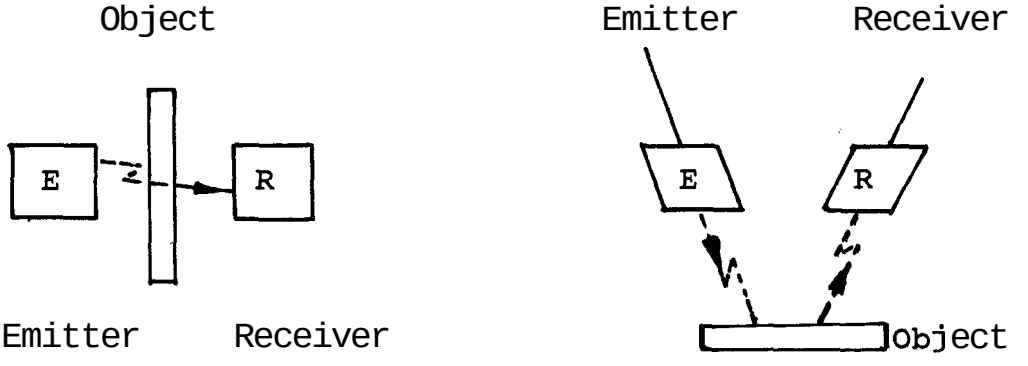

Fig. 2. Types of photo sensor

2.3 Phototransistor

Both the bipolar and unipolar transistors are suitable for use as photodetectors, Like the transistor, a phototransistor can have high gains with **"transistor action".** When the photons of light strike on the surface of the base of the phototransistor, they energize carriers, which contribute a photocurrent in the collector. -- According to **Einstein's** photon theory, the energy E of a single photon is given by

$$E = h\nu$$

If the energy carried by the photon is absorbed by the. carriers, and it is enough to overcome the energy barrier,- the electrons will be injected across the base to the collector.

The injection efficiency depends on the difference in the bandgap between the collector-emitter region and the thickness of the base. Phototransistor differs from a conventional bipolar transistor by having a large base - collector junction to collect more light photons.In addition, a darlington connection is used to obtain a higher photo sensitivity or gain. This however increases the response time. These structures and their equivalent circuits are shown in Fig. 3.[1]

Circuit Design

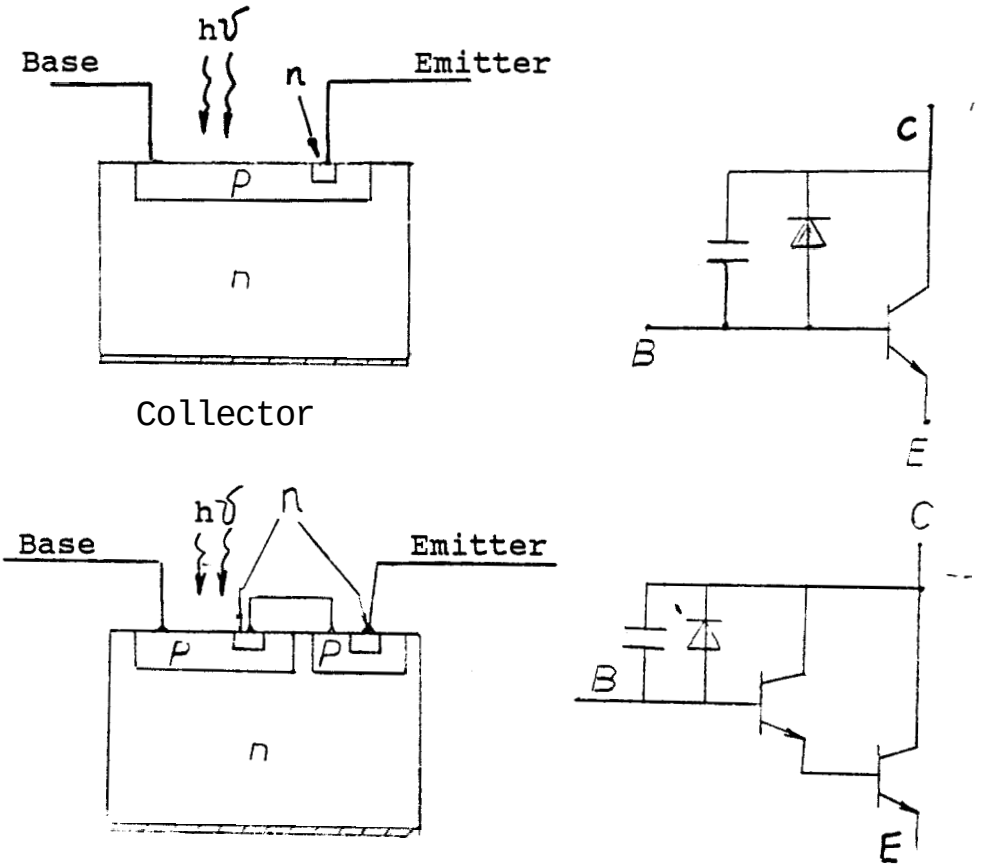

Fig. 3. (A) Bipolar phototransistor (B) Photo-Dariington connection

1. J.S. Jayson And Knight,"Opto-Isolator",Applied Solid Science, Vol.6. 1976 pp.119-168

The purpose of this section is to demonstrate how to obtain a digital output signal (HI or LO). If we consider the worst case, the temperature of the environment will affect the dark current I_{CEO} and the voltage V_{BE} . See Fig. 3. and 4.. Furthermore, from the following analysis the rules of the basic circuit design used to interface the logic circuit will be developed.

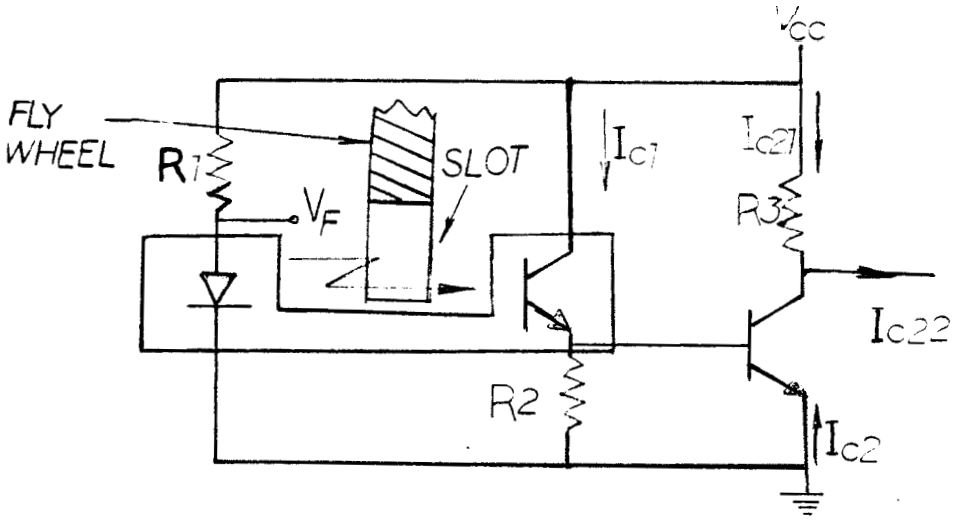

Fig. 4. The basic circuit of photo sensor

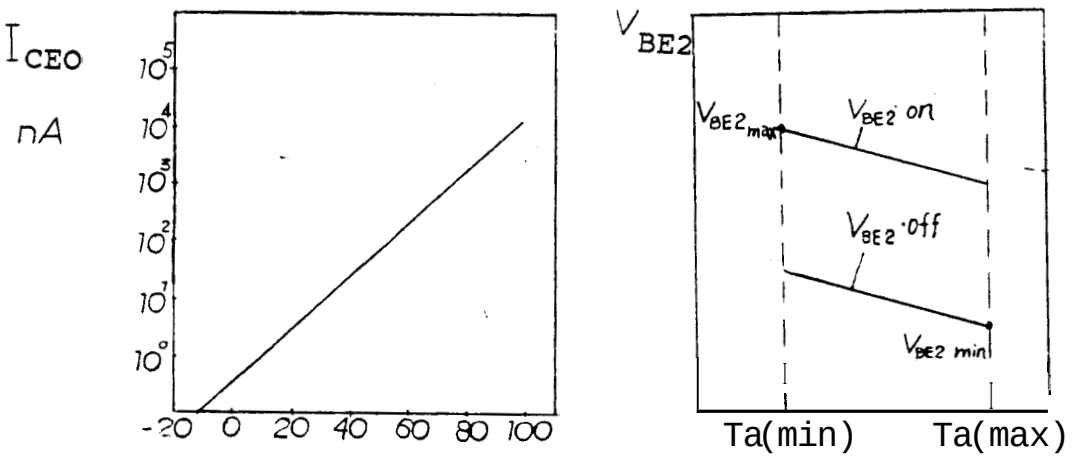

Ta : the temperature of environment

Fig. 5. The temperature characteristic
(from the Data Sheet of Pansonic Elec. Corps)

(1). resistor R1

the consuming power of LED = $(V_{CC} - V_F)V_F / R1$ < the rated power of LED

so, $$R1 > \frac{(V_{CC} - V_F)V_F}{\text{rated power of LED}}$$

(2). resistor R3

If R3 is increased, the I_{C2} will be decreased. However, if I_{C2} is too small, this circuit will be easily interfered by noise. In general $I_{C2} = 0.5 - 1$ mA; therefore,

$$Vcc/R3 < Ic = 0.5 \sim 1 \text{ mA}$$

(3). h_{FE} and I_{B2}

Because the luminosity of LED will decrease gradually, the gain h_{FE} and I_{B2} must be set at the minimum for the worst case.

(4). for Tr2 off

$$(I_{CEO(MAX)} + I_{C1(MAX)})R2 / A_{(MIN)} < V_{BE2(off,min)}$$

where, $$A_{(MIN)} = \frac{\text{the value of } I_{C2} \text{ , when P.Tr1 ON}}{\text{the value of } I_{C2} \text{ , when P.Tr1 OFF}}$$

(5). for Tr2 on

$$(I_{C1(MIN)} - I_{B2(MIN)})\ R2 > V_{BE2(on,max)}$$

Applying these rules to the circuit in the Fig. 4., we see that if the phototransistor Q1 on, the output voltage of the transistor Q2 will be high (4.93V), and if Q1 is off, the output voltage of Q2 is low (0.1V).

2.5 Summary

There are three processes in photo detection: (1) carrier generation by incident light, (2) carrier transport (3) interaction of current with the external circuit to provide the output signal. Comparing the use of a photo sensor with a micro switch, the photo sensor will have following advantage: (1) easy to interface with TTL and MOS logic circuits, (2) quick response, (3) accurate, (4) longer life, (5) smaller volume. The disadvantages are sensitivity to temperature and oil spots on the light-collecting elements which may change or reduce the life of the photo sensor.

CHAPTER III

STRAIN GAGE

3.1 Basic Definition

If a force F is exerted on a bar along the X- axis, it should make balance or internal stress, which is uniformly distributed over the cross sectional area A, exist inside the bar. The stress S on the plane of section is F/A (Fig. 6.).

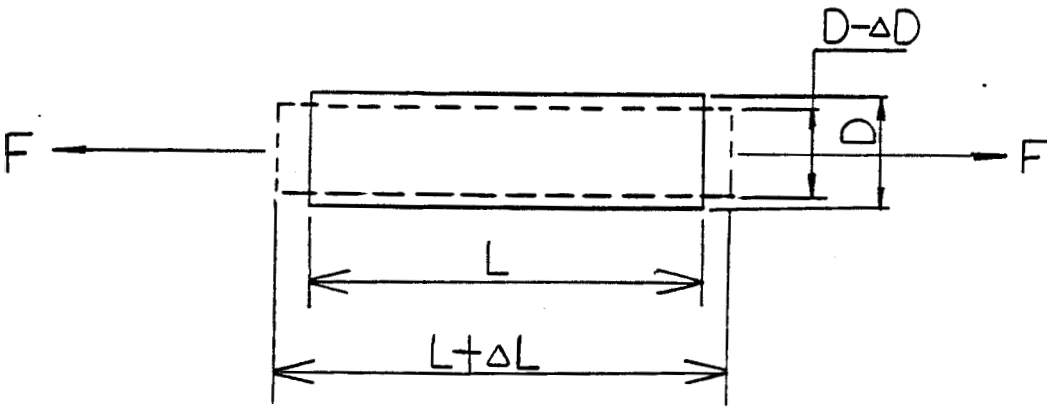

Fig. 6. Stress strain

The stress induced by the bending moment is defined as bending stress. Consider the following example. Consider a beam which is supported at both ends with a force acting in the middle (Fig. 7a.). From the free body diagram the bending moment is

$M = Fr / 2$, when $r < a$.

At the cross sectional area shown in Fig. 7b., an internal bending stress develops in order to balance the bending moment. The bending stress will vary linearly from zero (at the neutral axis) to a maximum compressive value (at the extreme top beam) and to a maximum tensile value (at the extreme bottom beam). See Fig. 7c.

If a beam is bent within the elastic range, the elastic line will have the relation $ds = \rho_c d\theta$. See Fig. 7b. If the θ is very small, then ds will be approximately equal to dx. The curvature is defined as $1/\rho_c = d\theta/dx$.

When a tensile force is applied to a bar, the bar

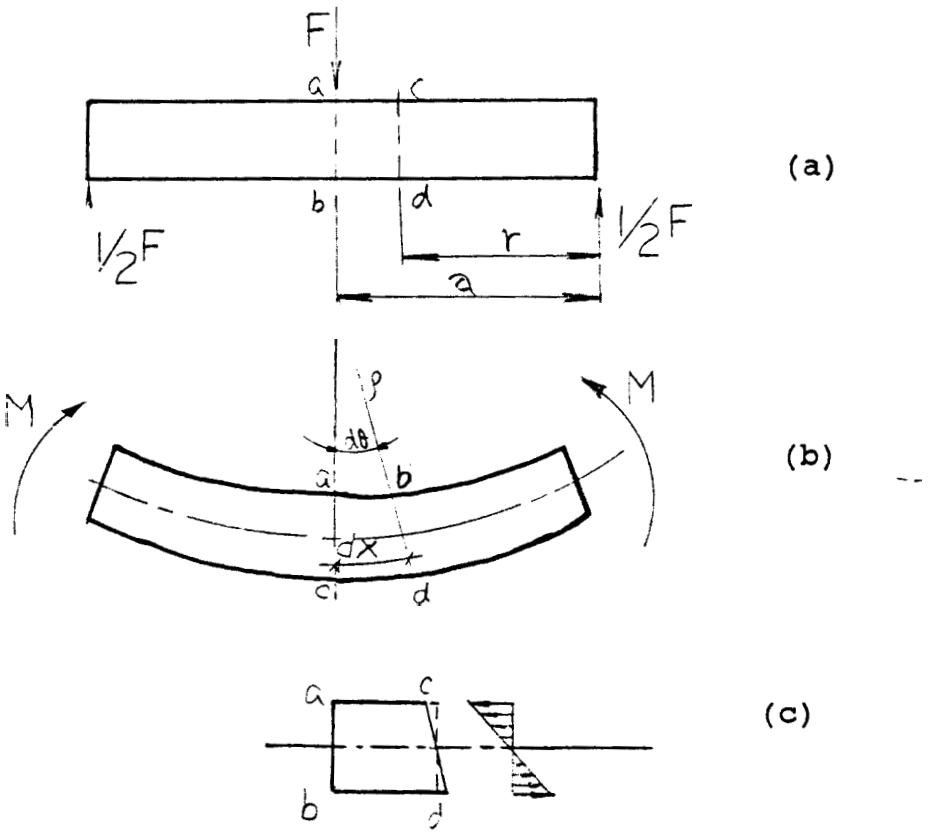

Fig. 7. Bending Stress

will be elongated. According to the definition of strain $\epsilon = \Delta L/L$. See Fig. 6.. The strain is dimensionless and it may be either tensile (positive) or compressive (negative). See Fig. 7c.. The purpose of a strain gage is to measure the strain in a structure.

Fig. 6. indicates there is a contraction in the transverse direction when the bar is stretched longitudinally. The equation defining the poisson's ratio is $\nu = -\frac{\epsilon_t}{\epsilon_l}$. where ϵ_t and ϵ_l are the strains in the transverse and longitudinal directions.

The shearing strain, ,is defined as the angular change in radians between the two line segments that were orthogonal in the undeformed state. Since the angle is very small for most metals,shearing strain is approximated by the tangent of the angle (Fig. 8.).

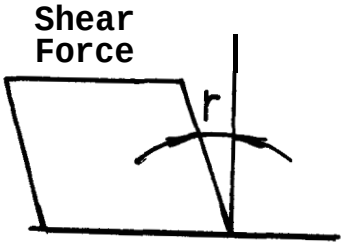

Fig. 8. Shear strain

Strain Sensitivity, Sa, is defined as the ratio of the fractional resistance change per strain along the axis of the gage. Strain gage manufacturers usually provide this calibration constant for each gage

$$Sa = \frac{\Delta R/R}{\Delta L/L} = \frac{\Delta R/R}{\epsilon_l}$$ ϵ_l Axial Strain

3.3 Resistance Change of Metallic Alloy Material

The resistance R of a uniform conductor with a length L, cross sectional A, and the specific resistance ρ_r is given by

$$R = \rho_r L/A \qquad \text{EQ.2}$$

Differentiating EQ.2, and dividing by the total resistance R, obtain

$$\frac{dR}{R} = \frac{d\rho_r}{\rho_r} + \frac{dL}{L} - \frac{dA}{A} \qquad \text{EQ.3}$$

If the diameter of the conductor is d_o, than the diameter will change to d_f (EQ.4) after the stress applied:

$$d_f = d_o\left(1 - \upsilon \frac{dL}{L}\right) \qquad \text{EQ. 4.}$$

therefore,

$$\frac{dA}{A} = \frac{d_f^2 - d_o^2}{d_o^2} = -2\upsilon\frac{dL}{L} + \upsilon^2\left(\frac{dL}{L}\right)^2 \approx -2\upsilon\frac{dL}{L} \qquad \text{EQ. 5}$$

Substituting EQ.5 into EQ.3, obtain

$$\frac{dR}{R} = \frac{d\rho}{\rho} + \frac{dL}{L}(1+2\upsilon) \qquad \text{EQ. 6.}$$

From the definition of the strain sensitivity of the metallic alloy, we get

$$S_A = \frac{dR/R}{\epsilon} = 1 + 2\upsilon + \frac{d\rho/\rho}{\epsilon} \qquad \text{EQ. 7.}$$

3.4 Resistance Change of Semiconductor Material

Basically the semiconductor strain gage consists of a small, ultrathin rectangular filament of a single crystal of silicon, which is usually a electrical anisotropic

material mounted on a carrier (like a diaphragm) to simplify handling. The resistivity ρ_r of a single-crystal semiconductor is given by

$$\rho_r = 1/eN\mu$$

where e = electron,or hole charge

N = number of charge carriers depending on concentration of impurity

μ = mobility of charge carriers.

The strain sensitivity of the semiconductor material will be

$$Sa = 1 + 2\nu + Ssc, \quad Ssc = \frac{d\rho_r}{\rho_r}/\epsilon$$

where Ssc is piezoresisitivity of semiconductor material, and the term $1+2\nu$ is due to dimensional change. Comparing the strain sensitivity Sa of semiconductor with the metallic alloy, the value of Ssc is from 40 to 200, which is larger than the value of metallic alloy(see Table 1), so the semiconductor strain gage will be more sensitive than metallic alloy. Because the differential pressure of pitot tube (discribed in chapter V) is very small, it needs

material	composition %	Sa
Advance	45 Ni, 55 Cu	2.1
Nichrome V	80 Ni, 20 Cr	2.1
Isoelastic	36 Ni, 8 Cr, 0.5 Mo, 55.5 Fe	2.1
Karma	74 Ni, 20 Cr	2.0

Table 1. Strain Sensitivity Sa in Metallic Alloys

2. James W. Dally and William F. Riely, Experimental Stress Analysis, New York: McGraw-Hill,Inc. p.123. 1978.
3. James W. Dally and William F. Riely, P.155.

a very sensitive strain gage to detect and transfer the pressure signal electrical signal. This is the most significant reason why we chose the semiconductor strain gage as the sensor in the flow meter.

3.4 Temperature Compensation

When the variations of temperature are very large, the strain gage will be elongated by the thermal expansion; therefore, for the precise measurement the temperature compensation should be considered due to the large temperature variation (50 °F) in the compartment of engine. Fortunately, a method of Wheatstone bridge (as shown in following paragraph) can solve the problem without adding any extra accessory, which could increase the weight of the car.

3.4.1 Wheatstone bridge Circuit

Considering the circuit of Wheatstone bridge (Fig. 9)

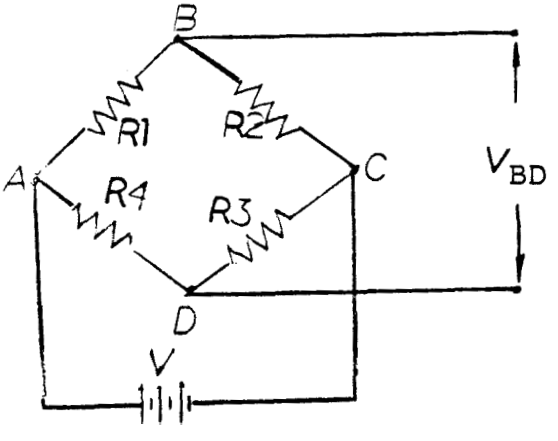

Fig. 9 Wheatstone Bridge Circuit

the voltage v_{AB} drop across R1 is

$$V_{AB} = \frac{R1}{R1 + R2} V \qquad (a)$$

and similiarly the voltage v_{AD} drop across R4 is

$$V_{AD} = \frac{R4}{R3 + R4} V \qquad (b)$$

The output voltage V yields

$$v_{BD} = v_{AB} - v_{AD} \qquad (c)$$

Substituting EQ. (a)(b) into EQ.(c), obtain

$$V_{BD} = \frac{R1R3 - R2R4}{(R1+R2)(R3+R4)} V \qquad \text{EQ. 8}$$

IF R1R3 = R2R4, the output voltage v_{BD} will go to zero, and then change each value of resistance R1, R2, R3, R4 by an incremental amount $\Delta R1$, $\Delta R2$, $\Delta R3$, $\Delta R4$. The variation of output voltage v_{BD} can be obtained from EQ. 8, which becomes

$$\Delta V_{BD} = \frac{(R1+\Delta R1)(R3+\Delta R3) - (R2+\Delta R2)(R4+\Delta R4)}{(R1+\Delta R1+R2+\Delta R2)(R3+\Delta R3+R4+\Delta R4)} \qquad \text{EQ. 9.}$$

By expanding EQ. 9, neglecting second order terms, and noting that R2/R1 = r and R1R3 = R2R4, EQ. 9 will become

$$\Delta V_{BD} = \frac{r}{(1+r)^2}\left(\frac{\Delta R1}{R1} - \frac{\Delta R2}{R2} + \frac{\Delta R3}{R3} - \frac{\Delta R4}{R4}\right) \qquad \text{EQ. 10}$$

Let the circuit sensitivity is defined $Sc = \Delta v_{BD} / \epsilon$ therefore the circuit sensitivity of Wheatstone bridge is

$$Sc = \frac{\Delta V_{BD}}{\epsilon} = \frac{V}{\epsilon} \frac{r}{(1+r)^2}\left(\frac{\Delta R1}{R1} - \frac{\Delta R2}{R2} + \frac{\Delta R3}{R3} - \frac{\Delta R4}{R4}\right) \qquad \text{EQ. 11.}$$

If you use strain gage in place of R1 as the active strain gage, which is used to measure the strain at a given point, and use another strain gage in place of R2 as the dummy gage, which is exposed to the same thermal environment

dummy gage which is exposed to the same thermal enviroment with the active gage in a Wheatstone bridge circuit. The difference is that the dummy gage is mounted on a small block, which has no received stress. Hence, the variation of resistance in the active gage is

$$\frac{\Delta R1}{R1} = \frac{\Delta R_\epsilon}{R1} - \frac{\Delta R_T}{R1} \qquad \text{EQ. 12.}$$

where R is the change of resistance due to the exerted force, and R is due to the temperature change. However, in the dummy gage the change of resistance is due to a change in temperature alone because no force is exerted on it; thus,

$$\frac{\Delta R2}{R2} = \frac{\Delta R_T}{R2} \qquad \text{EQ. 13}$$

Substituting **EQ. 12.** and **13.** into **EQ. 10.** if we choose $R1 = R2 = R_g$ which is the resistance of strain gage, it is obvious that the ΔR_T terms are canceled out from **EQ.** 14. and the output signal still is same as **EQ. 10.**

$$\Delta V_{BD} = V \frac{r}{(1+r)^2}\left(\frac{\Delta R_\epsilon}{R1} - \frac{\Delta R_T}{R1} - \frac{\Delta R_T}{R2} - \frac{\Delta R3}{R3} \frac{\Delta R4}{R4}\right) \qquad \text{EQ. 14.}$$

From the EQ. 14, we can see that the temperature of environment will not affect the result. In the same manner, if two strain gages are mounted on the surface of a circular diaphragm clamped by two cylinders, then the strain gage will have temperature compensation as described in the following paragraph.

According to the stress distribution of the circular plate (see aAppendix F and Fig. 10.), when r equals

to 0.629a, the stress is zero, i.e., this point acts like a dummy position, where the temperature is the same as the center of the diaphragm and doesn't have any stress. Therefore, if we set one Wheatstone bridge circuit on the circular plate by putting one dummy strain resistor at r = 0.629a, and putting active strain

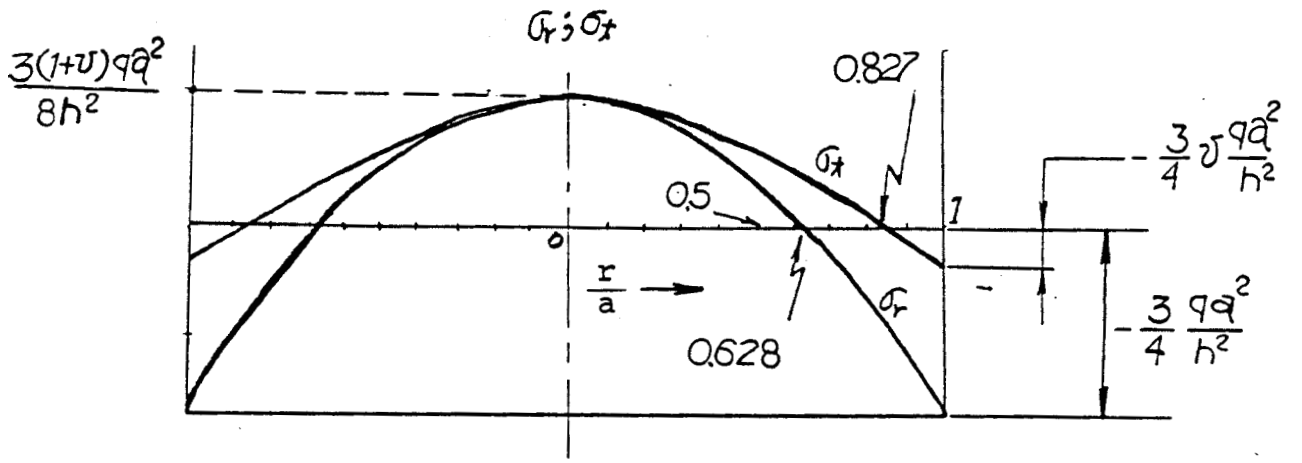

NOTE:
a = diameter of circulr plate q = load intensity
h = thickness of circular plate υ = poison ratio
σ_t = tangential stress σ_r = axial stress
r = 2 X distance from center

Fig. 10. Stress Distribution in Circular Plate

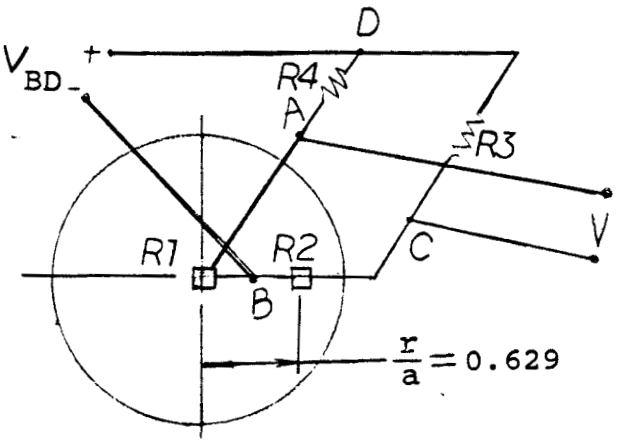

Fig. 11. Strain Gage Mounted on surface of circular diaphragm with Temperature Compensation in the Wheatstone Bridge Circuit

resistor at the center of the diaphragm, we will get a strain gage of temperature compansation (Fig. 11.) without adding a auxiliary circuit.

Because the strain is induced by the stress, the external load (or pressure) has a relationship with the output voltage of the strain gage as shown in the following. Those strain gages, which are products of Omega Engineering, Inc., are used to measure pressure.

Specification of strain gage (from Omega Engineering, Inc)

output: 1 to 6 Vdc
Linearity: + 1.5% Full Scale
Compensated Temperature Range: 0 To 145 F
Response Time: lms
Gage Type: Solid State Piezo-Resisitive
Diaphragm Material: 10 inch Square Silicon Chip.

Parts #	Range(PSIG)	Sensitivity (V/PSIG)
1.	-5 to 0	1.0
2.	-15 to 0	0.33
3.	0 to 5	1.0
4.	0 to 15	0.33
5.	0 to 30	0.167
6.	0 to 60	0.083
7.	0 to 100	0.050
8.	0 to 125	0.033

Table 2. Specification Data of Strain Gage

From the Table 2., the advantages of semiconductor strain gages are (1) linear (2) a wide range of temperature compensation (3) many different ranges of pressure and sensitivity available (4) small size (5) quick response.

CHAPTER IV

OXYGEN SENSOR

4.1 Introduction

The main reason for incomplete combustion in the engine is that a perfect air/fuel ratio was not achieved. With a perfect air/fuel ratio, there would be just enough oxygen to burn all of the gasoline. Therefore, a sensor is installed at the exhaust pipe to detect whether complete combustion took place, and to inform the computer, so the rate of injected fuel can be adjusted. This sensor must meet the following requirements:

1. Small in size and light in weight.
2. Stand high temperatures.
3. Generate a signal large enough to be easily detected.
4. Long life.

These requirements are difficult to meet, because of the hostile environment in the exhaust pipe. The ceramic solid electrolyte oxide cell can meet all these requirements.

4.2 solid oxide cell

4.2.1 Basic concept

There are two reasons why the zirconia electrolyte was chosen for the oxygen sensor (Fig. 14.). One is that

it has a reasonable electrical conductivity at high temperature, the other is that it will generate a voltage when it is exposed to enviroments of different oxygen concentrations. The conductive mechanism is described as follows (Fig. 14.). When the zirconia electrolyte is exposed to oxygen, it becomes a carrier of free electrons. The platinum plate nearest the atmosphere is exposed to more oxygen, so it has more electrons, i.e., it has oxide reaction (at the anode):

$$2O^{2-} \longrightarrow O_2 + 4e^-$$

On the contrary, the plate nearest the exhaust gas encounters fewer atoms of oxygen, giving it a positive charge, i.e., it has reductive reaction (at the cathode):

$$O_2 + 4e^- \longrightarrow 2O^{2-} ;$$

therefore, if the two plates are connected into a complete circuit, current will flow. The characteristic of the zirconia electrolyte will be discussed as following.

4.2.2 The Characteristic of ZrO_2

Zirconitum oxide (ZrO_2) is a non-conducting material which undergoes two transformations. One is the change in crystal form from monoclinic (Fig. 12.) to tetragonal (Fig. 3 . i.e., the polymoric transition, when the temperature is changed from low to high. The other occurs when CaO, or MgO is added to ZrO_2. It then transforms to a cubic fluorite structure which is a stable material.

The stabilized ZrO_2 has high conductivity at

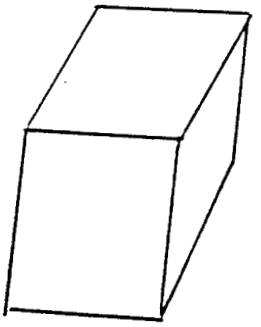

Fig.12. Monolinic Cube

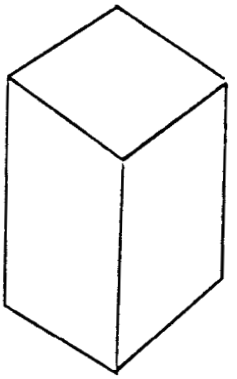

Fig. 13. Tetragonal Cube

elevated temperature and X-rays show the presence of O^{2-} ion vancancies in the crystal lattice. When ZrO_2 is doped with oxides of metals having a less than 4 valence, many anion vacancies will occur and raise the conductivity. Furthermore, a number of experiments of adding Ca and Y in the ZrO_2, show they can stabilize the ZrO_2 over the wide range of temperature. When the concentration of Y is at 8% and at about 12% Ca, there are about 7.5% of possible anion sites vacancies.

Kingery and co-workers used the diffusion of O^{2-} isotope through $(ZrO_2)_{0.85}$ $(CaO)_{0.15}$ and obtained the following results:

1. The diffusion coefficient of O^{2-} ions is sufficiently large to account for the entire observed conductivity.

2. The resistance was found to be independent of the partial pressure of O_2, and to depend only on the O^{2-} ion conductivity.

4. James Patrick Hoare, The Electrochemistry of Oxygen New York: Interscience Publisher, 1968, pp 105-110

3. The resistance of $(ZrO_2)_{0.85} \cdot (CaO)_{0.15}$ is about 15 ohm-cm,and of $(ZrO_2)_{0.9} \cdot (Y_2O_3)_{0.1}$ 9 ohm-cm.

4.3 Implement the Oxygen Sensor

To implement the sensor, the contact surface of the sensor and exhaust gas must be wide , the distribution of the gas can be homogeneous to spread on the sensor, and the gas can be absorbed by the sensor. Therefore, the sensor is coated with a porous material Al_2O_3 on the surface. Also, in order to obtain a homogeneous spread of the exhaust gas deposit porous platinum,which is difficult to be oxided , at each side of the electrolyte - ZrO_2-CaO,

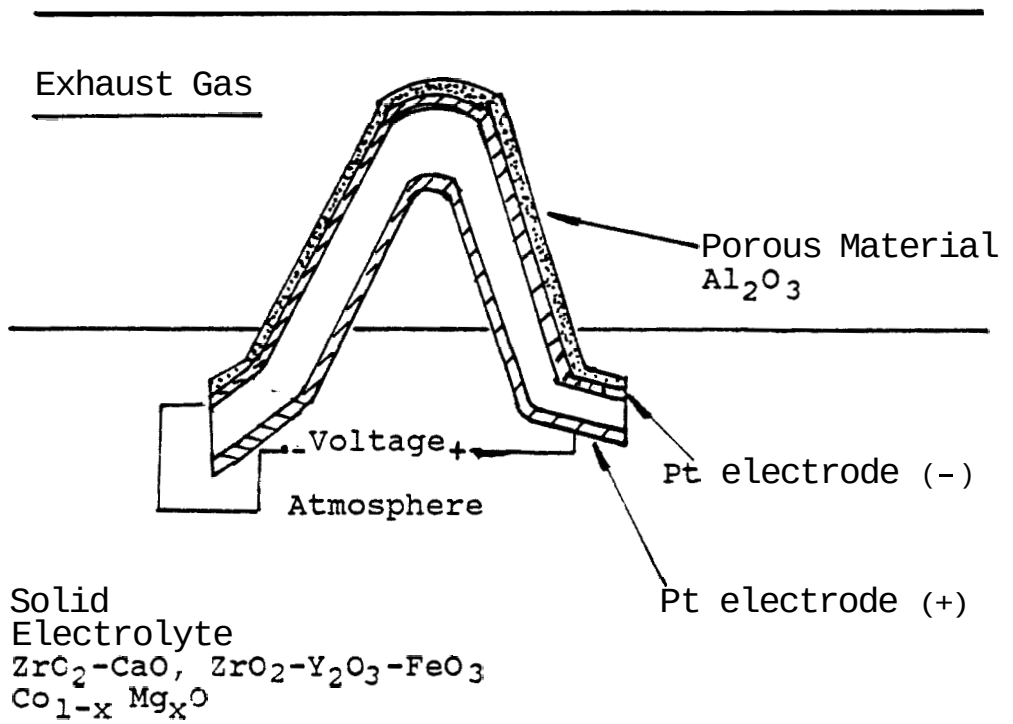

Fig. 14 Oxygen sensor

ZrO_2-Y_2C_3-FeO_3, and $Co_{1-x}Mg_x$, as electrodes (Fig. 22.) Consequently the behavior of the sensor is like a switch (Fig. **15.**). When the mixture is richer than switch point, where A/F ratio = 14.7 (or called Stoichiometric ratio, the output voltage of oxygen sensor is high, and when the mixture is leaner than switch point, the output is low.

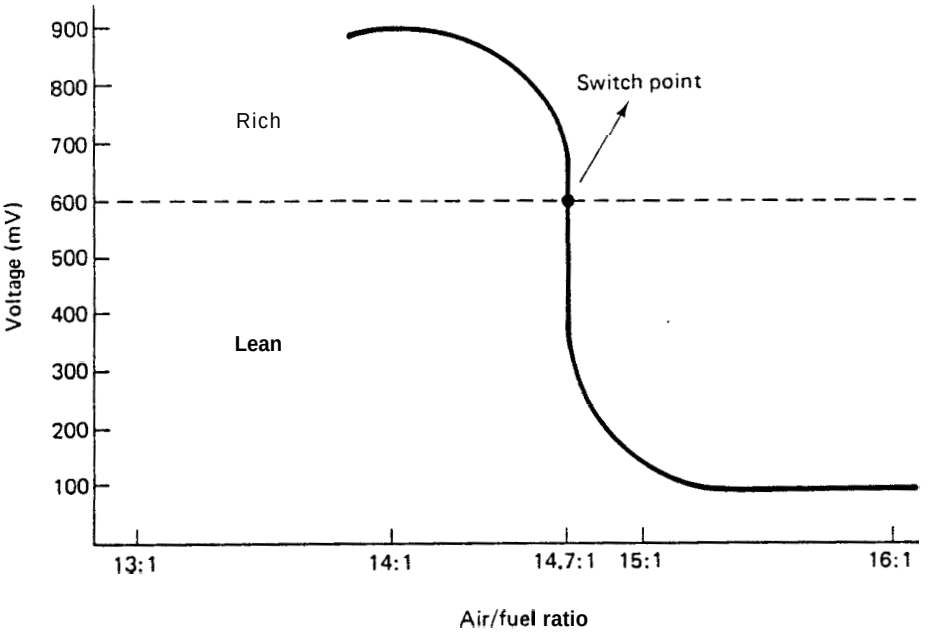

Fig. **15.** Sensor Voltage Curve (Courtesy of General Motors Corporation.)

4.4 The Catalyst Converter

What is the catalyst ? A catalyst is a substance that increases the rate of a reaction without being consumed. It may form an intermediate with one or more of the reactants. The intermediate then decomposes to form the products and to regenerate the catalyst. It just provides a pathway with a lower energy barrier between reactants and products, and has no effect on the position of equilibrium,

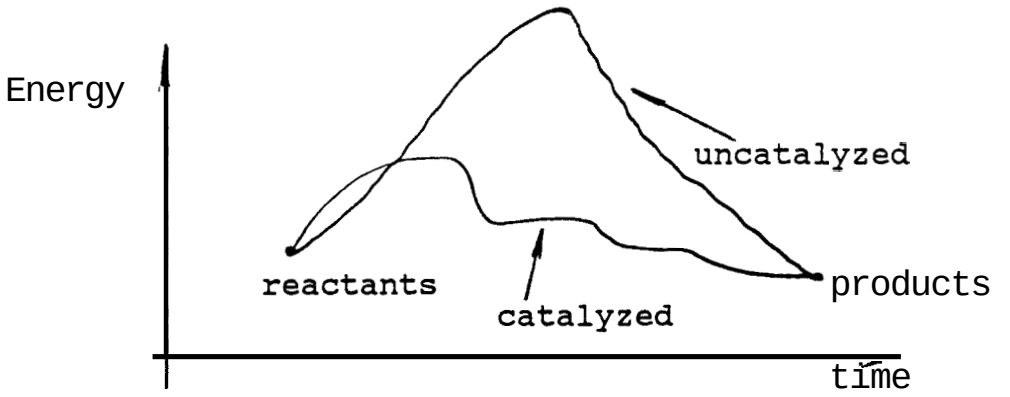

Fig. 16. The Effect of Catalyat

as show in Fig. 16.

If the automobile is installed with the catalyst converter at exhaust gas system, the emissions of carbon monoxide, hydrocarbons, and nitrogen oxides of the exhaust gas, which are the sources of air pollution, can be converted to harmless gases. The catalysts in the converter are primarily platinum and palladium, deposited in a thin layer on a porous material that has a very large surface area. Some of the reactions that occurred in the reducing converter are

$$2C0 + 2N0 \longrightarrow N_2 + 2C0$$

$$3H_2 + 2N0 \longrightarrow 2NH + 2H_2O$$

$$2H_2 + 2N0 \longrightarrow N_2 + 2H_2O$$

$$CO + H_2O \longrightarrow CO_2 + H_2$$

Some of the reactions that take place in the oxidizing converter are

$$2CO + O_2 \longrightarrow 2CO_2$$

$$4HC + 3O_2 \longrightarrow 4CO + 2H_2O$$

$$2H_2 + O_2 \longrightarrow 2H_2O$$

4.5 Applications of Oxygen Sensor and Catalyst Converter

One automobile manufacturer developed a control system using the oxygen sensor and the catalyst converter to clean the exhaust gas and control the A/F ratio.

From the Fig. **15.** and Fig. **17.** the generating voltage of oxygen sensor is abruptly decreased at the **Stoi-**chiometric ratio A/F = 14.7. This is the theoretical value of a perfect combustion reaction. Also the catalyst converter is controlled so that it can obtain the highest clean efficiency when the A/F ratio reaches the **Stoichiometric** ratio. According to these relationships, it is easy to control the A/F ratio in the processor. If the air fuel ratio is not right at the **stoichiometric** ratio, then the combustion will be incomplete; therefore, the oxygen sensor will generate the correlative voltage (HI, or LO) to tell

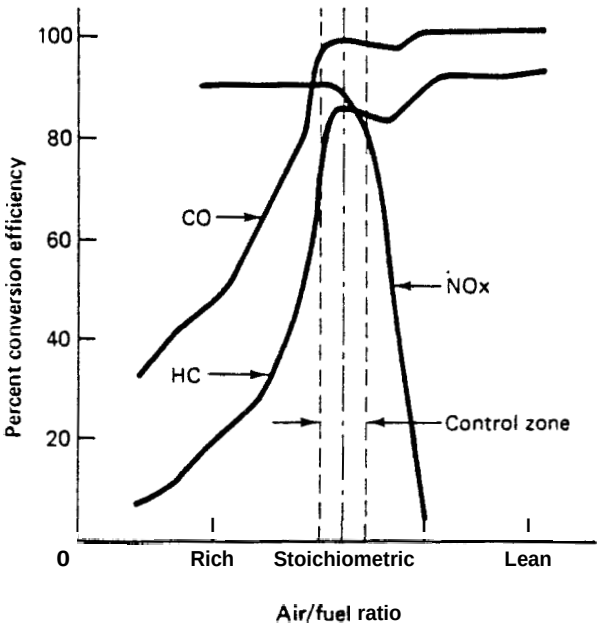

Fig. **17.** Clean Efficiency of Catalyst (courtesy of General Motor Corps.)

the computer to correct the quanties of injected fuel, until the output voltage of oxygen sensor at the switch point which A/F ratio = 14.7, so that the catalyst converter can obtain the highest clean efficiency. The block diagram of the emission control system is shown in Fig. 18. The exhaust gas must pass the oxygen sensor before passing the catalyst converter, because the exhaust gas will be converted to another gas in the catalyst converter.

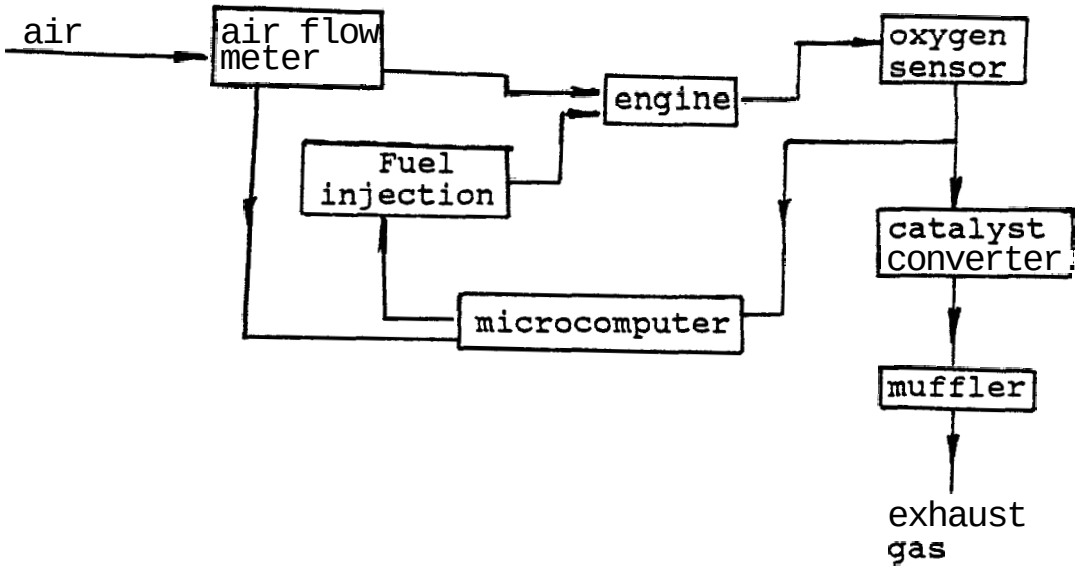

Fig. 18. Emission Control System

If the response time of an oxygen sensor is not considered,,the interface circuit of the oxygen sensor will be realized by two voltage comparators, which can provide two bits of data to the computer. To simplify the oxygen sensor, the oxygen sensor will be replaced by two switches in the simulation of the fuel injected system (chapter

VIII): therefore, the status of two switches will produce two bits of data into the computer. The simulating processes are shown in table a, and the circuit is shown in Fig 19.

output voltage	SW 1	SW 2	DATA BITS	COMMENTS
at switch point	off	off	00	right A/f ratio
HI	off	on	01	mixture too lean
LO	on	off	10	mixture too rich

Table a. The status of oxygen sensor

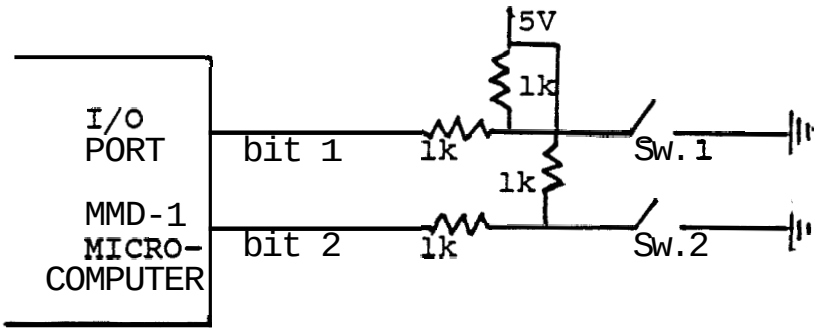

Fig. 19. Simulated Circuit of Oxygen Sensor

CHAPTER V

FLOW METER

5.1 Introduction

A variety of flow measurement techniques suited to gas, liquid , or slurry media have been developed. These measuring systems may be grouped as follows:

1. combining differential-pressure flow sensing element and strain gage like Venturi tube, pitot tube which can measure the differential pressure.
2. using mechanical flow sensing element like a float in variable area or spring-resistance plug turbine.
3. using electromagnetic flow rate tranducer
4. using the ultrasonic device, if the flow media can transmit the sonic wave.

In the automobile, it is important to control the air/fuel mixture for cleaning the exhaust gas, which is discussed in chapter IV; therefore, how to measure the air flow mass rate accurately and to interface with microcomputer to control the fuel injection will be very important. Considering the environment of the engine compartment, there are some difficulties attached to implementing the flow meter: (1) the high temperature which will affect the accuracy of the measure instrument (2) small space in the intake manifold, (3) physics quantities must

be large enough to be picked for measuring (4) easy to interface with the computer.

5.2 Basic Concept

According to the difficulties discussed in the previous section, it is best to choose the pitot tube as the sensing element of the differential pressure of the air flow with semiconductor strain gages as the tranducers, which can tranduce the differential pressure value to the electrical signal, and has high strain sensitivity (see chapter III). Note two strain gages are used to detect the static and dynamic pressure of the pitot tube as show in the block diagram (Fig, 20.).

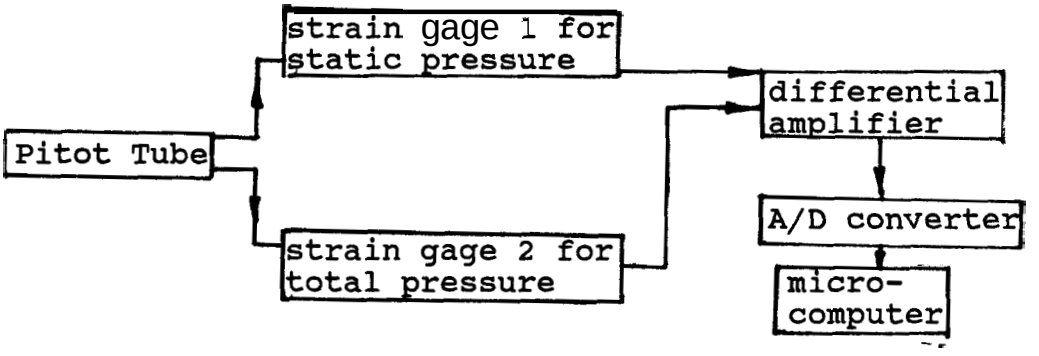

Fig. 20. Block Diagram of Flow Meter

At the beginning, it is necessary to amplify the signals of strain gage with a non-inverting amplifier if the signal is so small that it could be interfered with. However, if the signal is large enough , the non-inverting amplifier can be omitted. Then use a differential

amplifier to obtain a differential voltage, which can be converted to digital signals by a A/D converter. Finally interface the A/D converter with the microcomputer.

5.3 Pitot Tube

For a non-viscous, irrotational, and steady two-dimensional flow, the Bernoullis equation (EQ. 15.) can be represented for each point along a stream line.

$$\frac{P}{rg} + \frac{v^2}{2g} + Z = \text{CONST} \qquad \text{EQ. 15.}$$

where rg is specific weight, v is the velocity, and P is the pressure. A typical Pitot-tube (Fig. 21.) consists of one dynamic tube surrounded concentrically by a closed outer static tube with annular space in between them. Small holes are drilled through the outer tube to measure the static pressure. We detect the static and dynamic pressure at the same height, so the z term in the Bernoulli's equation can be omitted. As a result, the EQ. 15. will become

$$\frac{P1}{rg1} + \frac{v_1^2}{2g} = \frac{P2}{rg2} + 0 \qquad \text{EQ. 16.}$$

which show the relation of pressure and velocity. Note that

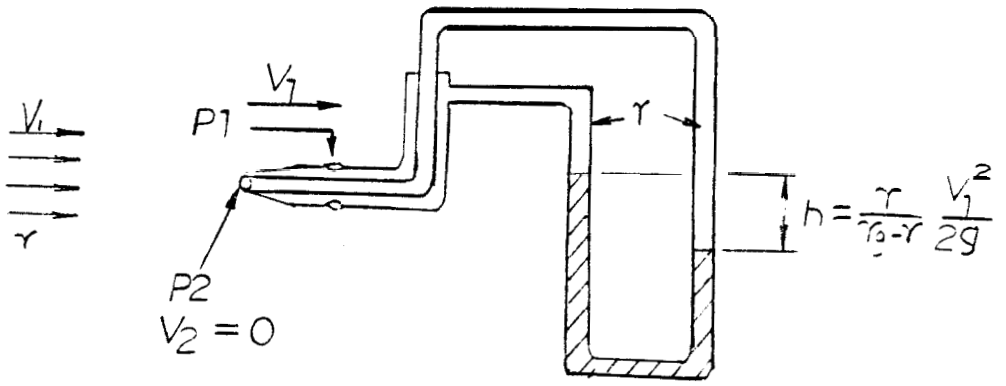

Fig. 21. Pitot Tube

the dynamic tube in the center measures the total pressure which is the sum of the static pressure and the dynamic pressure. According to the pressure-velocity relationship EQ. 16, obtain

$$V_1 = \sqrt{\frac{2(P1-P2)}{\rho_a}} \qquad \text{EQ. 17.}$$

where rg = $\rho_a g$, the density of air.

The term of (P1-P2) can be measured from two strain gages; therefore, the velocity of the air flow can be obtained in EQ. 17. For the steady flow, the mass flow rate m will be

$$\dot{m} = \rho_a A v \qquad \text{EQ. 18.}$$

where A is the pipe area.

Substituting EQ. 17 into EQ. 18, then obtain

$$\dot{m} = A\sqrt{2(P1-P2)\rho_a} \qquad \text{EQ. 19.}$$

which can show the relation of the air flow mass rate and the different pressures. Consequently, if we know the tranducing characteristic of the strain gages, it is easy to find out the relation of the air flow rate and the electrical signal (voltage), which has some examples shown in Table 1 (P. 21.)

5.4 Air Flow Meter in the Automobile

For four or more cyclinders (and a four stroke cycle), the flow is considered steady and equal to EQ. 20.[5]

5. Edward F. Obert Internal Combustion Engines, 1968 Scranton: International Textbook Company, p387.

$$\dot{m} = \eta_v \frac{\rho_a \times D \times n}{1728 \times 2 \times 60} \quad \text{(lb/sec)} \qquad \text{EQ. 20.}$$

where $\eta_v = \frac{\dot{m}t}{\dot{m}a}$; volumetric efficiency. See Note 1

$\dot{m}t$ = actual mass of air inducted per intake stroke
$\dot{m}a$ = theoretical mass of air to fill the piston displacement, volume
ρ_a = density of the atmosphere air (lb/ft^3), the typical value as shown in table 3.
n = speed of engine (rpm)
D = displacement of engine (volume, in^3)

atmosphere (in.Hg)	(lb/ft^3)
30	0.0764
29	0.0739
28	0.0713
27	0.0688
26	0.0622

Note: the temperature is 60 °F

Table 3 Density of the Atmosphere Air

Note 1:

Usually the value of η_v is depended on the speed and the time of opening valve (Fig. 22.). For example, consider the case where the inlet valve closes at 40 deg after BDC. At very slow speeds, the charge of air inducted when the piston reaches BDC would again approach m . But now the piston rises on the return (compression) stroke, and since the inlet valve is still open, a part of the inducted charge is pushed back into the inlet manifold. A unit air charge of only m would be inducted (as the limit at zero speed). However; as the speed is increased, the pressure drop from atmosphere to cylinder increases since the piston is moving faster. Because of this pressure difference, air rushes into the cylinder and the air column in the inlet manifold is accelerated. When the piston approaches BDC, the cylinder pressure is rising toward the pressure at the inlet ports, and this pressure is being reinforced by the momentum of the air column in the inlet manifold-by the deceleration of the air column. Consequently, as the piston first dwell at BDC and then returns on the compression stroke, charging continues until cylinder and inlet port pressures are equal. Thus the air charge increases with speed increase (C to D, Fig.22.). With further increase in speed, fluid friction losses become greater than the

gain in delay charging, and the air charge decreases (D to E, Fig. 22.). Note BDC: Bottom Dead Center.

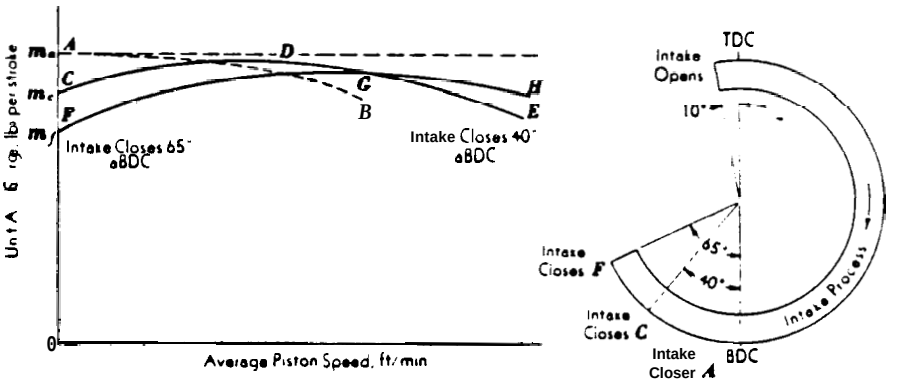

Fig.22. The Effect of inlet valve timing on the air Charge (from Edward F. Obert, P.478.)

Set EQ. 19 = EQ. 20, then

$$m = A\sqrt{2(p1-p2)\rho_a} = \frac{\eta_v \cdot \rho_a \cdot D \cdot n}{1728 \times 2 \times 60}$$

and,

$$P = \frac{\rho_a (\eta_v \times D \times n)^2}{8.6 \times 10\ A} \qquad \textbf{EQ. 21}$$

where, A is the area of intake manifold.

Suppose a engine, whose specification is shown as following, is simulated in this project,

D = 110 in = 1800 c.c,
n = 400 rpm to 8000 rpm,
ρ_a = 0,0739 lb/in,
d = 2 in. the diameter of intake manifold
A = π in^2
η_v = 1 (considering in the ideal condition)

then by EQ. 21. obtain table 4.

5.5 Circuit Design of Flow Meter

6. Edward F. Obert, PP 470-478.

5.5.1 The Non-Inverting Amplifier

For the non-inverting amplifier (Fig. 23.), the gain of the voltage is

$$\frac{V_o}{V_S} = \frac{R1+Rf}{R1} = \frac{Rf}{R1} + 1 \qquad \text{EQ. 22.}$$

It is important to note that the output voltage of op amp will be clamped at Vsat if the magnitude of the output is over the rated saturation voltage, which is provided by the manufacturing company. If the output signals of strain gages is large enough and no noise interferes, we can directly connect the strain gages to the differential amplifier.

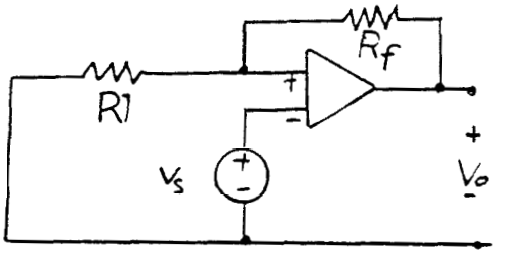

Fig. 23. Non-Inverting Amplifier

5.5.2 Differential Amplifier

There are two methods to obtain the differential voltage of two tranducers. One is by using the differential amplifier as shown in Fig. 24., and the other is by reversing the connection of Wheatstone bridge circuit as shown in Fig. 25.

Differential Voltage by Integrated Circuit

In the differential amplifier (Fig. 24.), if we choose

R1 = R2 and R3 = R4, the output will be

$$V_o = \frac{R3}{R1}(Vs2 - Vs1) = \frac{R4}{R2}(Vs2 - Vs1) \qquad \text{EQ. 23.}$$

where V_o will be different output voltage of two strain gage (Vs2, Vs1) (or two non-inverting amplifier).

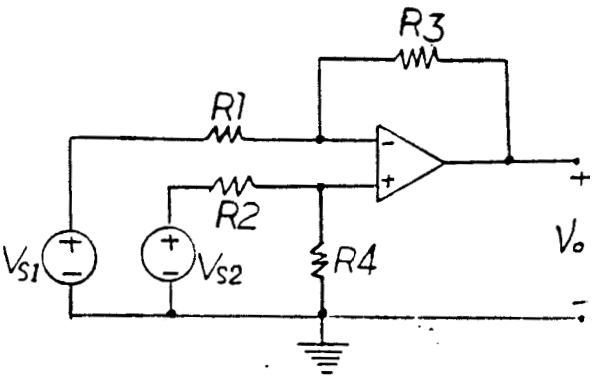

Fig. 24. Differential Amplifier.

Differential Voltage of two Wheatstone Bridge Circuit

In the same manner if two Wheatstone bridge circuit are connected as in Fig.25., the differential voltage of two strain gage is V_o

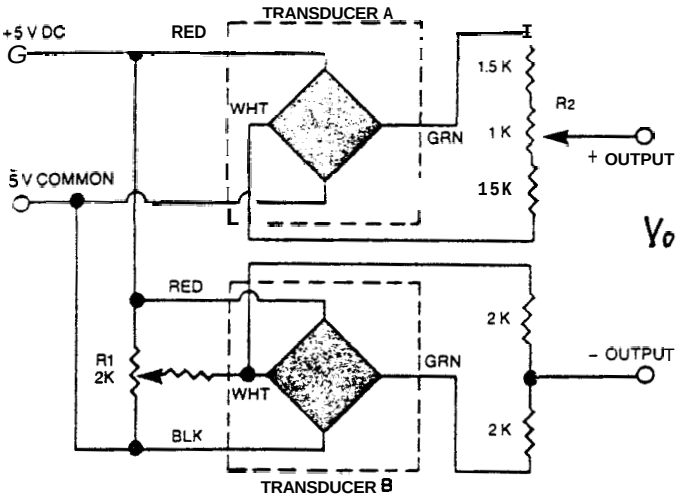

Fig. 25. Differential Voltage of Two Wheatston Bridge Circuit (From Measurement Handbook, Omega Engineering, Inc. 1986)

5.6 Data Acquisition of A/D converter

Usually the A/D converter has the limitation of input voltage range, so we must adjust the differential voltage of the previous state to be accepted by the A/D converter. If we use an 8 bit converter, the air flow mass rate can be divided into 255 steps (see Appendix B), so that each step of air flow mass rate which can be programmed to obtain the correlative quantities of injected fuel, and which is stored in the storage area in the computer,(described in chapter VIII).

Some companies already have some integral circuits of the differential pressure gage with two semiconductor strain gages such that the products of Omega Engineering, Inc. If a differential pressure gage (model: PX83-015DV, Fig. 26.), which sensitivity is 1 volt/PSID, is used in this flow meter, the data of this flow meter is shown in Table 4. Note the simulated engine is the same as in the previous section. Substituting the specification data of the simulated engine into EQ. 20, and 21, obtain

$$\dot{m}a = 3.9 \times 10^{-5} \times n$$

and $$\Delta P = 2.188 \times 10^{-5} \times n^2 .$$

Due to the circuit sensitivity of the differential pressure gage is

$$Sc = V/\Delta P = 1 \text{ volt/PSID} ,$$

where PSID = differential pressure in lb/in^2,

so that $V = 2.188 \times 10^{-5} \times n^2$

In this project, the differential pressure gage is replaced by a DC source, so that the characteristic curve of the differential pressure - voltage in the flow meter can be simulated by the DC source (Fig. 27.)

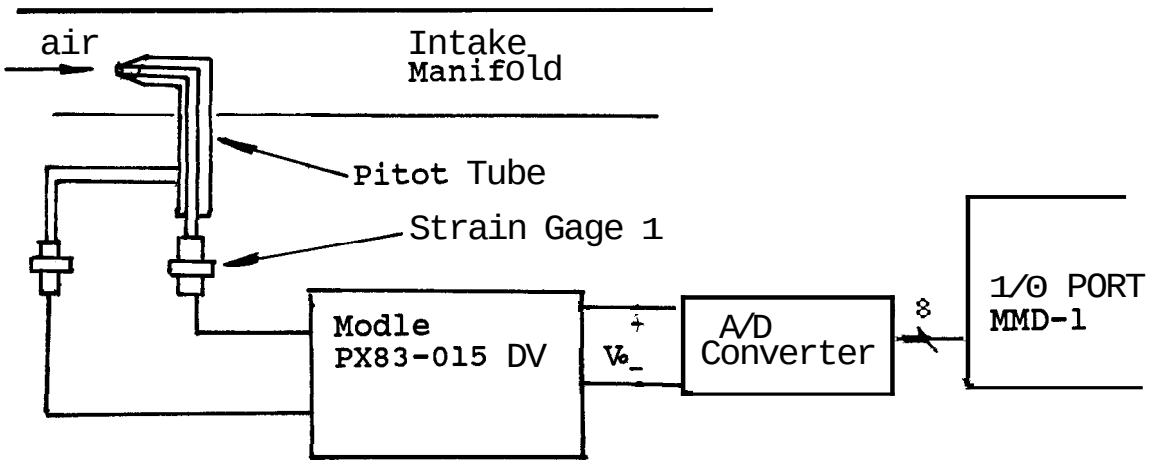

Fig. 24. Circuit of Flow Meter

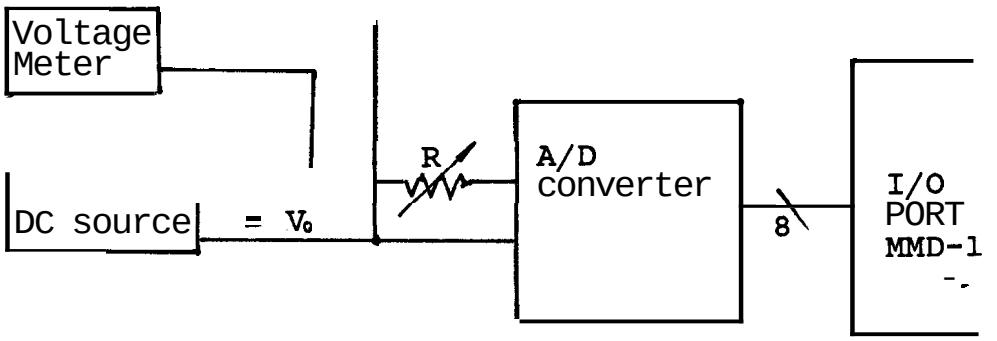

Fig. 27. Simulation Circuit of the Flow Meter

Speed (rpm)	ma (lb/sec)	PSFD (lb/ft)	PSIG = Voltage (lb/in) V
600	0.02352	7.8768	0.0547
700	0.02744	10.7120	0.0743
800	0.03136	14.00043	0.0972
900	0.03528	17.7228	0.1231
1100	0.04312	26.4748	0.1838
1200	0.04704	31.5072	0.0218
1300	0.05096	36.9772	0.2567
1400	0.05488	42.8848	0.2978
1500	0.05880	49.2300	0.3418
1600	0.06272	56.0128	0.3889
1700	0.06664	63.2332	0.4391
1800	0.07056	70.8912	0.4923
1900	0.07448	78.9868	0.5485
2000	0.07840	87.5200	0.6077
2100	0.08232	96.4908	0.6700
2200	0.08624	105.8992	0.7354
2300	0.09016	115.7452	0.8038
2400	0.09408	126.0288	0.8752
2500	0.09800	136.7500	0.9497
2600	0.10192	147.9088	1.0271
2700	0.10584	159.5052	1.1076
2800	0.10976	171.5392	1.1922
2900	0.11368	184.0108	1.2778
3000	0.11760	196.9200	1.3675
3100	0.12152	210.2688	1.4602
3200	0.12544	224.0512	1.5559
3300	0.12936	238.2732	1.6546
3400	0.13328	252.9328	1.7565
3500	0.13720	268.0300	1.8613
3600	0.14112	283.5648	1.9692
3700	0.14504	299.5372	2.0801
3800	0.14896	315.9472	2.1941
3900	0.15288	332.7948	2.3111
4000	0.15680	350.0800	2.4311
4100	0.16072	367.8028	2.5542
4200	0.16464	385.9632	2.6803
4300	0.16856	404.5612	2.8094
4400	0.17248	423.5968	2.9416
4500	0.17640	443.0700	3.0768
4600	0.18032	462.9808	3.2151
4700	0.18424	483.3292	3.3565
4800	0.18816	504.1152	3.5000

Table 4 Data of Flow Meter

CHAPTER VI

DIGITAL ENGINE SPEED DISPLAY

6.1 Introduction

Knowing the engine speed is useful information for the drivers, who can check the power of the engine with the revolution speed to learn the perfomance of their car. Also, the revolution speed of the engine can be transferred to the linear speed of an automobile by the software of the microcomputer, or by the hardware of the logic circuit. In the automobile the digital display will gradually replace the analogue display of mechanical type in the future. Usually, there are three ways to realize the digital speed meter in the automobile engine. The first is to pick up the current pulse frequency of the coil by the current transformer. The second is to pick up the pulse frequency of secondary voltage of the coil. The last is to use the magnetic material attached to the shaft of the distributor (or to the fly wheel) because the pulse of the current and of the voltage in the secondary winding of a coil and the speed of the distributor shaft (or fly wheel) have a relation to the crankshaft speed of the engine. In this research a photo sensor is installed to pick up the revolution signal of the motor from one slot cut in the fly wheel, whose speed is equal to the speed of the engine crankshaft.

When the slot of the fly wheel passes the photo sensor, it will create a pulse to trigger the counters (SN **7490**). Also, according to the sample hold time, the contents of counters will appear on the display.

6.2 Signal Sequence of the Speed Display

The digital speed display is implemented by a logical circuit which is actuated by a photo sensor. Besides the interface circuit of the photo sensor, there are a time gate to control the sample hold time, counters (SN 7490), a one shot multivibrator (OSM, SN 74123), decoders

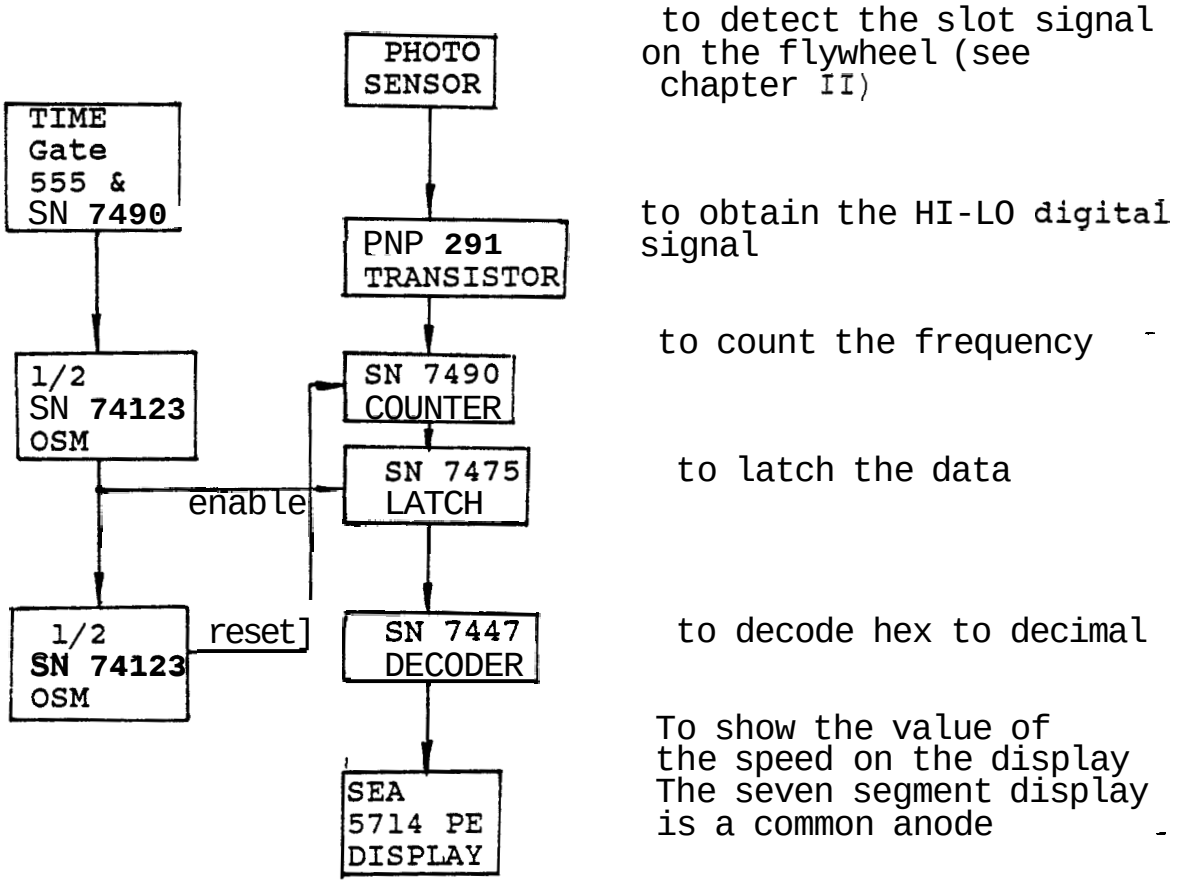

Fig. 28. Signal Sequence of the Speed Display

(SN 7447) and seven segment displays (common anode). The flow chart of the signal sequence is shown in the Fig. 28. and the circuit is shown in Fig. 29.

6.3 Time Gate

Because the engine speed is unstable, the sample hold time of the speed meter should be chosen appropriately, so that the display is not changed so rapidly that the value is difficult to check, and so long that it could lose accuracy. If we consider the sample hold time is 6 sec, then the engine speed (in rpm) will be 10 times the value shown on the display, because 10 times 6 secs is one minute. From the timing chart of the time gate (Fig. 31.) when the 6 sec time gate is in falling edge, the pulse counter needs a pulse to enable the latch SN7475s to release its content to the decoders, and then issue another pulse to reset all counters to zero for the next cycle; therefore, an SN74123 which has a dual one shot multivibrator is used to produce these two triggering pulses. Now a problem arises in obtaining the 6 sec time gate.

consider an astable 555 timer, which is often called a free-running multivibrator because it produces a continuous train of rectangular pulses.[7] According to the astable operation circuit of the 555 timer (Fig. 30.), it needs a very large resistor Rb 4.32 Mohm (when Ra is 500

7. Albert P. Malvino Electronical Principles, third edition, (New York: McGraw-Hill Inc., 1984) pp.630 - 650.

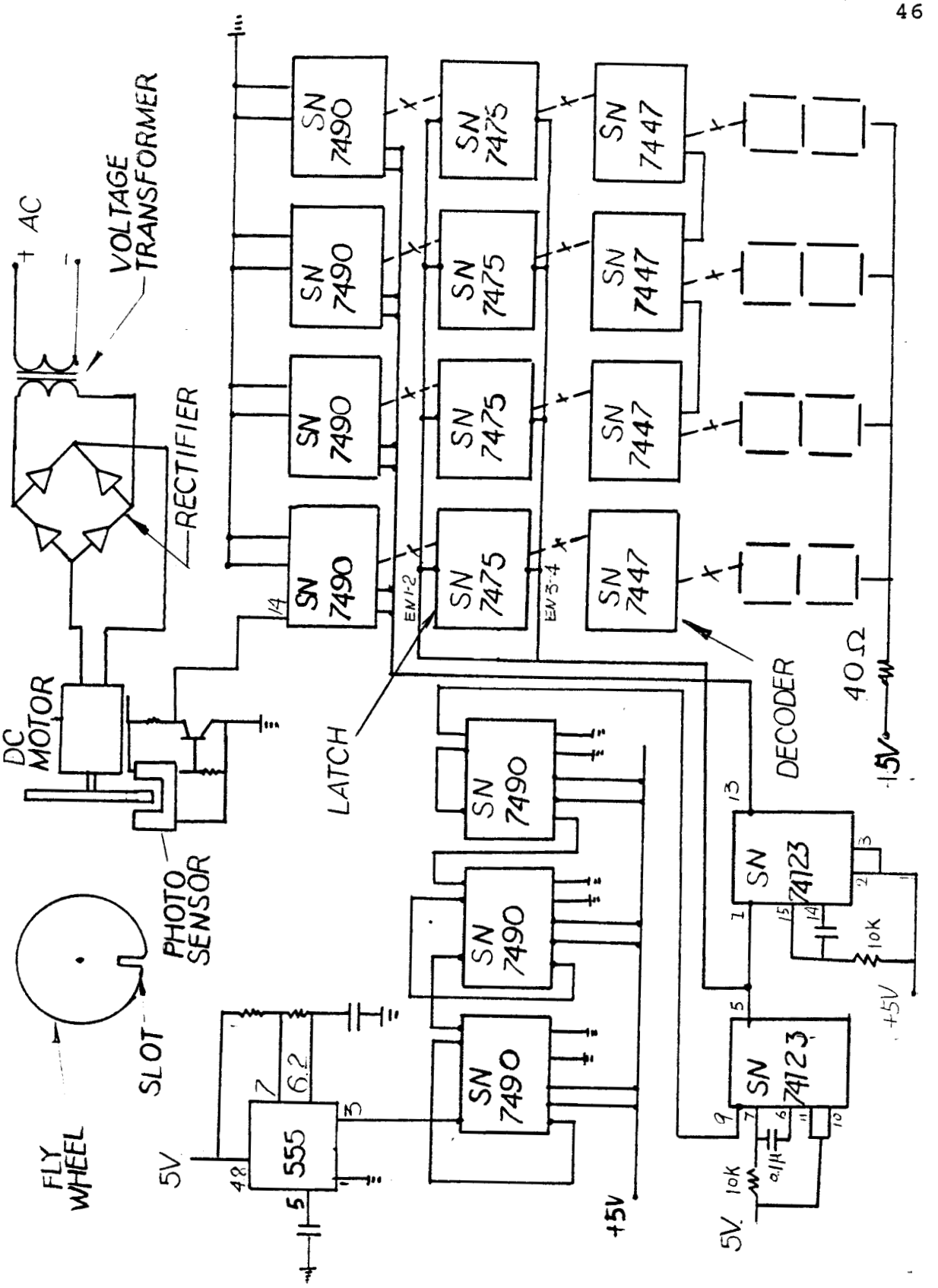

Fig. 29. The Circuit of Digital Speed Display

and C is 1 uF, EQ. 24.) to obtain a 6 sec time gate. It's period T issued by the timer is

$$T = \frac{1.44}{(Ra + 2Rb)C} \qquad \text{EQ. 24.}$$

and the duty cycle is

$$D = (W/T) \times 100\ \% = \frac{Ra + Rb}{Ra + 2Rb} \times 100\%$$

If Ra is much smaller than Rb, the duty cycle approaches 50 percent.

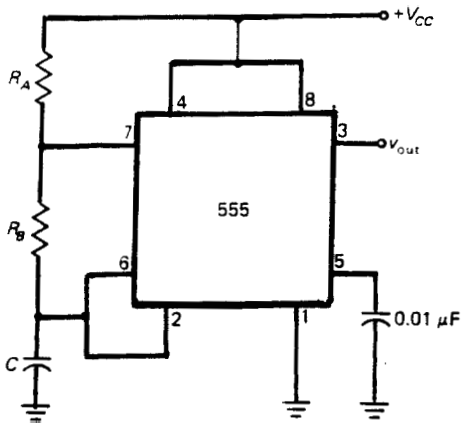

Fig. 30. Astable timer circuit

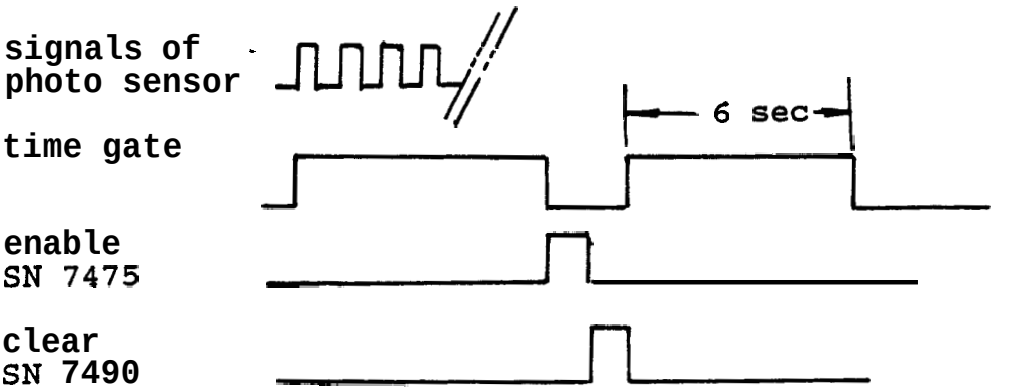

Fig. 31. Timing Chart of the time Gate

If a pulse counter, which can count from 1 to 1000 is connected with the timer to count the smaller pulse issued by the timer, then the time gate is 1000 X pulse width of the timer. On the other hand, after 1000 pulses, which period is 6m sec, have gone into the counters, then a falling edge of the 6 sec time gate will appear on the third counter (SN7490). Note the pulse counter consists of three SN 7490s, which can count from 1 to 10 and which are connected in series, so that it can count from 1 to 1000 to obtain the 6 sec time gate. Then the falling edge of the 6 sec time gate will trigger the first OSM to issue a square wave to enable the latch SN 7475, and at the same time, the first OSM will trigger the second OSM to clear all contents of counters to zero. A complete circuit of the digital speed display is shown in Fig. 29.

CHAPTER VII

SIMULATION OF ADVANCE IGNITION SYSTEM

7.1 Traditional Advance Ignition System

The components of the conventional ignition system, Fig. **32**. include an ignition coil, an ignition switch, a resistor, a distributor which houses the breaker points, a cam, a condensor, a rotor, spark plugs and advance mechanisms (see Appendix A). In this conventional system, it is just adequate for low and medium speeds and loads, but when the speed is high, its drawbacks become apparent as following:

1. Poor performace at high engine speeds because of current limitations and inertia (point bounce) caused by the mechanical breaker points.

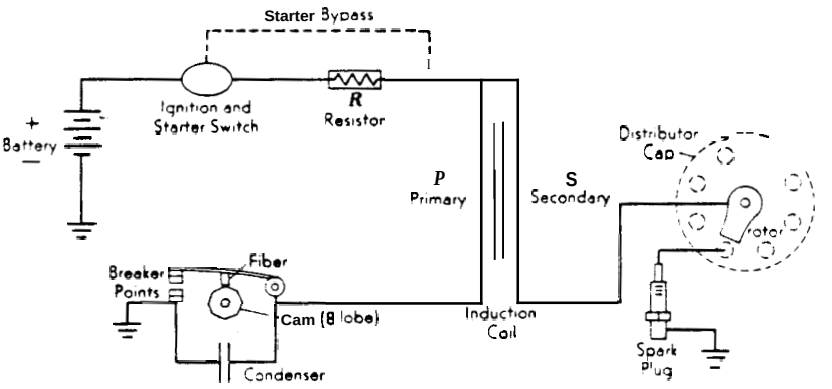

Fig. **32**. The Conventional Ignition System
(From Edward F. Obert, P. 532)

2. Relatively a short life of the breaker points because of high current flow at low speeds.

3. Relatively short life of the spark plugs because of the high energy discharge at low speeds.

4. Poor starting because of slow -opening of breaker points at cranking speeds.

Most of these disadvantages are caused by the inefficient method of interrupting the primary circuit - the mechanical breaker points.

In addition, since the combustion of fuel does not take place at the same time as the spark firing, in order to obtain the best power with the lowest fuel consumption, the spark should occur before the piston reaches the top dead point in the compression stroke. Most automobile engines, in order to make the ignition advance, are equipped with two mechanisms (1). the vacuum advance (2). the centrifugal advance.

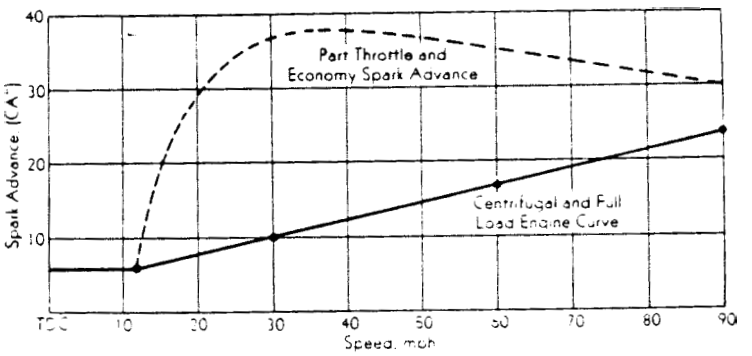

Fig. 33. Perfomance of Advance Mechanisms
(From Edward. F. Obert, p. 535)

advance (see Appendix C) and these effects of advance mechanisms' performance are shown in Fig. 33.

7.2 Basic Concepts

Because the electronic industry is making great progress, many mechanical parts can be replaced by some electronic parts. The advance mechanism and breaker point are replaced by a microcomputer, a photo sensor, and a few transistors. Perhaps, if this new system (Fig. 34a.) is successfully installed in the automobile, it can be integrated as a special microprocessor, which can be produced for sale in a large quantities. The timing chart of the new ignition system is shown in Fig. 34b. and the procedure is shown as follows:

STEP 1. To detect the position of the piston.

STEP 2. To count the engine speed.

STEP 3. To fetch the time bytes of the map in the storage

STEP 4. To fire the spark plug.

Note that a four stroke engine needs two revolutions = 720 to finish one cycle (see APPENDIX C).

7.3 STEP 1: To Detect the Position of Piston

The interface circuit is shown in Fig. 34. Owing to the non-regular waveform from the transistor, it is necessary to add a one shot multivibrator (called OSM ,SN 74123), which after being triggered can release a square wave to control the pulse width. This pulse width is

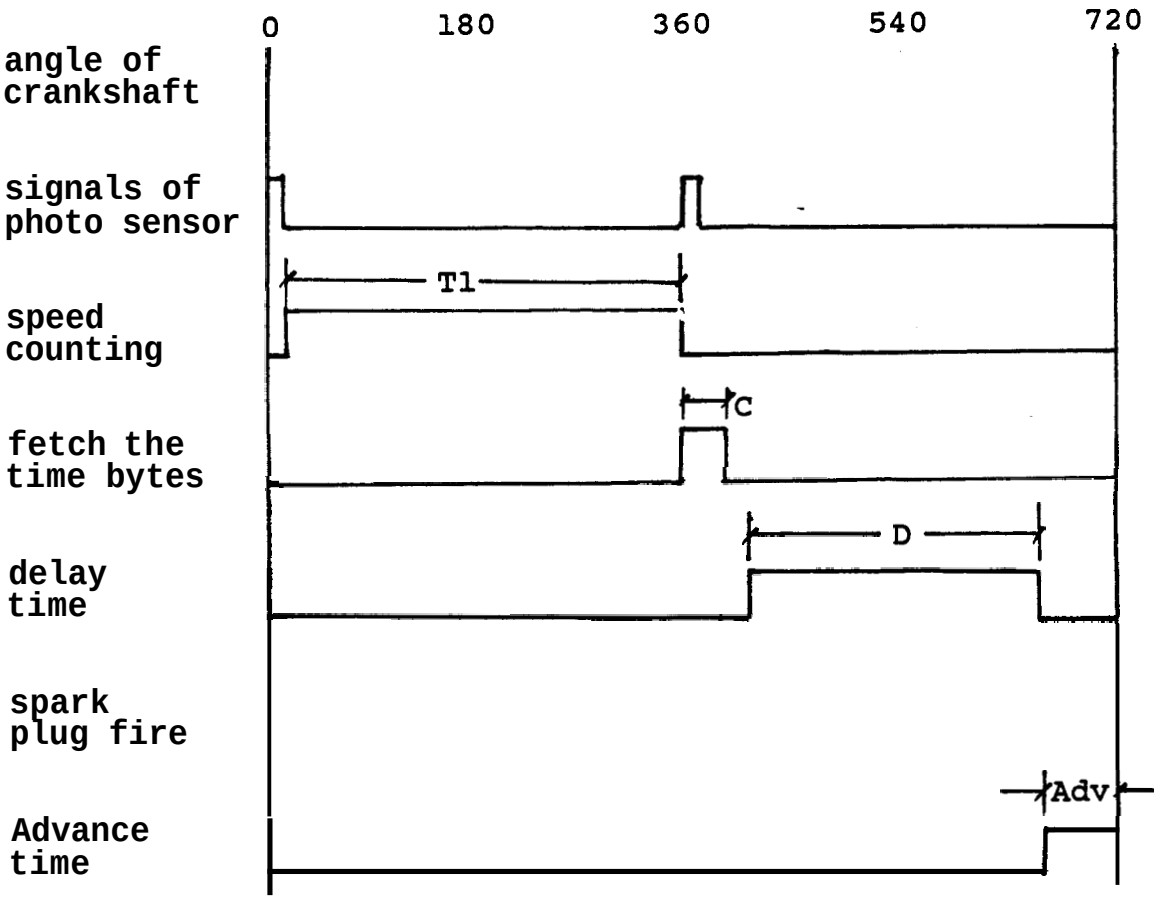

Fig. 34b. Timing Chart of the ignition system

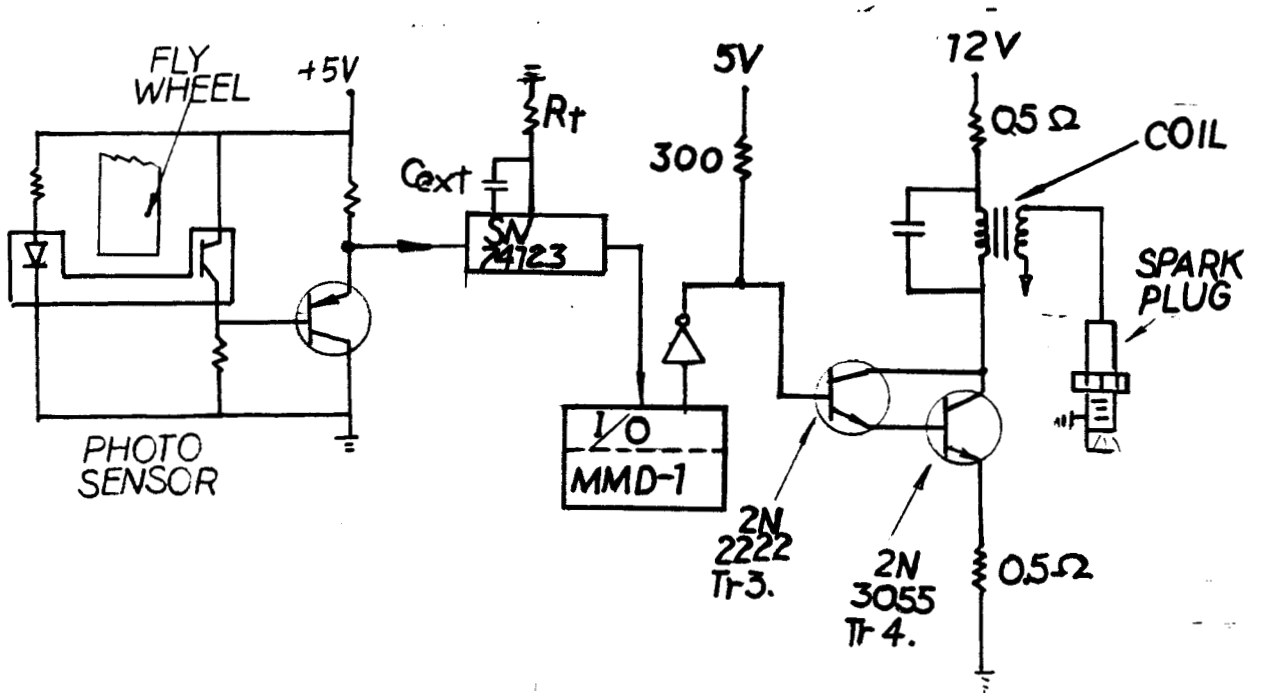

Fig. 34a. New Ignition System

very important for counting speed. This will be explained in the next section. Note that the pulse width of OSM is primarily a function of the external capacitor Cext and resistor Rt (Fig. 34.). For Cext > 1000 pF the output pulse width (tw) is defined as:

$$tw = K\ Rt\ Cext\ (\ 1 + 0.7/Rext\ ), \qquad \text{EQ. 25.}^{8}$$

where K is 0.32 for SN 74123, 0.37 for SN 74L123

Rt is in kilo-ohm

Cext is in pF

and, tw is in nanoseconds.

From the circuit, when the slot of the plate rotated by the DC motor passes the photo sensor, the rising edge of output voltage of Tr2 will trigger the one shot multivibrator to issue a squar wave to inform the computer that the slot has just reached the photo sensor. In the same way if the photo sensor is installed to the fly wheel of the engine, it is equivalent to notifying the micrcomputer that the piston of the engine is at the top dead point.

7.4 STEP 2: To Count the Engine Speed

In the microcomputer each command has individual operating cycles, which can be checked from the manual of microcomputer. According to the oscillator frequency of

8. Application Data of Integrated Circuits, manual of Texas Instruments Inc. P6-81

the computer, it is easy to count the execution time of the computer program. For example, there is a 750KHz oscillator in the MMD-1 microcomputer, so that one cycle time of pulse is 1/750k = 1.33 usec. Note u = 10 . If the subprogram 1 is executed from the address 003 000 to 003 020, the time of execution will be:

10+7+10+10+7+5+5+10 = 64 cycles

Thus, 64 cycle x 1.33 usec/cycle = 85.12 usec = time A Considering subprogram 1, whose flow chart is as shown in Fig. 35., the pulse width of the one shot multivibrator must be less then execution time A, which is between two " IN " commands (from 003 000 to 003 020) and greater than the execution time B, which is the time of only one loop from 003 021 to 003 030.

Time B = (10+5+7+10) x 1.33 = 42.56 usec

If the pulse issued by the one shot multivibrator is larger than time A, it will be detected twice consecutively by two "IN" commands of the computer program, and the speed will be zero. If the pulse width of the one shot multivibrator (OSM) is too narrow to be detected in the counter loop (from 003 021 to 003 030), it may be missed once and the speed will double. In order to make the pulse width of the one shot multivibrator have more tolerance, one block of dummy program (from 003 012 to 003 017) is inserted between two "IN" commands to make a dummy time, which can make time A longer. Note that in the dummy program the command MOV

B,B is nonsensical, due to no data change in the program.

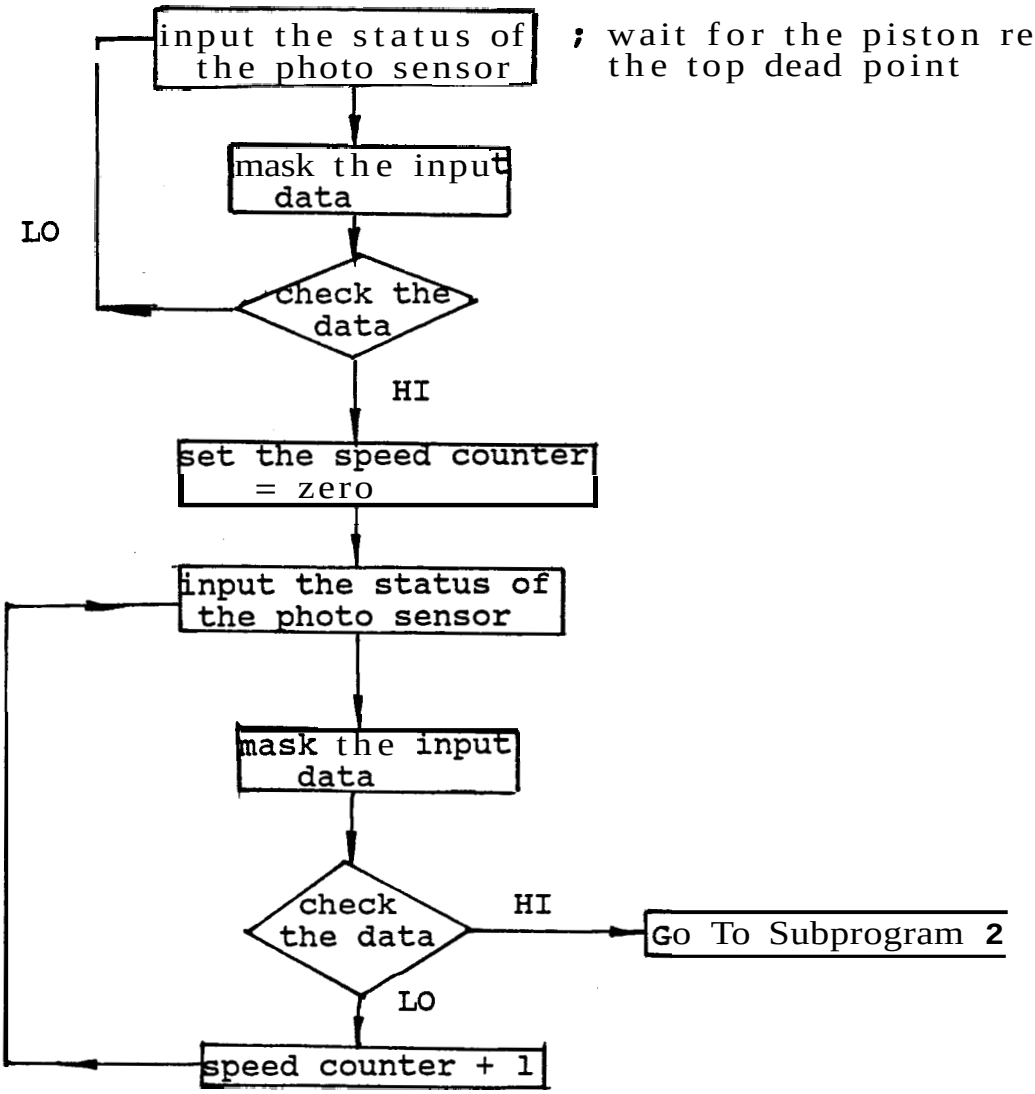

Fig. **35.** Flow Chart of the Speed Counter

ADDRESS	MNEU	OP CODE	CYCLE	REMARK
003 000	**IN**	333	10	
001	**003**	003		
002	**ANI**	346	7	
003	**200**	200		
004	**JNZ**	302	10	
005	**000**	000		time A
006	**000**	000		
007	**LXID**	021	10	
010	**000**	000		
011	**000**	000		
012	MVIC	016	7	

013	001	001		
014	MOV B,B	100	5	
015	DCR C	015	5	
016	JNZ	302	10	
017	012	012		
020	003	003		
021	IN	333	10	
022	003	003		
023	INXD	023	5	
024	ANI	346	7	time B
025	200	200		
026	JNZ	302	10	
027	021	021		
030	003	003		

Subprogram 1

In subprogram 1, the register pair (16 bits) D and E is set to be the speed counter in a loop (from 003 021 to 003 030), so that the content of the DE pair can be used to calculate the total computer cycle when running the program. If the execution time of one loop (from 003 021 to 003 030, which has 5+7+10+10 = 42 cycles) is set equal to B, then time B = 42 x 1.33 = 42.5 usec

If the content of the speed counter is

000 144 in octal = 1x8 + 4x8 + 4 = 100 in decimal,

then the execution time T1 between two HI output signals of photo sensor will be

T1 = a revolution period = content of speed counter x time B + time E, where E is the execution time from 003 000 to 003 016.

Thus T1 = (10+7+10+10+7+5+5+10) x 1.33 + (100 x 42.5)

= 4335.12 usec,

which means that in this period the engine has rotated one

revolution; therefore, the engine speed is

$$v = 60/4335.12 = 13840 \text{ rpm}$$

In general, if the content is N in decimal, the engine speed v (rpm) is

$$v = 60 \times 10E06 /(85.12 + N \times 42.56) \quad \text{EQ. 26.}$$

7.5 STEP 3: To Fetch the Data from the Map

From Fig. 33, each engine speed has a correlative advance angle, which can be transferred to the advance time as follows:

$$\text{Advance time (Adv)} = \text{Advance Angle} \times (T/360)$$
$$= \text{Advance Angle} /(60 \times v), \quad \text{EQ. 27.}$$

where the period of a revolution T = 60/v (sec/rev).
If the X axis (rpm axis) of Fig. 33., is divided in a sample division, then these sample data can be used to find its function value (advance angle) in the Y axis (advance angle axis). Furthermore, the advance angle can be transferred to the advance time (Adv, EQ. 27.). Thus, according to the Adv, the time bytes can be decided and stored in the computer as explained in following.

```
Begin:  003 000  IN    333
            001  003   003
              Subprogram  1        ;Speed counting (step 1)
        003 021  IN    333
            022  003   003
                        .
            026  JNZ   302
            027  021   021
            030  003   003

             Subprogram  2          ;To fetch the data of the
                                     time bytes (step 2)
```

```
          Subprogram   3          ;To execute the delay
                                    time (step 3)
       003 221  MVIA  076
           222  200   200
           223  OUT   323         ; Spark Fire (step 4)
           224  002   002
           225  JMP   303         ; time Adv start
           226  000   000         ; restart
           227  003   003
                 .
           240
               Data area         ; time bytes
           300
```

Program A Schematic Program of Advance Ignition System

According to the program A and Fig. 34b. the sum of the execution time from 003 031 to 003 223 and Adv is equal to the next revolution period T2 of the motor, i.e.,

period T2 = C + D + Adv = T1,

where C = execution time of fetching data (subprog 2)

D = delay time.

Adv = advance time

thus, D = T2 - C - Adv. EQ. 28.

Supposed the engine speed is smooth, the previous revolution period T1 is equal to the present revolution period T2; therefore, T2, C, and Adv all are knowns. Note that time C is just the execution time of fetching the time bytes from the map. It is very fast for the computer operation; therefore, in this cycle it still has a lot time (time D or called delay time) before firing the spark plug in this four stroke engine (Fig. 34b.). From EQ. 28. D is a dependent variable which is the function value of speed (rpm), but in the computer the format of the motor speed

is the content of DE pair (speed counter); therefore, the content of DE pair is an independent variable in this program. According to EQ.26. 27. and 28., there are predetermined sample data shown in Table 5, which lists the relationship between the content of the speed counter and time D (delay time). Furthermore, time D can be programmed to become a time byte, stored in the memory map. Note that the memory capacity of MMD-1 is small, so the sample division of the contents of the speed counter is set to 2 and the range of sample data is from 146 (850 rpm) to 22 (4800rpm) (see Table 5., the column of speed counter). According to Fig. 33. if the speed is out of this range (850 - 4600rpm), the advance angle is constant, so that it is easy to be realized by hardware or software, information which is not included in this thesis.

In the 8080, it is easy to fetch the time bytes in the map (Fig. 36.). First, store the predetermined data (time bytes) in the storage area (from 003 240 to 003 300) before running the program. Second, use the command of LXIH, address to load the start address of memory, which store the contents of the minimum speed (850 rpm). Third, set the reference speed vr equal to the minimum speed. Fourth, design a loop to compare continuously the reference speed with the content of the speed counter. If the contents of the speed counter are not greater than the contents of reference speed, then the memory address plus one and the contents of the reference speed minus 2 and go

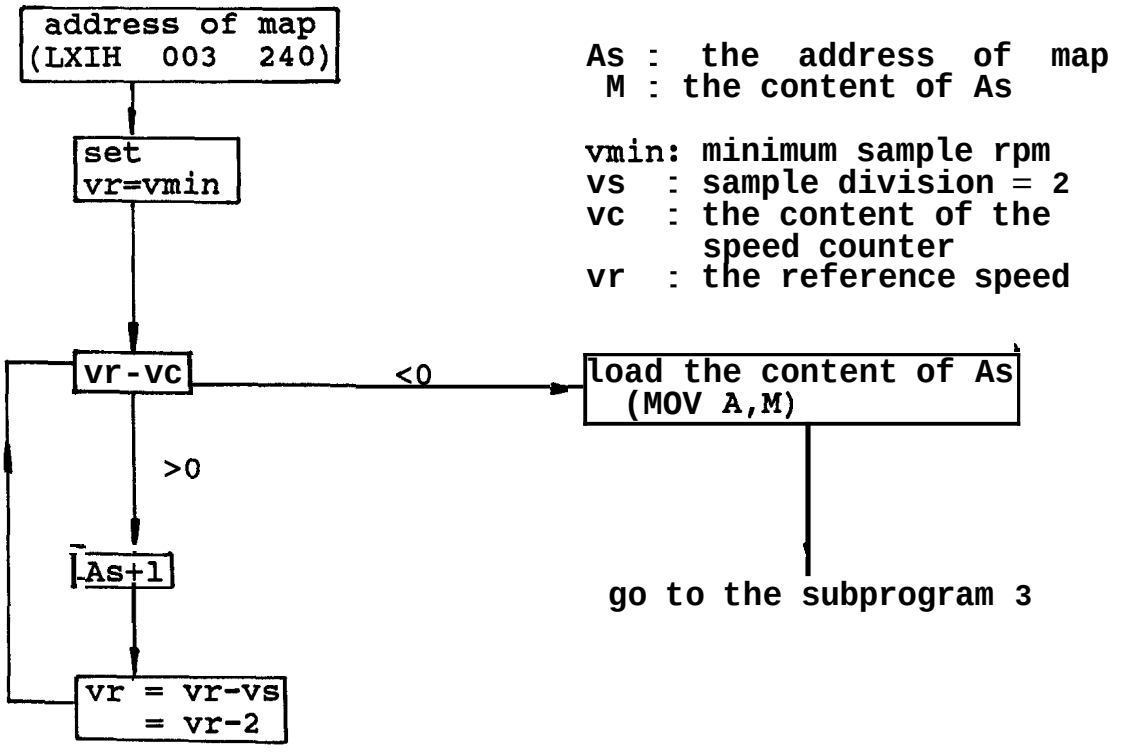

FIg. 36. Flow Chart of Fetching Data

to the next loop to compare again. Finally, use the command of MOV A,M to load the content (time bytes) of memory address into the accumulator (see subprogram 2, from 003 062 to 003 214 in the main program, Appendix A), and its flow chart is shown in following (Fig. 36.).

From the table 5, the delay time D is from 100ms to 0.1ms, so the subprogram 3 must satisfy with each condition. But the subprog 3 does nothing,just going round and round in a loop(s) of instructions until the program tells it to get out of the loops at a predetermined (programmed by subprog 2) time and to go back to the main program. There is a time delay subroutine built in MMD-1 (CALL 277,000), whose delay time base is 10ms, and dependent on the content of B risters. For example, if the content of B

is 001, then it has 10ms time delay. Subprog 3 consists of two blocks. In the first block the minimum delay time is 10ms, and 35 usec is in the second block. On the other hand, the content of B can delay one time base (=10ms), and the content of DE pair can delay from 35 usec to 10ms (time base = 35 usec). (Note now the content of DE pair has been changed from the content storing the speed to the content storing time bytes). As a result, the contents of B, and DE pair can be predetermined from Table 5, which is calculated by hand according to EQ.26. 27., and 28. These contents are called time bytes in the following discussion. In addition, the content of DE pair is stored by two consective addresses in the datd area (M) for 8080 (or 8 bit processor), or one address for 8088 or 8086 (or 16 bit processor). In the computer controlled system it is easy to change the contents of time bytes to obtain best ignition time with doing some experiments, i.e., it is programmable for this system.

```
003 100  006   MVIB
    101  B1     B1
    102  315   CALL  ;    the first block
    103  277    277
    104  000    000

    105  021   LXID
    106   E1     El
    107   D1     D1
    110  033   DCX D
    111  172   MOV A,D ;   the second block
    112  263   ORA, E
    113  302   JNZ
    114  105   105
    115  003   003
```

subprogram 3

The main program A for the advance ignition is shown in Appendix A.

7.6 Step 4: To Fire the Spark Plug

In general, it needs an average current of 5A in the primary winding of the coil to obtain a good spark, but the output current of the computer is just around 5ma. How to use the small current of the computer to drive the large current will be the subject of this section. Usually, there are three solutions to the drive current problems by the regular switching transistor : (1) by more drive current (2) by more stage of amplification and (3) by higher transistor gains. The Darlington circuit combines the latter two advantages, and it is composed of a 2N2222 transistor and an HEC 2N3055 power transistor. The 2N2222 (the first stage) is a high speed, medium power transistor to obtain enough output current to drive the second stage, and the HEC 2N3055 (the second stage) is a 15 Amp , 115 Watts power transistor to bear the large load current in the primary winding. In this circuit, the average load current is so large 4.7 Amp that it needs a heat sink to dissipate the heat. From Fig. 34., If the output of computer is HI, the primary circuit will on (Tr3, Tr4 on), and the coil will store energy. When the output is changed to LO, the primary circuit will off (Tr3, Tr4 off), and the magnetic field will collapse with consequent current flow in the secondary winding. The voltage rises at the spark plug

until it reaches a value that can break down the spark gap, like the breaker point open in the conventional ignition system (Fig. 32.), and the spark occurs.

content of DE	rpm	Adv Angle	Adv usec	time C (usec)	time D (usec)	time bytes
150	846	6	1181	294	69446	376
146	880	7	1545	419	67560	330
144	880	8	1700	351	66014	171
142	898	9	1670	515	64630	204
140	917	10	1810	563	63057	127
136	936	11.5	2047	610	61445	051
134	957	13	2264	658	60941	033
132	978	14	2386	706	60643	022
130	1000	15	2500	754	56746	200
126	1023	16	2600	802	55249	226
124	1047	17.5	2786	850	53670	151
122	1073	18.5	2873	898	52147	075
120	1100	20	3030	946	50569	020
116	1128	21	3102	993	49096	377
114	1158	22	3166	1041	47606	331
112	1189	23	3225	1089	46148	257
110	1222	24	3273	1137	44690	111
106	1257	25	3314	1185	43233	114
104	1294	26.5	3413	1233	41721	031
102	1333	28	3500	1280	40231	007
100	1374	30	3639	1328	38701	370
76	1419	31.5	3700	1377	37207	315
74	1466	33	3752	1425	35750	244
72	1517	35	3845	1468	34238	171
70	1571	35.5	3766	1516	32910	123
66	1629	36	3683	1564	31585	055
64	1691	36.5	3597	1611	30274	001
62	1759	37	3505	1660	28945	376
60	1832	36.7	3340	1707	27644	332
56	1611	36.3	3166	1755	26476	271
54	1998	35.9	2994	1804	25233	225
52	2093	35.5	2820	1851	23989	105
50	2202	35	2649	1899	22699	115
46	2313	34.62	2495	1947	21498	052
44	2441	34.17	2333	1995	20252	007
42	2591	33.66	2165	2042	18950	377
40	2746	33.12	2010	2092	17750	335
36	2929	32.5	1849	2138	16496	271
34	3137	32	1700	2187	15240	225
32	3377	31.4	1549	2234	13984	116
30	3658	30.7	1398	2282	12722	111
26	3989	30	1253	2330	11458	051
24	4387	29	1101	2378	10197	006
22	4871	28	958	375	10984	034

Table 5. Data of Advance Ignition System

CHAPTER VIII

SIMULATION OF DIGITAL FUEL INJECTION

8.1 Introduction

Recently, many countries have established regulations limiting the composition of exhaust gas to prevent the air pollution. According to the investigation, the crankcase, fuel tank, and carburetor contribute just 40% of the total hydrocarbon pollution produced; therefore, most of the pollution problem is made by exhaust gas. Responding to the pressure from the government, the automakers have improved some pollution problems by modifing or adding new devices, such as computer control and feedback control, From 1960 to 1973, they reduced unburned hydrocarbon emissions by 85% and carbon monoxide by 70%.[9] How to use the microcomputer with the feedback signal of the oxygen sensor to control appropriate injected fuel will be discussed in this chapter and the details of the oxygen sensor, which can detect whether the combustion of the engine is complete or not, is shown in Chapter IV. If the combustion is complete, there is much less air pollution.

8.2 Digital Fuel Injection by Close Loop Control

9. Tom Weathers,Jr. and Claud C. Hunter, Automotive Computers and Control System.,(Englewood Cliffs: Prentice-Hall,1984), pp30 - 44.

In general, there are three approaches to realizing the electronic fuel injection by the car maker:(1) the intake manifold pressure control, (2) the air-flow control, (3) the mechanism control,(see Appendix D, for examples). This system will use air flow control. The component of the system consists of a stepper motor, A/D conver, air flow meter and oxygen sensor (Fig. 38.). Due to the semiconductor strain gage in the air flow meter (see Chapter V) having a linear property of voltage-strain and the steps of the stepper motor being easily transferred to discrete data, both of them will play very important roles in this system. The stepper motor (48 step/cycle) will be used to transmit the gear-rack set, whose function is supposed to be the same as described in Appendix A (Bosch Fuel Injector), to meter the quantities of injected fuel The air flow meter is used to obtain the value of air flow mass. Because there is an 8 bit A/D converter to convert the analogue signal of the differential pressure gage to the digital signal, the air flow in the intake manifold will have 255 divisions between from closed to fully open of the throttle valve. Then transmit the data of the A/D converter to the microcomputer, that is to tell the computer how much air flow is drawn into the cylinder. By this data of the A/D converter the computer does some mathematical operation and checks the status of the oxygen sensor, so that the computer will output one signal to command the stepper motor to rotate needed steps, which is correlative to the quantities

of injected fuel.

Note that there are two stepper motors in this digital system, which will be discussed later. One is for the main fuel injection system (or called running mode), which can control 4 fuel injectors in each cylinder, and the other is for the auxiliary fuel injection system, or cold start mode, which just has one fuel injector for enriching the fuel mixture.

8.3 Operation of Stepper Motor and A/D Converter

8.3.1 Stepper Motor

The stepper motor is a device used to convert electrical pulses into discrete mechanical rotational movements.

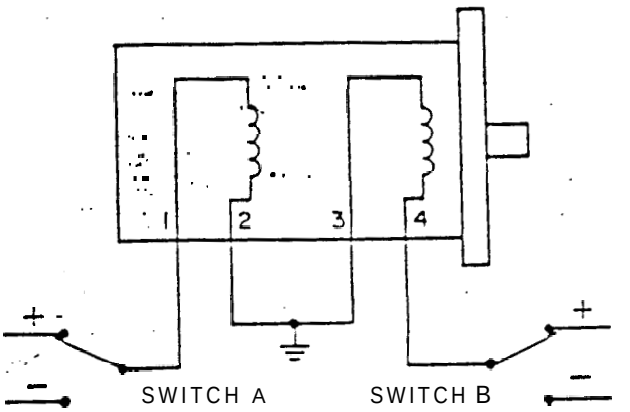

(a)

STEP	COIL A	COIL B
1	+	+
2	+	−
3	−	−
4	−	+
1	+	+

CW ROTATION

CCW ROTATION

(b)

Fig. 37. Schematic diagram of the stepper motor

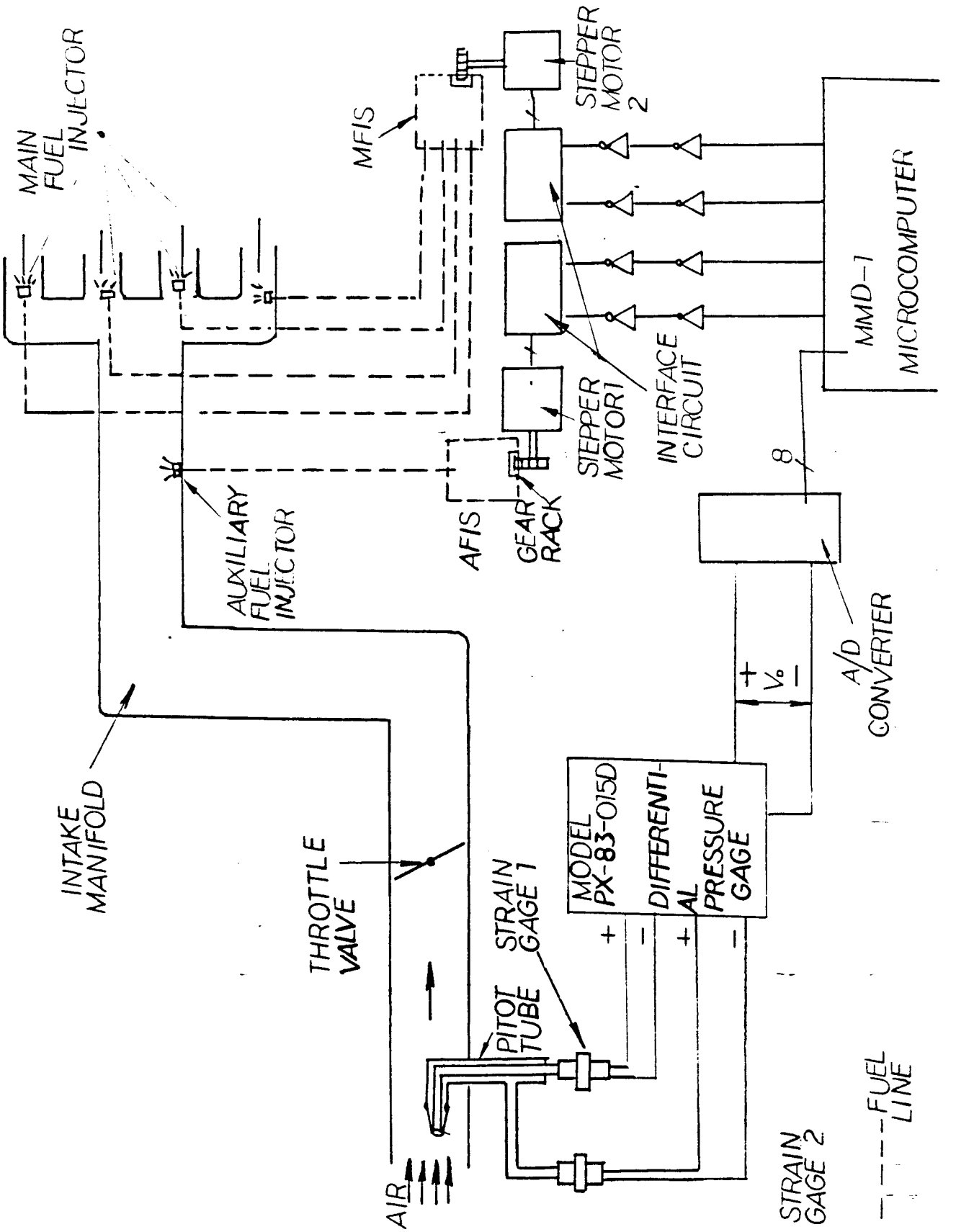

Fig. 38 The Digital Fuel Injection System

In a typical motor, electrical power is applied to two coils (Fig. 37a.). According to the interaction between the rotor and the stator (opposite poles attracting and same poles repelling), the directions of the stepper motor depend on the winding polarity change, and the steps of the stepper motor depend on how many pulses are input to the coils. For example, each 4-step switching sequence (Fig. 37b.), causes the rotor to move 1/4 of a pole pitch for a two phase motor; therefore, a 12 pole pairs per stator coil, and a permanent magnet rotor would move 48 steps per rovolution or 7.5 per step.

The mechanical requirements of the stepper motor installed in the automobile are as following:

1. the shaft torque of the stepper motor is large enough to transmit the gear-rack set.
2. It is small, accurate, and can stand heavy vibration.
3. one step can meter one unit of specified fuel, which depends on the mechanical design.

These requirements are not discussed here, because they are the responsibility of the mechanical engineer. It is only necessary to assume that one step of the stepper motor can accurately meter one unit of fuel as desired.

From Fig. 38., two stepper motors with an interface circuit of the PC board (made by N.A.P.C. Company) between the power supply of the motor and the microcomputer, are used. The only requirement is to use two SN 7402s to amplify the output current of the microcomputer to drive

the interface circuit. There are two control signals into the PC board. One is to decide the direction of the stepper motor, and the other is to switch the polarity. The program of controlling stepper motor is as following:

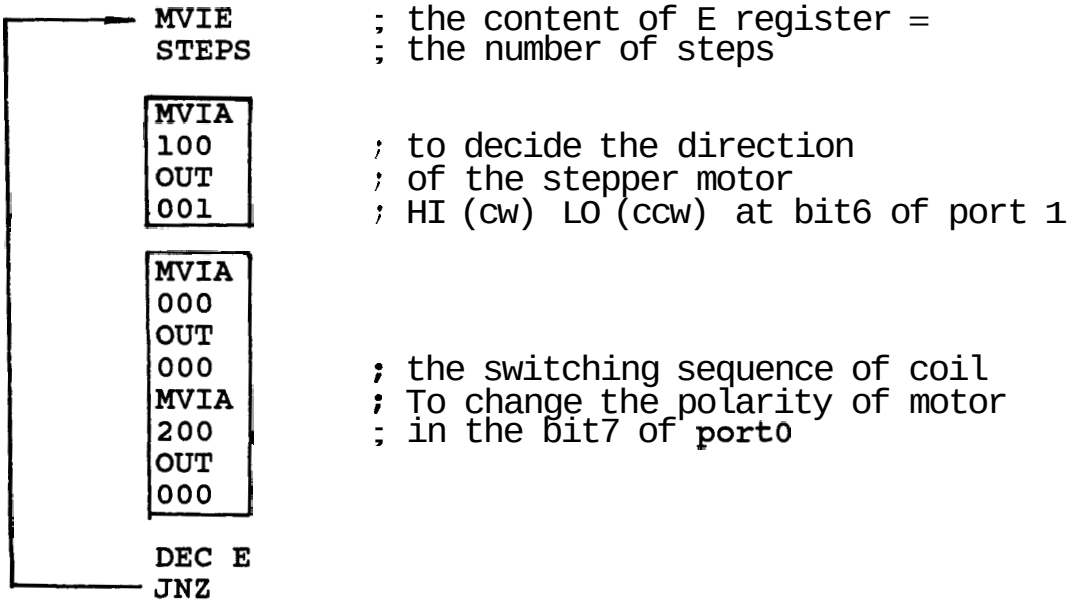

8.3.2 A/D converter

The LR-36 Analog to Digital Converter (see Appendix B) will accurately digitize signals over a + 25 volt range with a AD7570 monolithic CMOS chip, a comparator, and a voltage reference (10V) circuit. The AD7570 is a monolithic CMOS A/D converter which uses the successive approximations technique to provide up to 8 or 10 bits of digital data in a serial or parallel format. To operate the A/D converter, it needs 5 input control signals as following:

1. Convert Start(STRT): to start the conversing procedure.

2. High Byte Enable(HBEN): for the 10 bits conversion, when it is high, digital data (only bit9 and bit8) from the latches appears on the data lines.
3. Low Byte Enable(LBEN): Same as HBEN, but controls bits 0 through 7.
4. Busy Enable(BSEN): To ask the AD5750, whether the conversion has finish or not.
5. Short Cycle 8-Bits(SC8): With a logic 0 input, the conversion stops after 8 bits.

The interaction circuit of the AD conversion system with MMD-1 is shown in Fig. 39., and according to the 5 input control signals the program of controlling LR-36 is as follows:

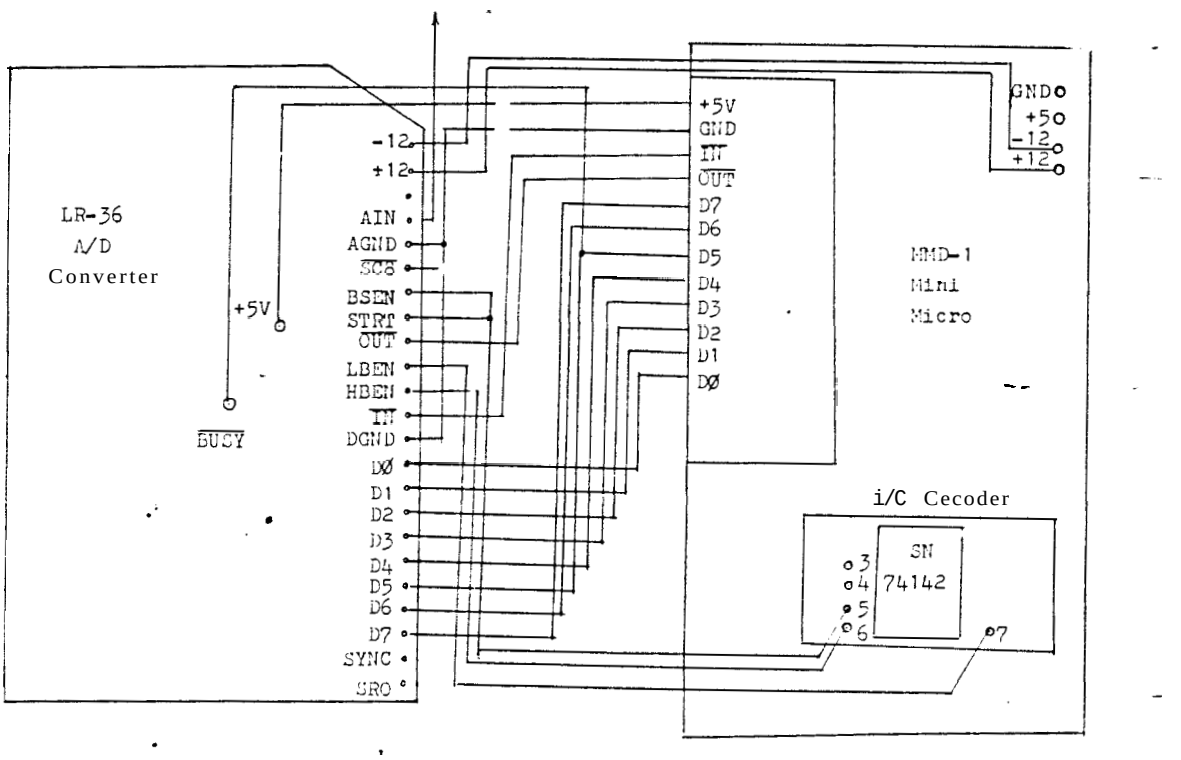

Fig. 39. Interaction Circuit of A/D converter with MMD-1

```
OUT   ; start A/D conversion
005
IN    ; ckeck the conversion status
005
ANI   ; mask the data of BUSY
00100000  at bit 5 of port 5
JZ    ; If the conversion is not complete,
002   ; chech again.
003
IN    ; If complete, read the data bits from port 4.
004
```

The program for controling A/D converter

Note the breakdown voltage of zerner diode IN961 is 10 V, which is set as the maxium reference voltage (see appendix B), so that the sample division of A/D converter is 10/255 = 0.039V. (see table 6)

8.4 Fuel Metering

The A/F ratio requirement in the engine is not constant as discussed in Appendix C.

where $A/F = \frac{\text{The air mass}}{\text{The fuel mass}}$

In general, there are three A/F conditions, which are dependent on the engine speed and load (Fig. 40.):

1. Idling : the mixture must be enriched.
2. Cruising: the mixture is constant and lean. --
3. High power: The mixture must be enriched;

therefore, the system needs one extra fuel injector to enrich the mixture as some car makers do, using a cold start valve (see Appendix D). For some computer control, besides the information of air mass from the air flow meter, the signals of the engine speed and cooling water temperature can be set at a point to adjust the A/F

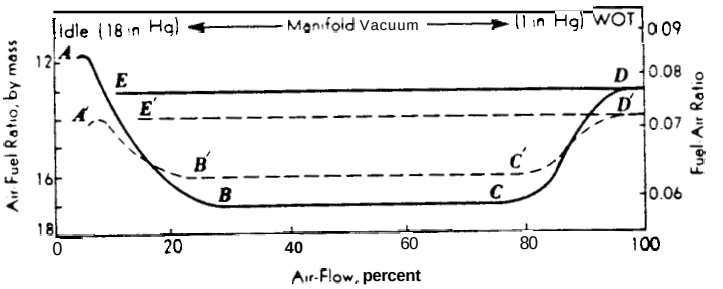

Fig. 40. Relation Between A/F and the speed

ratio as the following:

1. A temperature switch: to be set at "on," when the cooling water temperature is below 80 F, which means that the engine needs a richer mixture at cold start.

2. A throttle position switch : When the throttle is fully opened, a lever will hit the switch to tell the computer that the engine now is fully loaded. On the other hand, if the switch is on, it represents the high power condition in the engine.

3. When either one of the above switches is on, it makes the auxiliary fuel injection system work.

In order to satisfy the different A/F ratio, there are two fuel injection systems (Fig. 38.) in this project. One is the running mode (or cruising speed system) for constant A/F ratio in the cruising speed, and the other is the cold start mode (or enriching system) for the idling and full load speed. In the cruising system, just the main fuel injectors, which include 4 separate fuel injector installed in the front of the intake valve of each cylinder, is used to meter fuel. The flow chart of the

cruising speed system is shown in Fig 41. Note, if the engine speed is increased, the stepper motor will be clockwise to meter more fuel than the previous revolution. In other words, if the engine speed is kept constant, the position of the stepper motor will not be changed; therefore, it needs a register to store the absolute position of the stepper motor (NA), and another register to store the relative steps (NR), which is a relative previous position of the stepper motor.

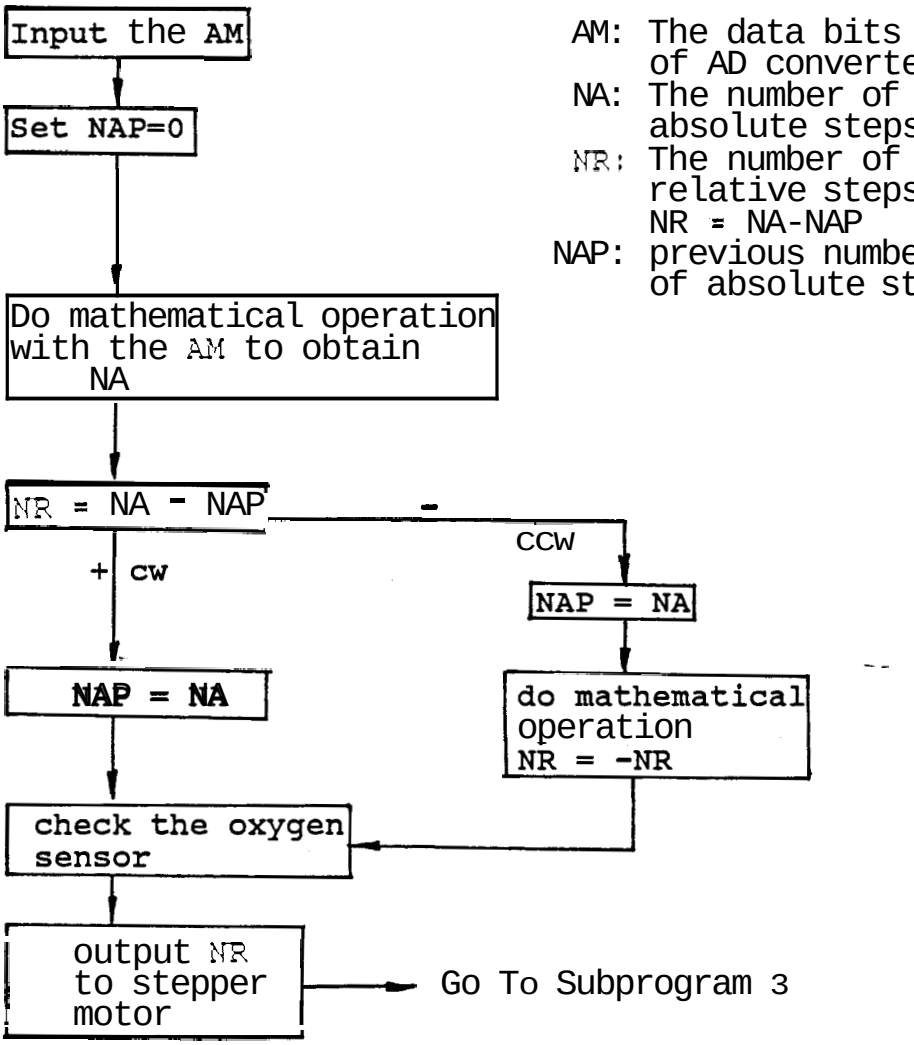

Fig. 41. Plow Chart of Running Mode

In the enriching system the A/F is not constant, so that it still needs a map based on the relationship between the speed engine and the quantities of fuel needed to enrich it. As a result, it needs a memory byte to store the quanties of enriched fuel, which is injected by the auxiliary fuel injector. This memory byte is called fuel byte, as the time bytes are called in the advance ignition (Chapter VII). If we combine the advance ignition and the digital fuel injection system, the flow chart is as shown in Fig. 42..

If the A/F ratio is constant in the cruising system, it is easy to design the program, which does not need a fuel byte in the data area. According to the data of the A/D converter, then do mathematical operations to obtain how many steps of stepper motor are needed to rotate. We already have the accurate metering devices of the stepper motor, whose data is as shown in Table 6. and its main program B for the running mode system is shown in Appendix A.

8.5 Timing of Fuel Injection

The fuel injection should occur in the intake stroke of the engine; the advance ignition is in the end of the compression stroke and counting the engine speed is in the power and exhaust strokes. The timing chart of the fuel injection is as shown in Fig. 43. In general, the fuel injection timing will rely on whatever kind of fuel is

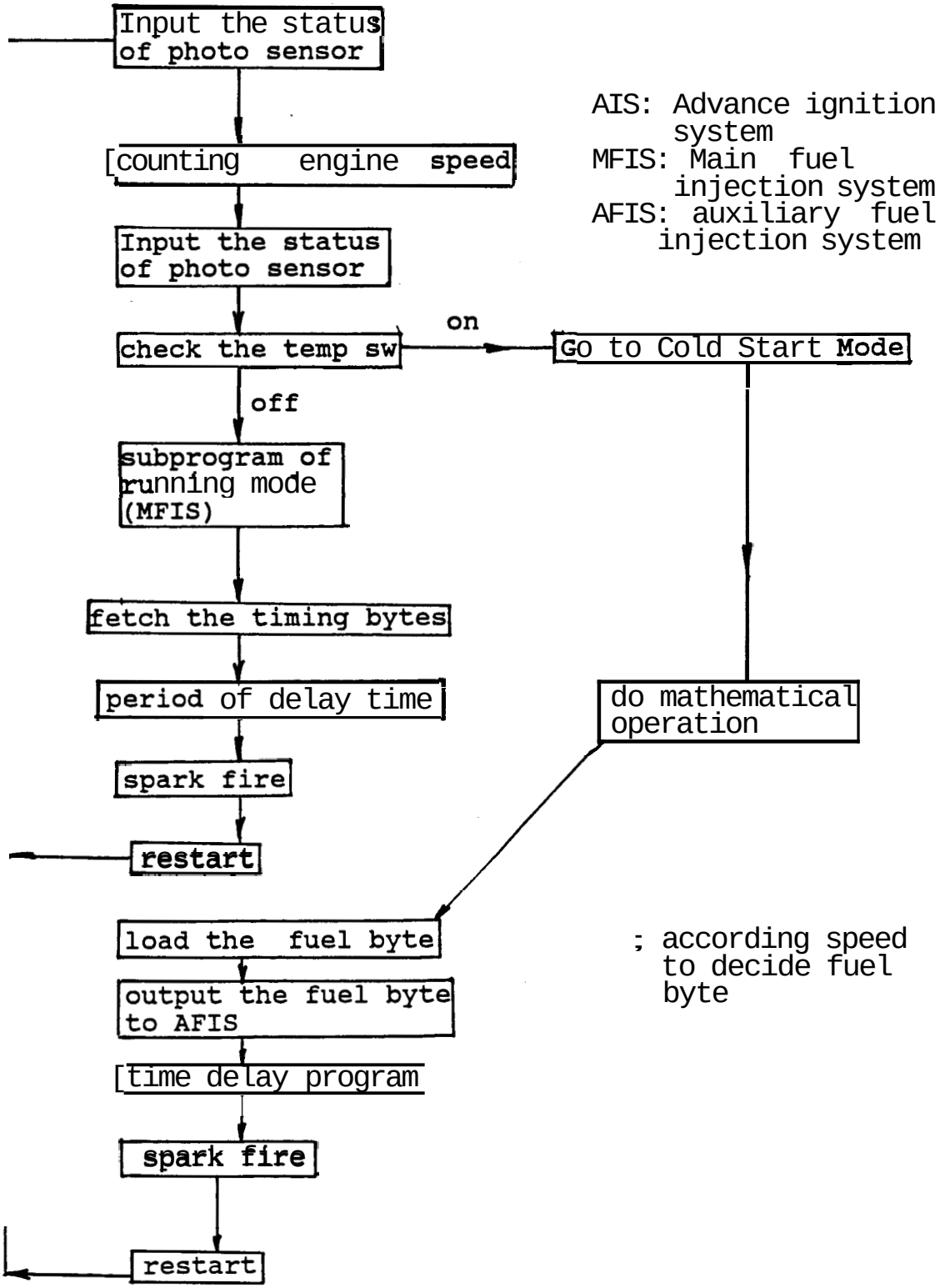

Fig. 42. Flow Chart of Combination System

used because each kind of fuel has different chemical properties. For the computer, the fuel injection timing is easy to control by setting the command of the fuel injection at the different position of the main program, or by setting a dummy timing program to control this problem as discussed in chapter VII.

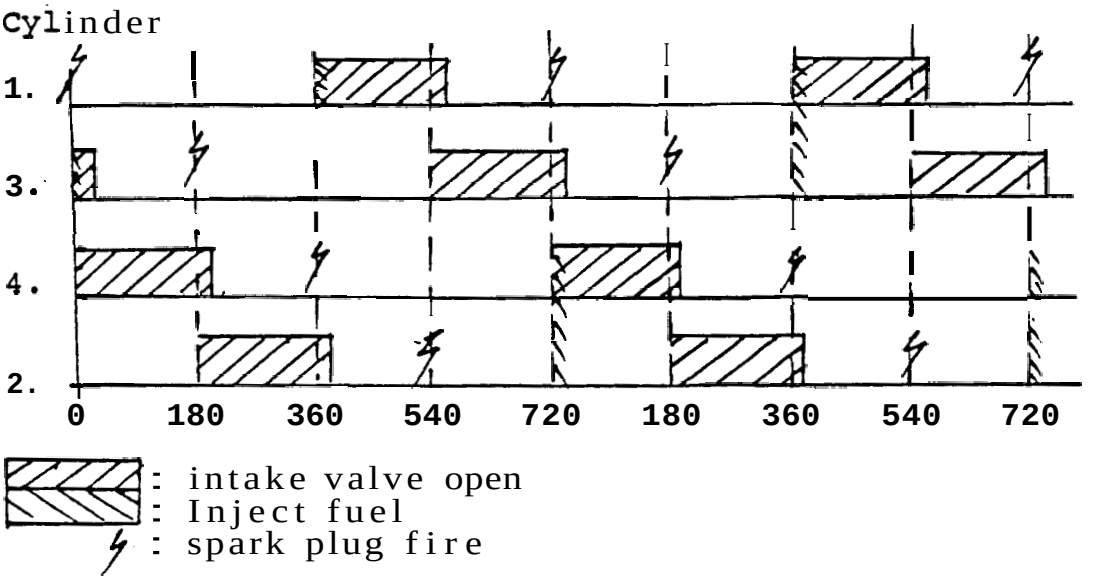

Fig. 43. Timing Chart of Fuel Injection

Speed (rpm)	ṁ (lb/sec)	Voltage V	Data Bits of A/D Converter
600	0.02352	0.0547	00 000 001
700	0.02744	0.0743	00 000 001
800	0.03136	0.0972	00 000 010
900	0.03528	0.1231	00 000 011
1100	0.04312	0.1838	00 000 100
1200	0.04704	0.2181	00 000 101
1300	0.05096	0.2567	00 000 110
1400	0.05488	0.2978	00 000 111
1500	0.05880	0.3418	00 001 000
1600	0.06272	0.3889	00 001 001
1700	0.06664	0.4391	00 001 011
1800	0.07056	0.4923	00 001 100
1900	0.07448	0.5485	00 001 101
2000	0.07840	0.6077	00 001 111
2100	0.08232	0.6700	00 010 001
2200	0.08624	0.7354	00 010 010
2300	0.09016	0.8038	00 010 100
2400	0.09408	0.8752	00 010 110
2500	0.09800	0.9497	00 011 000
2600	0.10192	1.0271	00 011 010
2700	0.10584	1.1076	00 011 100
2800	0.10976	1.1922	00 011 110
2900	0.11368	1.2778	00 100 000
3000	0.11760	1.3675	00 100 010
3100	0.12152	1.4602	00 100 101
3200	0.12544	1.5559	00 100 111
3300	0.12936	1.6546	00 101 010
3400	0.13328	1.7565	00 101 100
3500	0.13720	1.8613	00 101 111
3600	0.14112	1.9692	00 110 010
3700	0.14504	2.0801	00 110 111
3800	0.14896	2.1941	00 111 000
3900	0.15288	2.3111	00 111 010
4000	0.15680	2.4311	00 111 101
4100	0.16072	2.5542	01 000 001
4200	0.16464	2.6803	01 000 100
4300	0.16856	2.8094	01 000 111
4400	0.17248	2.9416	01 001 011
4500	0.17640	3.0768	01 001 110
4600	0.18032	3.2151	01 010 001
4700	0.18424	3.3565	01 010 101
4800	0.18816	3.5000	01 011 001
5500	0.21560	4.6000	01 110 101
6000	0.23520	5.4712	10 000 011
6500	0.25400	6.4106	10 100 011
7000	0.27442	7.4489	10 111 110
7500	0.29456	8.5599	11 011 010
8000	0.31433	9.7223	11 110 101

Table 6 Data of Fuel Injection

CHAPTER IX

CONCLUSION

9.1 Sensor

In the future the sensor will play an important role because human beings always want everything to be easy and safe. On the other hand, more devices will be automated so that more sensors will be developed and installed on the devices to provide the information of environment to the controller. Furthermore, the controller can refer to the information to decide what is the next step of the execution. This project is one of the examples. Although there are four sensors in this simulated engine, it is obvious that the information available is not sufficient. For example, in Chapter VIII, we need (1) a temperature switch to tell the controller to switch from the cold start mode to the running mode, (2) a throttle valve position switch to tell the controller to enrich the mixture when the throttle valve is fully opened, and (3) a "knock" sensor, which can detect the abnormal vibrations (or abnormal detonations), to tell the controller to correct the quantities of injected fuel. Furthermore, more sensors are needed in the other systems, e.g. the security system, the transmission system, and the brake system, etc.

9.2 Microcomputer

Microcomputers will be as important as the engine in the automobile. The microcomputer MMD-1 has two drawbacks, which are dependent on the requirements of the engine's performance. One is not enough memory capacity to store the time bytes and fuel bytes. In the Chapter VII it needs four time bytes to control the advance ignition and in the Chapter VIII it needs two fuel bytes to control the quantities of injected fuel. Due to the small memory capacity of MMD-1 (8 bits Processor), the time bytes are reduced to two bytes by using the larger sample division. As a result, the system could lose accuracy. The other drawback is that the oscillator frequency (750 KHz) is too small. Note that in the SDK-86 (16 bits processor) there is a 4M Hz oscillator frequency. A faster frequency will have a smaller cycle time to make the smaller division of the sample time (or time base) as described in Chapter VII. Also, from table 5 (see Chapter VII) the higher speeds have lower uSPD (usec/deg). In comparing a 750kHz computer with a 4MHz one as follows, the result will show the high frequency computer has a more accurate answer. From subprogram 1, there are 64 cycles in this loop program which means that in the worst case there is a maximum error time base of 64 cycles time.

	cy time usec/cy	max time error	angle error
750kHz	1.33	85.12	0.56
4M Hz	0.25	16	0.105

Note: usec = 10^{-6}sec, cy: computer cycle
deg = degree error: for 64 cycle loop

Why? Because after the computer has finished the first IN command, the slot (on the fly wheel), reaches the photo sensor. The computer must wait until the next loop comes again to detect the signal. As a result, there is a 85.12 usec maximum time base error in the 750 kHz, and there is a 16 usec time base error in the 4 MHz. If you consider the motor speed at 1100 rpm, the motor will rotate 0.0066 degree in one usec, so that the angle error of 750 kHz will be 0.65 , and 0.105 error in the 4M Hz as shown in the above table. Thus to solve these drawbacks, three solutions are available (1) using a PROM to increase the memory space and (2) redesigning a special processor to decrease the computer load. The processor is designed in the automobile and it could be just a chip of integrated circuit including all functions of the automobile. (3) using other hardware to decrease the load of the computer. Recently, the computer industry has successfully developed 32 bit computers which have powerful memory capacity and faster frequency. These could increase the possibility of all-computer-control automobiles.

9.3 Summary

This thesis concentrates on the technical possibilities of using new sensors to make more economical fuel consumption and less air pollution in automobiles. Although it is not feasible to install them in an automobile for extensive experimentation and testing, it is feasible

to electrically simulate these tests in the laboratory. The simulation system can be modified easily to incorporate various designs and operating conditions. For example, if an automobile engine is tested in the laboratory and the advance angle of ignition at 2000 rpm needs to be adjusted, the test engineer just changes the contents of time bytes in the computer without resetting or replacing components and then tests it again. However, the most important idea of this thesis is to show that there is still great **potential** for improvement and that there are many possible ways to adapt the automobile to the requirements of the people and the demands of the society in the future. Furthermore, the electronic industry will be more important in the future. **As** I discussed before, more mechanisms will be replaced by the electronic parts which will be improved to stand the worst environments. In addition, it is necessary for mechanical engineers (or mechanics in garages) to learn more about electronic technology. Because more electronic devices like **"black boxes"** will be put into automobiles, before mechanical engineers redesign, or mechanics fix the automobile, they need to understand what the functions of electronic devices are.

APPENDIX A

Microcomputer Pr

PROGRAM OF ADVANCE IGNITION SYSTEM

Address	Mneu	Op Code	Comments
000	IN	333	; input the status of photo
001	003	003	sensor at bit7 of port 3.
002	ANI	346	; mask the data 10 000 000
003	200	200	
004	JNZ	302	; if bit7 LO, check again.
005	000	000	
006	003	003	
007	LXID	021	; set the content of speed
010	000	000	counter to zero.
011	000	000	
012	MVIC	016	; the content of C is to
013	001	001	; control the dummy time.
014	MOV B,B	100	; dummy command
015	DCR C	015	
016	JNZ	302	
017	012	012	
020	003	003	
021	IN	333	; input the status of photo
022	003	003	sensor.
023	INX D	023	; speed counter + 1.
024	ANI	346	; mask data.
025	200	200	
026	JNZ	302	; if bit7 LO, check again.
027	021	021	
030	003	003	
031	MVI C	016	; to obtain the sample data
032	004	004	from the speed counter.
033	MOV A,D	172	
034	ANI	346	
035	00001111	017	; HI byte of content of speed
036	RLC	007	counter is divided by 16.
037	DCR C	015	
040	JNZ	302	
041	036	036	
042	003	003	
043	MOV B,A	107	
044	MVI C	016	
045	004	004	
046	MOV A,E	173	; LO bytes of the content of
047	ANI	346	speed counter is divided by
050	11110000	360	16.
051	RRC	017	
052	DCR C	015	
053	JNZ	302	
054	051	051	
055	003	003	
056	ADD B	200	; the contents of the DE pair
			become 8 bits

```
057     OUT         323   ; the sample data of speed
060     000         000     shown on the port 1.
061     MOV D,A     127
062     CPI         376   ; compare with the minium
063     150         150     speed.
064     JM          372   ; if speed > 850 rpm jump
065     101         101     to 003 101.
066     003         003
067     LXIH        041   ; load the start address
070     240         240     of the map.
071     003         003
072     MOV A,M     176   ; load the time bytes of 850
073     OUT         323     rpm.
074     001         001
075     MOV E,A     137
076     JMP         303
077     133         133
100     003         003
101     CPI         376   ; compare with the greatest
102     016         016     speed 4600 rpm.
103     JM          372   ; if speed > 4600 rpm
104     125         125     jump to 003 125.
105     003         003   ; if 860<v<4600, go on.
106     LXIH        041   ; load the address of next
107     237         237     sample data.
110     003         003
111     MVIA        076
112     152         152
113     SUI         326   ; sample data - 2
114     002         002
115     INXH        043   ; the address of map + 1
116     CMPD        272     compare again.
117     JM          372   ; if < 0, to load the time
120     130         130     bytes.
121     003         003
122     JMP         303   ; if > 0, go back to compare
123     113         113     next sample data.
124     003         003
125     LXIH        041   ; the address of time bytes
126     303         303     at speed = 4600 rpm.
127     003         003
130     MOV A,M     176   ; load the time bytes.
131     OUT         323
132     001         001   ; time bytes shown on the
133     MOV E,A     137     port 1.
134     MOV A,D     127   ; load the present speed.
135     MVIC        016   ; to decide how many 10ms
136     132         132     delay time needed.
137     CMP C       271   ; compare with the speed =
140     JM          372     132.
141     150         150
142     003         003
143     MVIB        006   ; when speed < 132, it needs
```

```
144     005         005    50ms time delay.
145     JMP         303
146     212         212
147     003         003
150     MVIC        016
151     102         102  ; compare with speed = 102
152     CMP C       271
153     JM          372
154     163         163
155     003         003
156     MVIB        006  ; if 132 < speed < 102,
157     004         004    it needs 40ms time delay
160     JMP         303
161     212         212
162     003         003
163     MVIC        016
164     064         064
165     CMP C       271  ; compare with speed = 064
166     JM          372
167     176         176
170     003         003
171     MVIB        006  ; if 102 < speed < 064, it
172     003         003    needs 30ms time delay.
173     JMP         303
174     212         212
175     003         003
176     MVIC        016
177     022         022
200     CMP C       271  ; compare with speed 022.
201     JM          372
202     204         204
203     003         003
204     MVIB        006  ; if 064 < speed < 022, it -
205     001         001  ; needs 10ms time delay.
206     MVIA        076
207     000         000
210     OUT         323  ; to store the energy in the
211     002         002  ; coil.
212     CALL        315  ; call subroutine of 10ms
213     277         277  ; time delay.
214     000         000
215     MOV B.B     100  ; to execute the time bytes.
216     MOV B,B     100
217     MOV B,B     100
220     MOV B,B     100
221     DCR E       035  ; time bytes - 1.
222     215         215
223     003         003
224     MVIA        076  ; prepare to fire spark.
225     200         200
226     OUT         323
227     002         002  ; spark fire.
230     JMP         303
```

```
231     000       000  ; restart.
232     003       003


240     350       350  ; storage area of time bytes
241     271       271
242     222       222
243     160       160
244     111       111
245     041       041
246     024       024
247     015       015
250     165       165
251     200       200
252     130       130
253     062       062
254     013       013
255     237       237
256     273       273
257     002       002
260     162       162
261     112       112
262     047       047
263     002       002
264     306       306
265     261       261
266     214       214
267     146       146
270     105       105
271     044       044
272     003       003
273     334       334
274     274       274
275     236       236
276     127       127
277     115       115
300     100       100
301     042       042
302     003       003
303     334       334
304     276       276
305     237       237
306     127       127
307     140       140
310     101       101
311     041       041
312     002       002
313     025       025
```

PROGRAM OF FUEL INJECTION

Address	Mneu	Op Code	
003 000	MVID	026	; set absolution step of SM
001	000	000	to 0.
002	MVIH	046	; set the reference status of
003	020	020	sensor (10).
004	IN	333	; input the status of OXY
005	007	007	; at bit 3,4 of port 7
006	ANI	346	; mask the data of oxygen
007	030	030	sensor at bit 3, 4.
010	CMPH	274	; compare with reference
011	JNZ	302	status of OXY.
012	023	023	
013	003	003	; yes,
014	MVIB	006	; the mixture is too heavy.
015	001	001	; cw steps + 1.
016	MVIC	016	; ccw steps - 0.
017	000	000	
020	JMP	303	
021	044	044	
022	003	003	
023	MVIH	046	; set the reference status
024	010	010	of OXY 01
025	CMPH	274	; compare with the data of
026	JNZ	302	OXY.
027	040	040	
030	003	003	; yes,
031	MVIB	006	the mixture is too lean.
032	000	000	; cw steps + 0
033	MVIC	016	
034	001	001	; ccw steps + 1
035	JMP	303	
036	044	044	;yes,
037	003	003	the mixture is right ratio.
040	MVIB	006	
041	000	000	; cw steps + 0
042	MVIC	016	; ccw steps + 0
043	000	000	
044	OUT	323	; start A/D conversion.
045	005	005	
046	IN	333	; check the A/D conversion
047	005	005	finish or not.
050	ANI	346	; mask the data of BUSY
051	040	040	at bit 5.
052	JZ	312	; yes, BUSY is high, check
053	046	046	again.
054	003	003	; A/D conversion finished.
055	IN	333	; input the data of air flow
056	004	004	meter at port 4.
057	ANI	346	; mask the data of flow meter

```
        060     374         374
        061     RRC         017   ; divide the data of flow
        062     RRC         017     meter by 4 to obtain steps
        063     MOV E,A     137   ; (NA) of SM.
        064     SUBD        222   ; obtain relative steps NR.
        065     JM          372   ; if minus, go to SMccw.
        066     133         133
        067     003         003
        070     MOV D,E     123   ; store the present NA to D.
        071     SBB B       230   ; correct the steps by OXY.
        072     ADD C       201
        073     JZ          312
        074     002         002
        075     003         003
        076     MOV L,A     157   ; store NR in L.
SMcw    077     MVIA        076
        100     000         000   ; SM cw.
        101     OUT         323
        102     001         001
        103     MVIA        076   ; rotate the needed steps
        104     000         000
        105     OUT         323
        106     000         000
        107     MVIA        076
        110     200         200
        111     OUT         323
        112     000         000
        113     MVIB        006 ; decide the delay time of
        114     001         001   each steps, 10ms.
        115     CALL        315 ; call the delay subroutine.
        116     277         277
        117     000         000
        120     DCR B       005
        121     JNZ         302
        122     115         115
        123     003         003
        124     DCR L       055 ; NR - 1
        125     JNZ         302
        126     103         103
        127     003         003
        130     JMP         303
        131     002         002 ; restart
        132     003         003
SMccw   133     CMA         057 ; let NR = -NR
        134     ADI         306
        135     001         001
        136     MOV D,E     123 ; store NA in D.
        137     SBB C       231 ; correct the injected fuel.
        140     ADD B       200   to obtain the NR.
        141     JZ          312
        142     002         002
        143     003         003
        144     MOV L,A     157 ; store NR in L.
```

```
145     MVIA        076 ; make SM ccw.
146     200         200
147     OUT         323
150     001         001
151     JMP         303
152     103         103
153     003         003
```

NOTE:

OXY: oxygen sensor.
SM : stepper motor.
NA : the absolute steps of stepper motor.
NR : the relative steps of stepper motor with the previous revolution.

APPENDIX B

LR-36 A/D Converter

LR-36 A/D CONVERTER

Basic Description

The AD 7570 is a monolithic CMOS A/D converter which uses the successive approximations technique to provide up to 10 bits of digital data in a serial and parallel format. Most A/D applications require the addition of only a comparator and a voltage or circuir reference.

In the successive approximations technique, successive bits, starting with the most significant bit (DB9) are applied to the input of a DAC circuit. The DAC output is then compared to the unknown analog input voltage (AIN) using a zero crossing detector (comparator). If the DAC output is less than AIN, the trial data bit stays in the "1" state, and the next smaller data bit is tried.

Each successive bit is tried, compared to AIN, and set or reset in this manner until the least significant bit(DB0) decision is made. At this time, the AD7570 output is a valid digital representation of the analog input, and will remain in the data latches until another conversion start (STRT) is applied. Fig. 44. is the AD7570 timing diagram, showing the successive trials and decisions for each data bit. When convert start (STRT) goes HI, the MSB(DB9) is set to logic "1" state, while DBO through DB8 are reset to the "0" state. Two clock pulses plus 200ns after STRT

returns LO, the MSB decision is made, and DB8 is tried. Each succeeding trial and decision is made at CLK + 200ns.

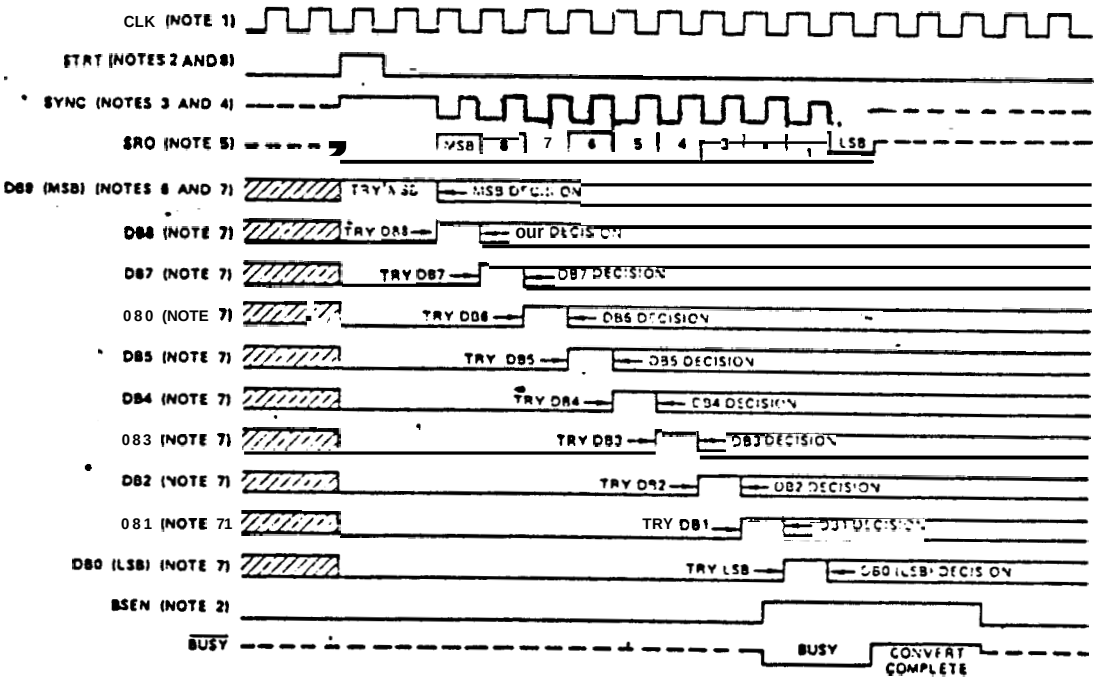

(a) AD 7570 Conversion Timing Sequence

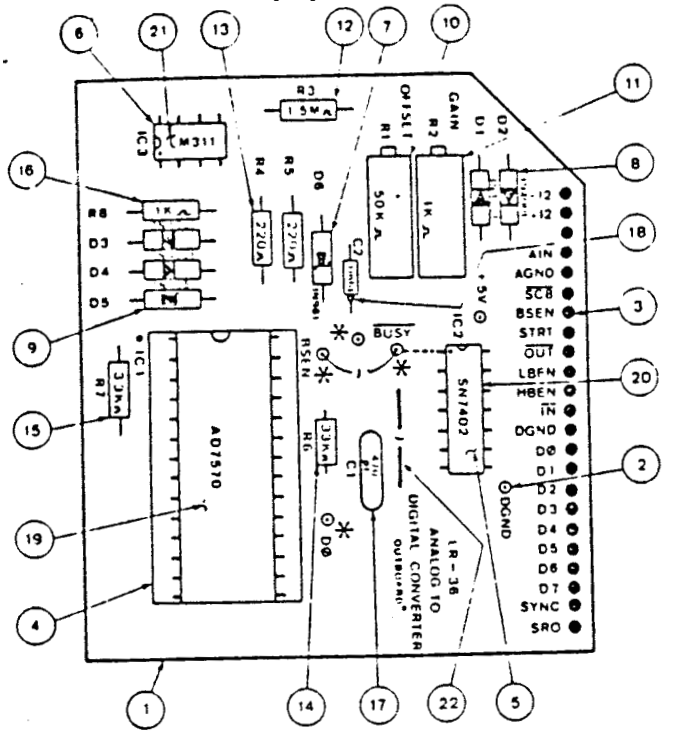

D	DESCRIPTION
1	P.C. Board, Mach.
2	BP-25 Pin
3	BP-26 Pin
4	AD7570JD
5	SN7402
6	LM311
7	IN961 (10V Zener)
8	IN4001
9	IN965 (15V Zener)
10	50K Heli Trimpot
11	1K Heli Trimpot
12	CCRES 1/4W 1.511 Ohm 5%
13	CCRES 1/4W 220 Ohm 5%
14	CCRES 1/4W 33K Ohm 5%
15	CCRES 1/4W 3.3K Ohm 5%
16	CCRES 1/4W 1K Ohm 5%
17	Cer Cap 470PFD
18	Tant Cap 1MFD 35V CS
19	28 Pin Socket
20	14 Pin Socket
21	8 Pin Socket

(b). outboard of LR 36

Fig. 44. The LR36 A/D converter

PIN NO.	MNEMONIC	FUNCTION
1	VDD	Positive Supply (+15V)
2	VREF	Voltage REFerence (±10V)
3	AIN	Analog INput
4	OUT1	DAC Current OUTput 1
5	OUT2	DAC Current OUTput 2
6	AGND	Analog GrouND
7	COMP	COMParator
8	SRO	SeRial Output
9	SYNC	Serial SYNChronization
10	DB9	Data Bit 9 (MSB)
11	DB8	Data Bit 8
12	DB7	Data Bit 7
13	DB6	Data Bit 6
14	DB5	Data Bit 5
15	DB4	Data Bit 4
16	DB3	Dara Bit 3
17	DB2	Data Bit 2
18	DB1	Data Bit 1
19	DR0	Data Bit 0 (LSB)
20	HUEN	High Byte ENable
21	LBEN	Low Byte ENable
22	VCC	Logic Supply (+5V to +15V)
23	DCND	Digital GrouND
24	CLK	CLocK
25	STRT	STaRT
26	$\overline{SC8}$	Short Cycle 8 Bits
27	$\overline{BSEN}$	BuSy EN
28	$\overline{BUSY}$	BUSY

Fig. 45. Function Table

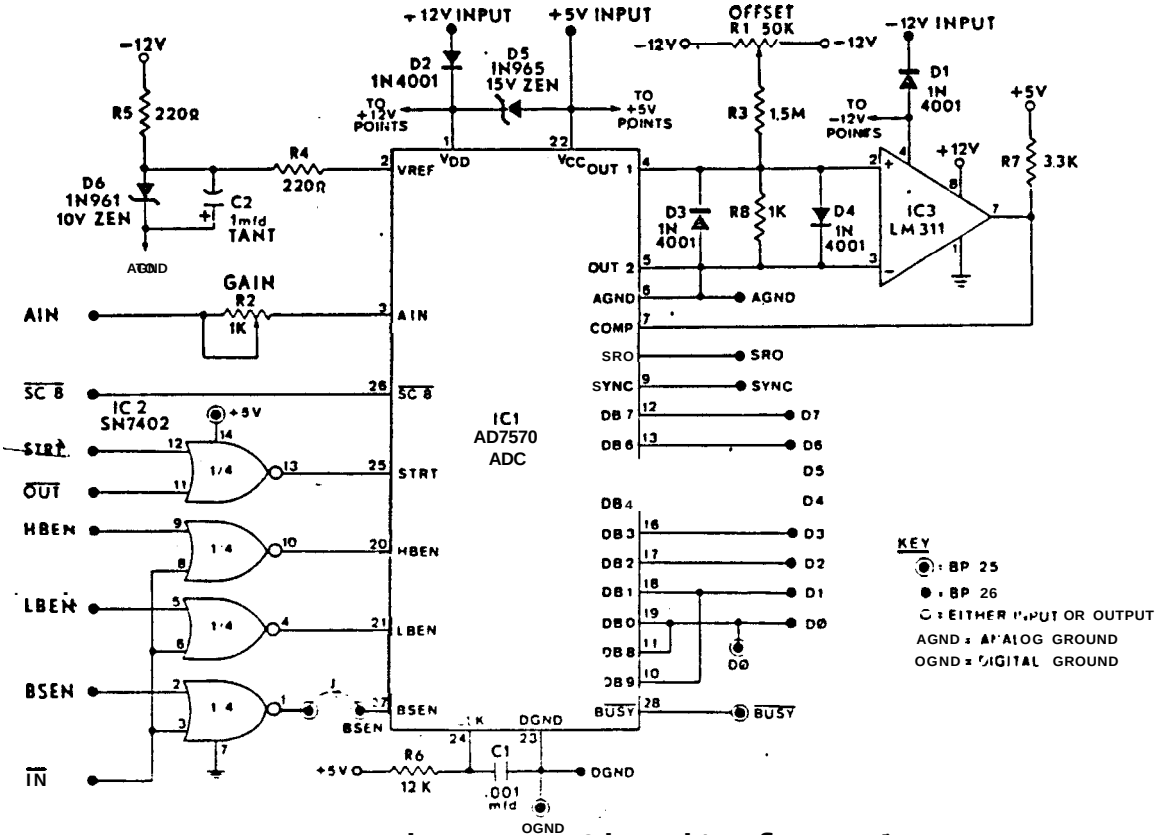

Fig. 46. Circuit of LR-36

10. Operation Mannual of LR-36 A/D Converter, E&L Instrument, Inc. Derby, Ct

APPEXDIX C

Overview of the Engine

Four Stroke Engine

The four strokes of the engine are (1) intake stroke (2) compression stroke **(3)** power or work strol-e **(4)** exhaust stroke as shown in Fig. **47.**[11]

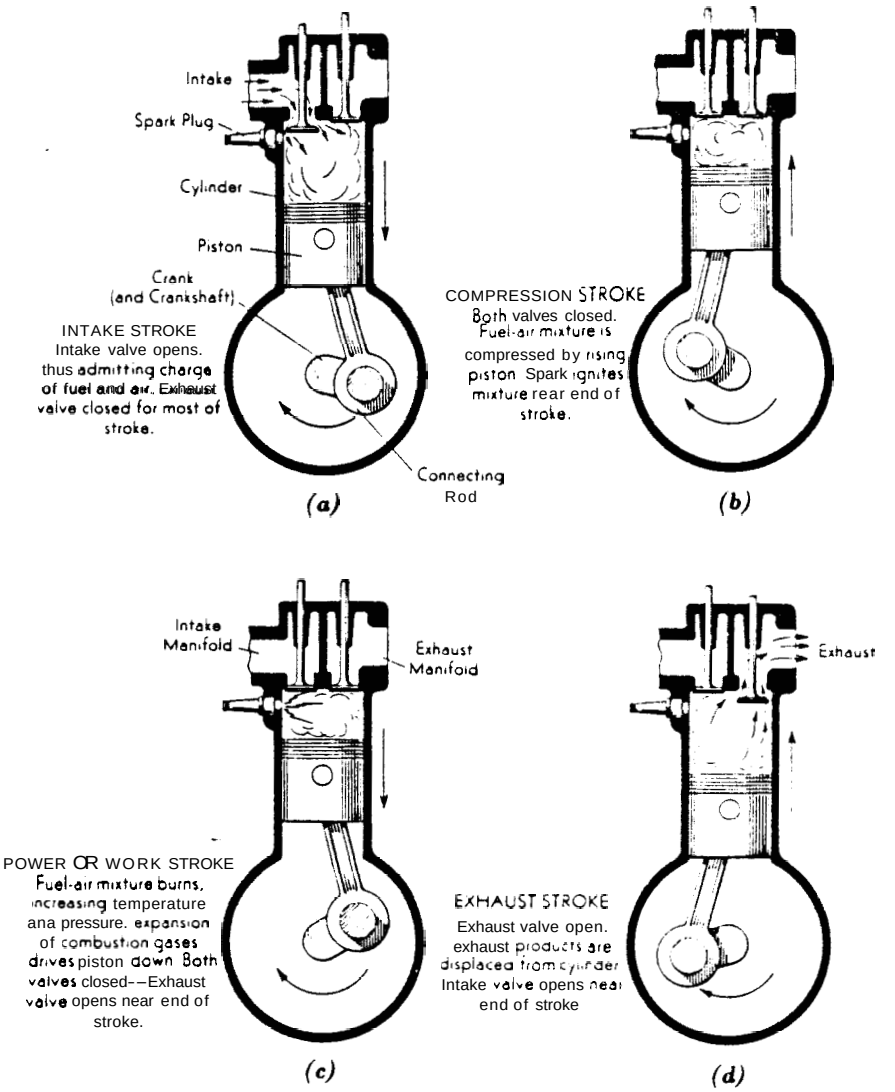

Fig. 47. Four Stroke Spark-ignition Cycle

11. Edward F. Obert, **P3.**

Carburetor

A carburetor is a mechanical device to meter the liquid fuel which meets the A/F ratio required of the engine. When the fresh air is drawn into the venturi tube of the carburetor from the atmosphere by the action of the engine pistons on the intake stroke, according to the theory of Bernuli the air will atomize the fuel, and mix it homogeneously (Fig. 48).

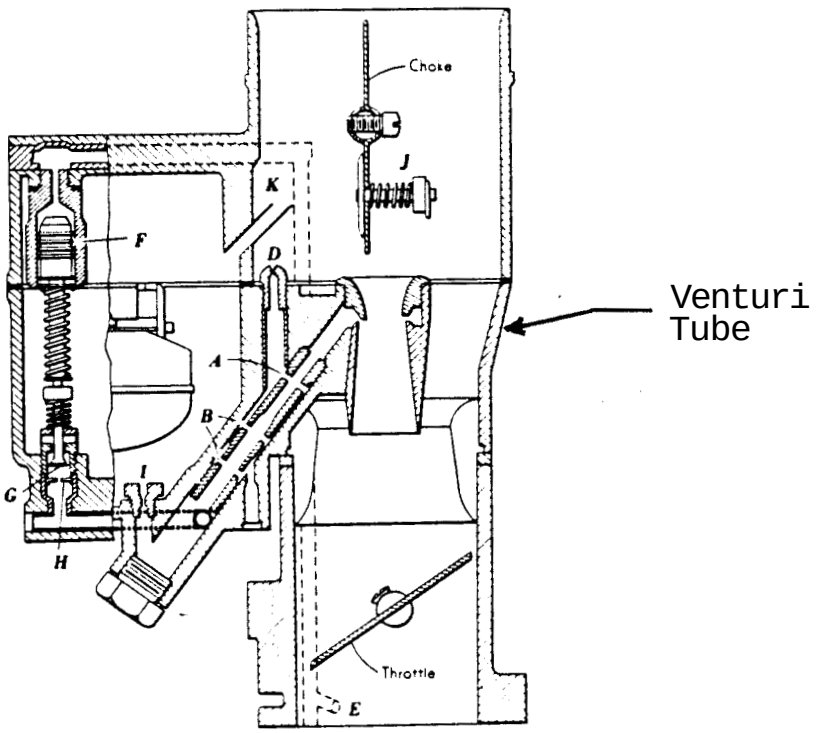

Fig. 48. Carburetor
(Courtesy of Bendix Aviation Corp.)

Engine Air-Fuel Mixture Requirements

Under actual conditions of successful operation, there are three general ranges of throttle position as shown in Fig. 46. The carburetor must modify the A/F ratio to satisfy following condition :

(1) Idling (mixture must be enriched)
(2) Cruising (mixture must be leaned)
(3) High power (mixture must be enriched)

(1). Idling Range. An idling engine is one operating at no load and with nearly closed throttle. The amount of fresh charge brought in during idling, hower, is much less than during full throttle operation,due to the restriction imposed by the throttle. The result is a much larger proportion of exhaust gas being mixed with the fresh charge, under idling conditions. Furthermore, the nearly closed throttle restriction tends to keep the pressure in the intake manifold considerably below atmospheric. When the intake valve opens, the pressure differential between the combustion chamber and the intake manifold results in backward initial flow of exhaust gases into the intake manifold. As the piston going down on the intake sroke, these exhaust gases are drawn back into the cylinder, along with the fresh air. As a result, the final mixture of fuel and air in the combustion chamber is diluted by exhaust gas; therefore, it is necessary to provide more fuel by enrichening the air fuel mixture.

(2). Cruising Range. In the cruising range from B to C, the exhaust gas dilution problem is relatively insignificant. The primary interest is how to obtain the best economy mixture.

(3). Power range. Since high power is desired, logically the engine requires a richer mixture to produce the best power mixture. In addition, enrichening the mixture reduces the flame temperature and cylinder temperature, thereby reducing the cooling and "knock" problems which will cause some damage in the engine.[12]

Advance Ignition System (Fig. 46.):

Since the combustion of fuel does not take place instantaneously, in order to obtain the best power and the lowest fuel consumption the spark should occur before the end of the compression stroke. Some of the major factors affecting the optimum spark setting are 1. type of fuel 2.

12. Edwart F. Obert pp.470-478

engine speed 3 air fuel ratio 4.part load conditions; therefore, the optimum spark setting must be regulated to account for changes in the load and speed of the engine. Most automobile engines are equipped with a mechanism that is integral with the distributor. The two mechanisms are the vacuum advance and the centrifugal advance.

The vacuum advance automatically compensates for the idling speed or part load. As the throttle is closed, in the intake manifold will exist a vacuum force to move the diaphragm away from the distributor and as a result the spark is advanced through a linkage mechanism. As the throttle is opened, the vacuum force will disapper and make the spark to occur closer to TDC.

The centrifugal advance automatically compensates for changes in the speed of the engine. From Fig. 49, we can see that one pair of the counterweights is attached with the cam shaft of the distributor. When the engine speed increases, it will create a centrifugal force to move the counterweights and advance the angular position of the cam relative to the drive shaft. In this new position, the breaker points open earlier, causing an advance in th spark setting.[13]

13. Paul W. Gill and Janes H. Smith, Jr. Fundamental of Internal Combustion Engine. John Wiley & Sons Inc.

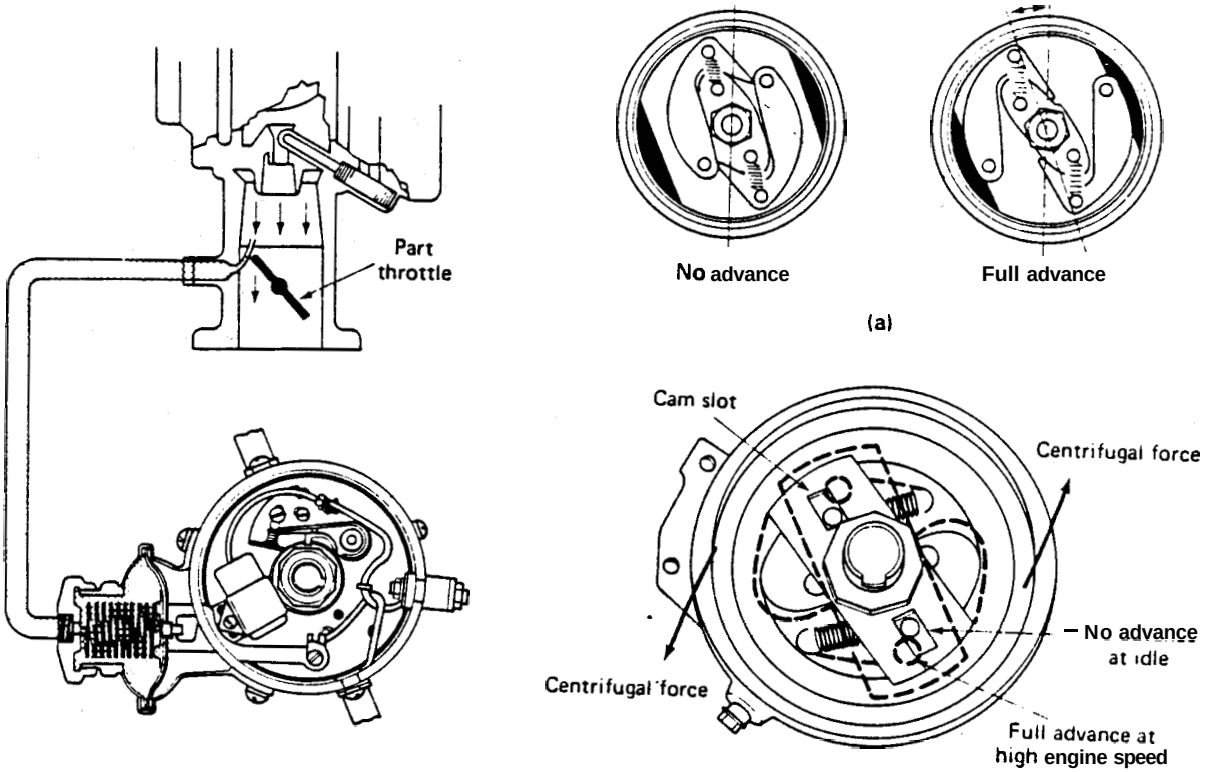

(a) Centrifugal Advance

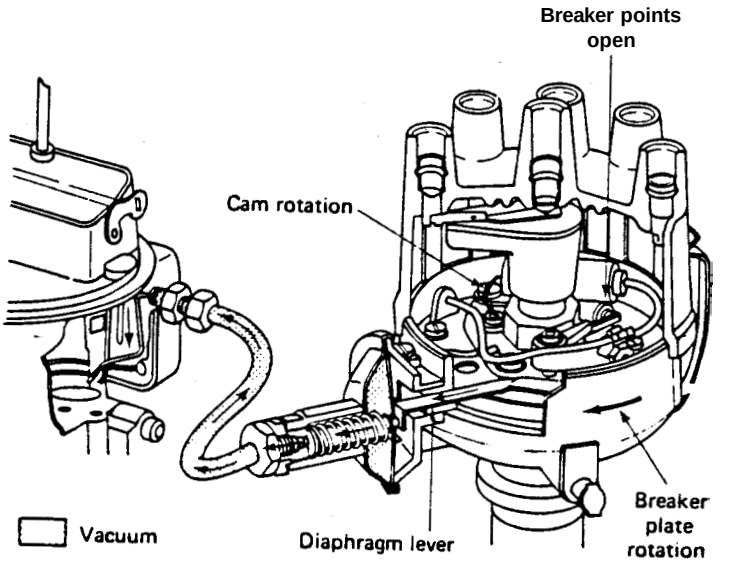

(b) Vacuum Advance

Fig. 49. Mechanisms of the Advance Ignition (From T. Weathers. and C. Hunter, Fundamentals of Electricity and Automotive Electronical System, Prentice-Hall, Inc., Englewood Cliffs)

Fuel Injector

A Bosch individual-pump assembly for a six-cylinder engine is illustrated in Fig. 50a, and a sectional view of one of the pumping elements, in Fig. 50b. When the plunger compresses the fuel, the delivery valve C opens and fuel flows through the discharge tubing D to the nozzle E. The spray pattern from the nozzle is formed by the orifices F, which are closed by a spring-loaded G valve. Note that the pump plunger is lifted by a cam on a camshaft driven by the engine.

The metering and compression processes of the plunger can be explained with the help of Fig. 50b. When the plunger is at the bottom of its stroke, ports A and A' are uncovered. Fuel enters the barrel under pressure from the fuel tank pump. When the plungers rise, the ports are sealed and the compressed fuel lifts the delivery valve C and begins the injection period. Fuel is injected only during the high-velocity portion of the plunger stroke. As the plunger continues to rise, the spill port A' into the sump, while the delivery valve snaps shut, with consequent end of the injection period. The position of the helical groove in relation to the spill port A' is changed by rotating the plunger with the rack or control rod R which corresponds to the throttle of engine. By moving the rack, the quantity of fuel injected can be varied from zero to that demanded at full load. Fig 50c., shows a shorter effective travel, say, half load, while in Fig 50c.(a) the slot in the plunger is in line with the spillport and no compression or delivery of fuel is obtained. This is the "stop" position for shutting down the engine. Note that the overall travel or displacement of the plunger is constant at all speeds and loads but the effective travel is controlled by the helix and spill port in proportion to the load (displacement metering).[14]

14. Edware F. Obert, pp 430-436.

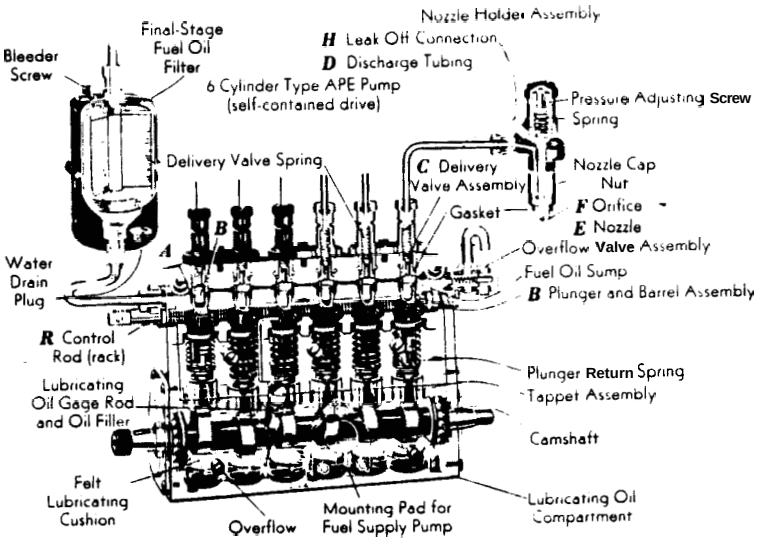

Fig. 50a. Bosch APE injection (Courtesy of American Bosch Corp.)

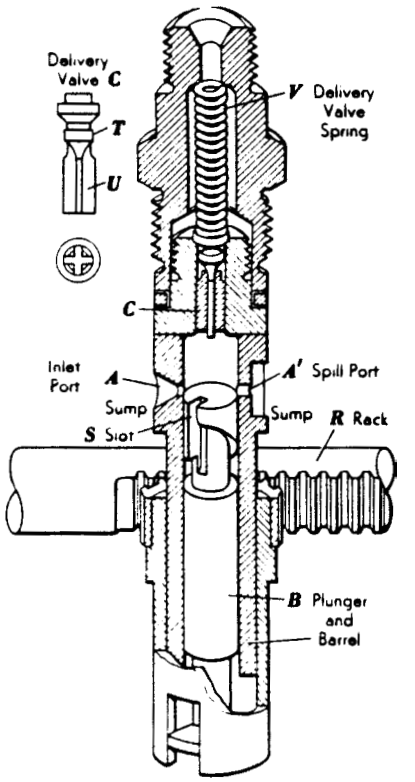

Fig. 50b. Section View of Bosch Pump Elements.(Courtesy American Bosch Corp.)

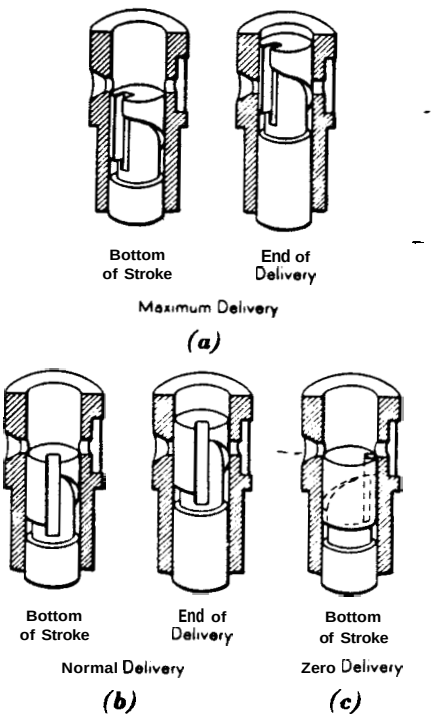

Fig. 50c. Position of the Helix for various load conditions (Courtesy American Bosch Corp.)

APPENDIX D

Examples of Fuel Injection

EXAMPLE OF FUEL INJECTION

Mercede Benz 280 CE (D-jetronic, pressure control)

The quantity of fuel injected is decided by the signal of pressure sensor (5) Fig. 51. When the position of the throttle valve is varied, the pressure of intake manifold will be different; therefore, convert the values of signal of the pressure sensor to different analogue pulse width signals to control the quantities of fuel being injected. In addition, the computer can use the signals of the air and cooling water temperature sensor to make the injected fuel more accurate. Also, the cold start valve can be used to inject more fuel to make the A/F ratio richer when the cold start or at full speed.

BMW 528i (L-Jetronic, Air Flow Control, Fig. 52.)

There is one position sensor to detect the position of the throttle valve, then use the signal to compute the quantities of fuel being injected. In this system the A/F ratio is kept at 1:15 in the cruise speed condition, but when the automobile is just started or in full speed, there is one cold start valve to inject extra fuel so that the A/F ratio is changed to 1:14. Furthermore, the computer can use the other information like the signals of air and cooling water temperature sensor, or oxygen sensor to correct the quantities of fuel.

VOLVO B21F (K- jetrontic , mechanical control, Fig.53.)

According to the theory of the lever, when the air flow beats the sense plate on the left hand side of the pivot, it will produce a balance force to push the plunger up or down, and the different positions of the plungers can meter the required fuel being injected.

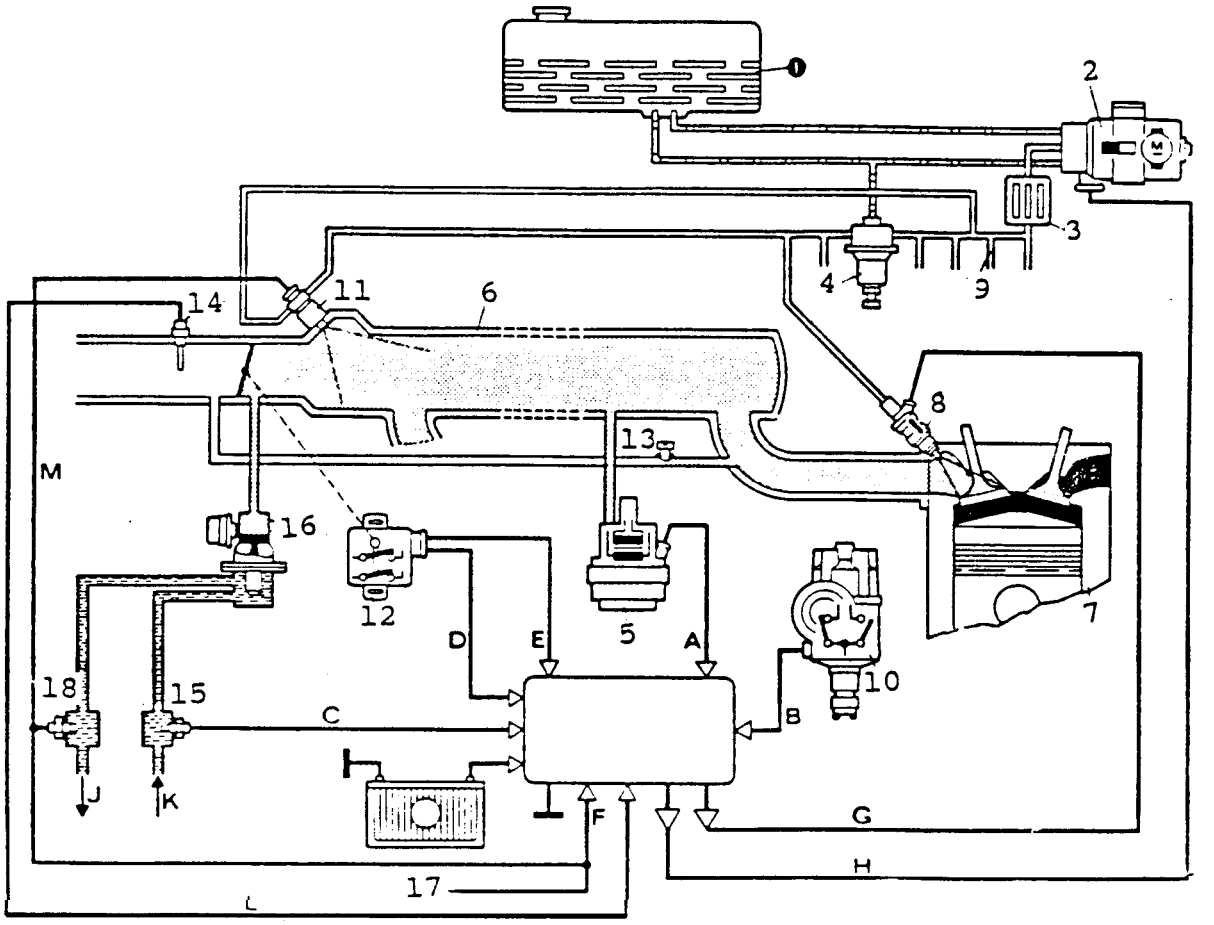

Fig. 51. Fuel Injection System (Pressure Control)
(Courtesy of Mercede Beze Automotive Corp.)

(1). fuel tank (2). fuel pump (3). fuel filter
(4). fuel pressure regulator (5). pressure sensor
(6). intake manifold (7). cylinder head (8). nozzle
(9). fuel tube (10). pulse trigger (11). cold start valve
(12). throttle valve switch (13). the regulation screw of idling speed (14). the temperature sensor of air
(15). the water temperature sensor A
(16). the regulator of auxiliary air
(17). the terminal of start motor
(18). the temperature switch

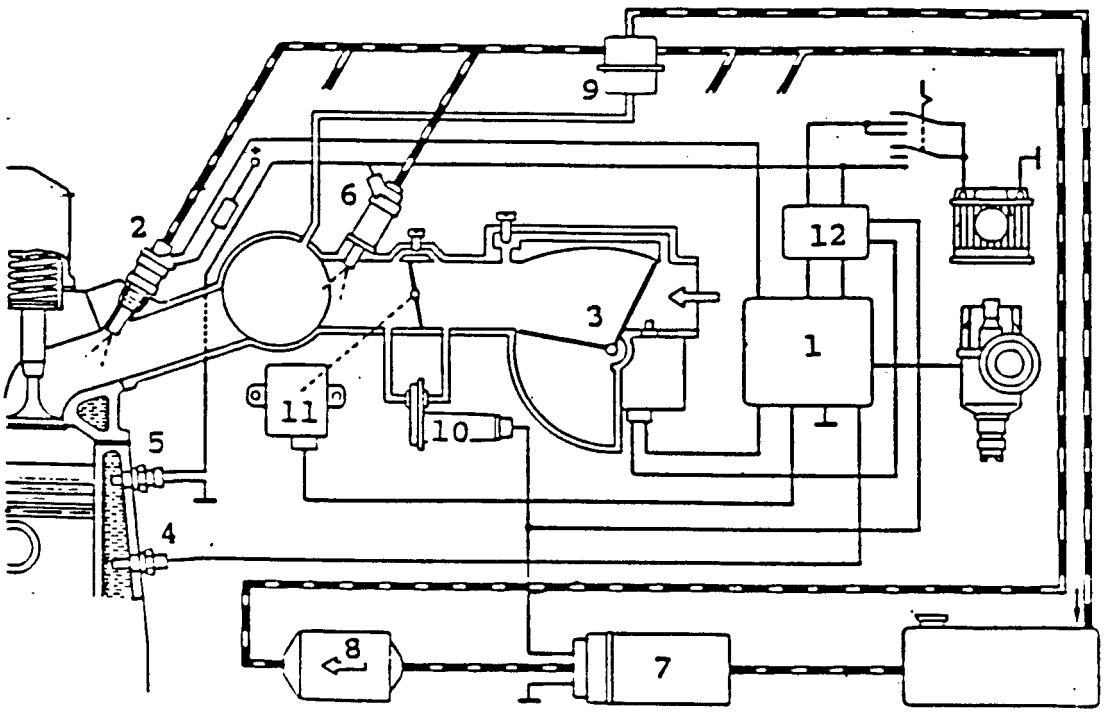

Fig. 52. Fuel Injection System (Air Flow Control)
(Courtesy of BMW Automotive Manf. Corp.)

(1). computer controller. (2). nozzle
(3). air flow sensor (4). the water temperature sensor
(5). the temperature timer. (6) cold start valve
(7). fuel pump (8). fuel filter
(9). the regulator air valve (13). throttle valve
(10).the auxiliary air valve.
(11). the throttle position switch
(12). relay set

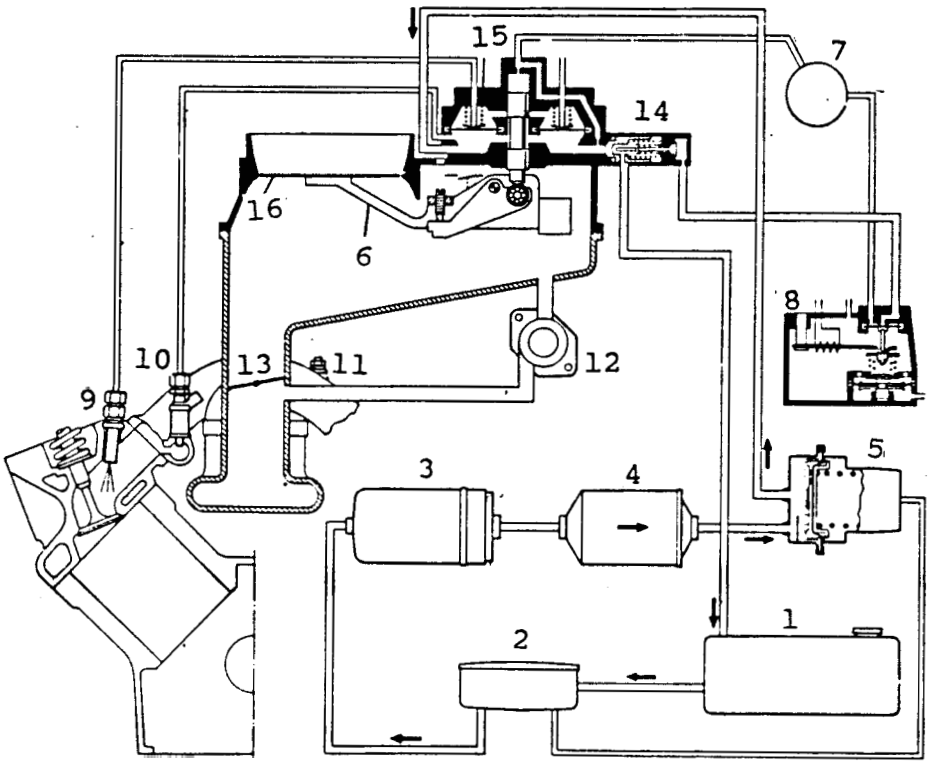

Fig. 53. Fuel Injection System (Mechanical Control)
(Courtesy of Volvo Automobile Corp.)

(1). fuel tank (2). muffler (3). fuel pump
(4). fuel filter (5). accumulator
(6). distributor (7). buffer
(8). warm-up regulator (9). nozzle
(10). cold start valve (11). the water temperature sensor
(12). auxiliary air valve (13). throttle valve
(15). the fuel pressure regulator
(16). the sensing plate

APPENDIX E

Stress Analysis of Circular Plate

STRESS ANALYSIS OF CIRCULAR PLATE

To simplify the problem of stress analysis of a circular plate with clamped edges, we must assume: (1) the circular plate material is homogeneous, (2) the modules of elasticity in tensible and compression are equal, (3) the bending deformation of the circular plate is symmetric, (4) after bending the transverse plane still remains plane, not distorted.

If we mount a radius a and thickness h circular diaphragm clamped by two cylinders (Fig. 54.), a load of

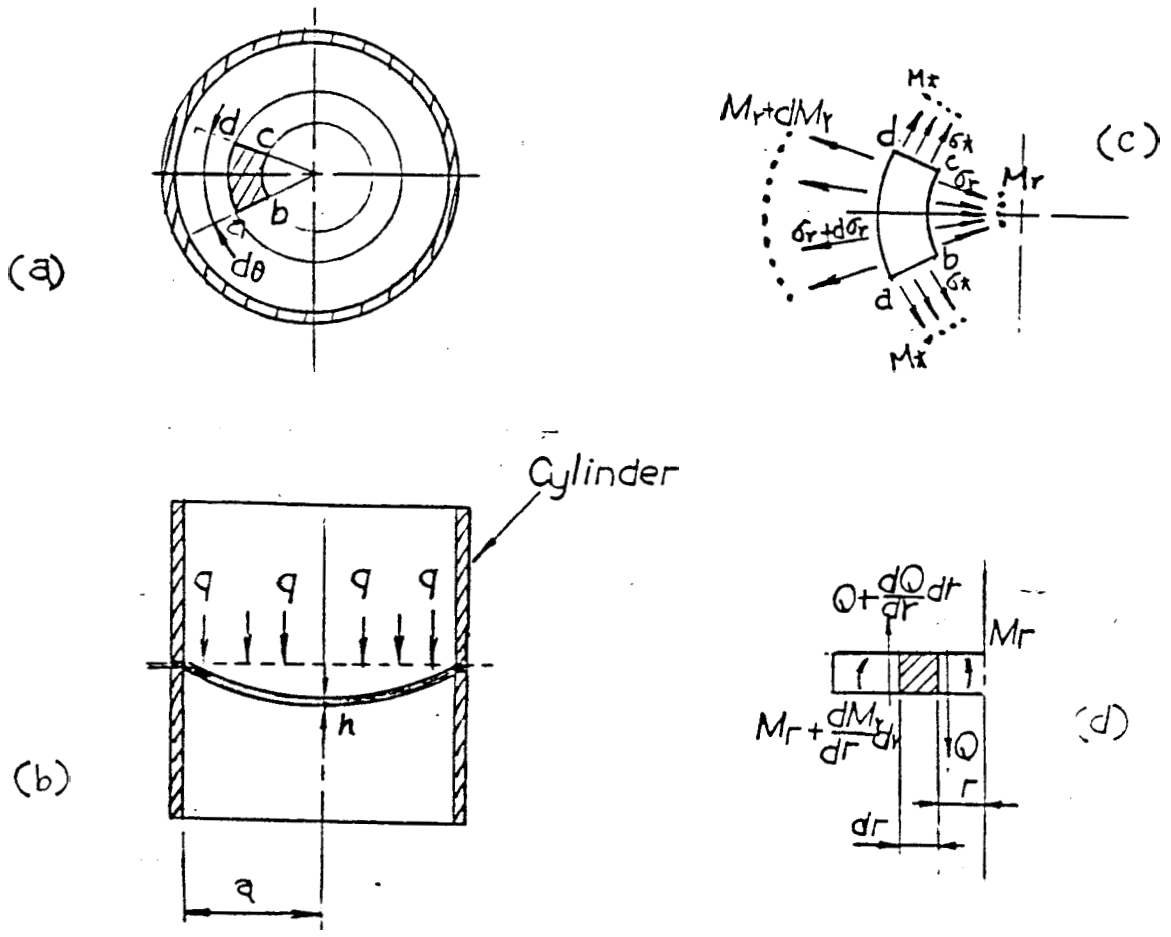

Fig. 54. Stress Analysis of the Circular Plate

intensity q uniformly distributed over the entire surface of the plate. The magnitude of the shearing force Q, at a distance r from the center of the plate is determined from the equation, which accord to the equilibrium law of force.

$$2\pi rQ=\pi r^2 q$$

where 2 rQ is the total shear force at circumference, and $\pi r^2 q$ is total external force within the circular plate of radius r; therefore Q = qr/2.

Because the external force intensity q exerts on the plate uniformly, it will create two bending moment M and M

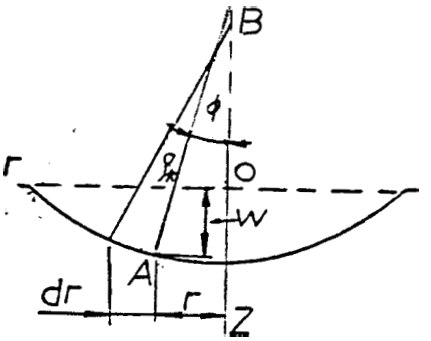

Fig. 55. The principal curvatures

which will induce equilibrium bending stress σ_r and σ_t (Fig. 54d.). Meanwhile, there exist two principle curvatures ρ_r and ρ_t due to the bending moment (Fig. 55.).

$$\frac{1}{\rho_r}=-\frac{d^2w}{dr^2}=\frac{d\phi}{dr}=\frac{\epsilon_r}{Z} \qquad \text{EQ. 30.}$$

$$\frac{1}{\rho_t}=\frac{-dw}{rdr}=\frac{\phi}{r}=\frac{\epsilon_t}{Z} \qquad \text{EQ. 31.}$$

According to the Hooks law, the unit elongation ϵ_r and ϵ_t in terms of the normal stress σ_r and σ_t, which are act on the element shown in Fig 54c.

$$\epsilon_r=\frac{\sigma_r}{E}-\frac{\nu\sigma_t}{E} \qquad \text{EQ. 32.}$$

$$\epsilon_t = \frac{\sigma_t}{E} - \frac{\upsilon\sigma_r}{E} \qquad \textbf{EQ.}\ 33.$$

Rearranging **EQ.** 32. and **EQ.** 33, we obtain **EQ.** 34 and **EQ.** 35.

$$\sigma_r = \frac{EZ}{1-\upsilon^2}\left(\frac{1}{\rho_r} + \frac{\upsilon}{\rho_t}\right) \qquad \textbf{EQ.}\ 34.$$

$$\sigma_t = \frac{EZ}{1-\upsilon^2}\left(\frac{1}{\rho_t} - \frac{\upsilon}{\rho_r}\right) \qquad \textbf{EQ.}\ 35.$$

If we integrate the bending stress σ_r and σ_t through all cross sectional area with z direction, the magnitude must be equal to the external moments Mr and Mt. In this way, we obtain the equations

$$\int_{-h/2}^{h/2} \sigma_r Z r\, d\theta\, dZ = M_r r\, d\theta \qquad \textbf{EQ. 36.}$$

$$\int_{-h/2}^{h/2} \sigma_t Z dr\, d\theta\, dZ = M_t dr\, d\theta \qquad \textbf{EQ. 37.}$$

substituting **EQ. 34** and **35** into **EQ. 36** and **EQ.** 37 respectively and integrating ,we obtain

$$M_r = \frac{Eh^3}{12(1-\upsilon^2)}\left(\frac{1}{\rho_r} + \frac{\upsilon}{\rho_t}\right) \qquad \textbf{EQ. 38.}$$

$$M_t = \frac{Eh^3}{12(1-\upsilon^2)}\left(\frac{1}{\rho_t} + \frac{\upsilon}{\rho_r}\right) \qquad \textbf{EQ. 39.}$$

Let $D = \frac{Eh^3}{12(1-\upsilon^2)}$ flexure rigidity

Replacing $1/\rho_r$ and $1/\rho_t$ by **EQ.** 30. and 31., obtain

$$M_r = -D\left(\frac{d^2w}{dr^2} + \frac{\upsilon dw}{r dr}\right) = D\left(\frac{d\phi}{dr} + \frac{\upsilon\phi}{r}\right) \qquad \textbf{EQ.}\ 40$$

$$M_r = -D\left(\frac{1}{r}\frac{dw}{dr} + \nu\frac{d^2w}{dr^2}\right) = D\left(\frac{\phi}{r} + \frac{\nu d\phi}{dr}\right) \qquad \text{EQ. 41.}$$

where the moment Mr acts along the circumferential sections of the plate, such as the section made by the conical surface with the apex at b, and Mt acts along the diametral section rz of the plate.

By considering the equilibrium of an element of the plate such as element abcd (Fig. 54c) cut out from the plate, the couple acting on the side bc of the element is

$$M_r d\theta \qquad \text{(a)}$$

the corresponding couple on the side ad is

$$\left(M_r + \frac{dM_r}{dr}dr\right)(r + dr)d\theta \qquad \text{(b)}$$

the couples on the sides ab and cd of the element are

$$M_t dr d\theta \qquad \text{(c)}$$

and the shearing force per unit length of the cylindrical section of radius r, the total shearing force acting on the side bc of the element is Qrd , and the corresponding force on the side ad is

$$\left[Q + \left(\frac{d\theta}{dr}\right)dr\right](r + dr)d\theta \qquad \text{(d)}$$

Neglecting the small difference between the shearing forces on the two opposite sides of the element, we can say these forces give a couple in the rz plane equal to

$$Qrd\theta dr \qquad \text{(e)}$$

summing up the couples of (a), (b), (c), and (d), and neglecting some small quantities of higher order, finally we obtain the following equation of equilibrium of the element abcd (EQ. 43.)

$$\left(M_r + \frac{dM_r}{dr}dr\right)(r+dr)d\theta - M_r r d\theta - M_t dr d\theta + Q r d\theta dr = 0$$

$$M_r + \frac{dM_r}{dr}r - M_t + Qr = 0 \qquad \text{EQ. 42.}$$

EQ. 43.

Substituting expressions EQ. 40. and 41. for Mr and Mt, EQ. 43. becomes

$$\frac{d^2\phi}{dr^2} + \frac{d\phi}{r dr} - \frac{\phi}{r^2} = -\frac{Q}{D} \qquad \text{EQ. 44.}$$

or, in another form

$$\frac{d^3w}{dr^3} - \frac{d^2w}{r dr^2} - \frac{dw}{r^2 dr} = \frac{Q}{D} \qquad \text{EQ. 45.}$$

EQ. 44. and 45. can be put in the following form

$$\frac{d}{dr}\left[\frac{1}{r}\frac{d}{dr}\left(r\frac{dw}{dr}\right)\right] = \frac{Q}{D} \qquad \text{EQ. 46.}$$

$$\frac{d}{dr}\left[\frac{1}{r}\frac{d}{dr}(r\phi)\right] = \frac{-Q}{D} \qquad \text{EQ. 47.}$$

Sometimes it is advantageous to replace the shearing force Q by the intensity q of the load distributed over the plate. Because $2\pi rQ = \pi r^2 q$, from which $Q = qr/2$, EQ. 46 and 47 will become

$$\frac{d}{dr}\left[\frac{1}{r}\frac{d}{dr}\left(r\frac{dw}{dr}\right)\right] = \frac{qr}{2D} \qquad \text{EQ. 48.}$$

By one integration in the EQ. 48, we get

$$\frac{1}{r}\frac{d}{dr}\left(r\frac{dw}{dr}\right) = \frac{qr^2}{4D} + C_1 \qquad \text{EQ. 49.}$$

By the second integration

$$\frac{dw}{dr} = \frac{qr^3}{16D} + \frac{C_1 r}{2} + \frac{C_2}{r} \qquad \text{EQ. 50.}$$

By the third integration

$$w = \frac{qr^4}{64D} + \frac{C_1 r^2}{4} + C_2 \log\frac{r}{a} + C_3 \qquad \text{EQ. 51.}$$

Now, let us calculate the constant C1, C2, C3.

For the clamped edge ,the slope of the deflection surface in the radial direction must zero for r = 0 and r = a .

Hence, from the **EQ. 50.**

$$\left(\frac{qr^3}{16D} + \frac{C_1 r}{2} + \frac{C_2}{r}\right)_{r=0} = 0 \qquad \textbf{EQ. 52.}$$

$$\left(\frac{qr^3}{16D} + \frac{Cr}{2} + \frac{C_2}{r}\right)_{r=a} = 0 \qquad \textbf{EQ. 53.}$$

From the **EQ. 52.**, C2 = 0. Substituting this into the **EQ. 53.** get $C1 = -qa^2/8D$.

With C1 the **EQ. 50.** becomes

$$\phi = -\frac{dw}{dr} = \frac{qr}{16D}(a^2 - r^2) \qquad \textbf{EQ. 54.}$$

and the **EQ.** 51. becomes

$$w = \frac{qr^4}{64D} - \frac{qa^2r^2}{320} + C_3 \qquad \textbf{EQ. 55.}$$

At the edge of the plate, the deflection is zero;therefore

$$\frac{qa^4}{64D} - \frac{qa^4}{32D} + C_3 = 0 \qquad \textbf{EQ. 56.}$$

and obtain C3 = qa / 64D

If substitute **EQ. 54.** into **EQ.** 40., 41., we get the bending moment Mr and Mt:

$$M_r = \frac{q}{16}\left[a^2(1+\upsilon) - r^2(3+\upsilon)\right] \qquad \textbf{EQ. 57.}$$

$$M_t = \frac{q}{16}\left[a^2(1+\upsilon) - r^2(1+3\upsilon)\right] \qquad \textbf{EQ. 58.}$$

If we consider at the bottom of the plate (z = h/2), the relationship of the bending stress and the bending moment is

$$\sigma_r = Mr(z / I) \; ; \quad \sigma_t = Mt(z / I)$$

where z = h/2 and I = $bh^3/12$; therefore,

$$\sigma_r = 6Mr/h \quad , \quad \sigma_t = 6Mt/h$$

The EQ. 57. and 58. will become

$$\sigma_r = \frac{3}{8}\left(\frac{q}{h^2}\right)\left[a^2(1+\upsilon) - r^2(3+\upsilon)\right] \qquad \text{EQ. 59.}$$

$$\sigma_t = \frac{3}{8}\left(\frac{q}{h^2}\right)\left[a^2(1+\upsilon) - r^2(1+3\upsilon)\right] \qquad \text{EQ. 60.}$$

As a result, the stress distribution of the circular plate along the radius a is shown in Fig. 10. (Chapter III).

BIBLIOGRAPHY

Books

Artwick, Bruce A. Microcomputer Interfacing. New Jercy: Prentice-Hall,Inc. 1980

Coughlin, Robert F. & Frederick F. Driscoll. Operational Amplifier and linear Integrated Circuits, Englewood Cliffs, NJ: Prentice-Hall, Inc., 1982.

PAO, Richard H. F., Fluid Mechanics New York: John Wiley & Sons, Inc. 1974.

Seiffert, Ulrich & Peter Walzer. The Future for Automoive Technology, Dover: Frances Pinter.

Sze, S.M. Physics of Semiconductor Devices, 2 Edition, New York: John Wiley & Son Company. 1981.

Timoshenko, S. and D. H. Young Elements of Strength of Materials 5 Edition. Princeton: D. Van Nostrand Company, Inc. 1969.

Van Vlack, Lawerence H. Materials Science for Engineers Addison-Wesley Publishing Company, Inc. 1970.